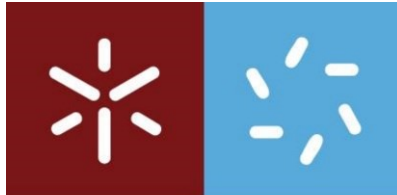


Universidade do Minho
Escola de Ciências

Study of the metabolic conditions involved in monocarboxylate transporter MCT1
internalization in human cancer cell lines

Jéssica Patrícia Azevedo Pinto

Study of the metabolic conditions involved in
monocarboxylate transporter MCT1
internalization in human cancer cell lines



Universidade do Minho

Escola de Ciências

Jéssica Patrícia Azevedo Pinto

**Study of the metabolic conditions involved in
monocarboxylate transporter MCT1 internalization
in human cancer cell lines**

Dissertação de Mestrado

Mestrado em Bioquímica Aplicada

Especialização em Biomedicina

Trabalho realizado sob a orientação de

Professora Doutora Sandra Cristina Almeida Paiva

Doutora Catarina Moura

Junho de 2021

DIREITOS DE AUTOR E CONDIÇÕES DE UTILIZAÇÃO DO TRABALHO POR TERCEIROS

Este é um trabalho académico que pode ser utilizado por terceiros desde que respeitadas as regras e boas práticas internacionalmente aceites, no que concerne aos direitos de autor e direitos conexos.

Assim, o presente trabalho pode ser utilizado nos termos previstos na licença abaixo indicada.

Caso o utilizador necessite de permissão para poder fazer um uso do trabalho em condições não previstas no licenciamento indicado, deverá contactar o autor, através do Repositório da Universidade do Minho.

Licença concedida aos utilizadores deste trabalho



Atribuição-NãoComercial-SemDerivações
CC BY-NC-ND

<https://creativecommons.org/licenses/by-nc-nd/4.0/>

Acknowledgements

I express my gratitude to all the people who, directly or indirectly, contributed to the accomplishment of this work. I would like to register my sincere thanks:

Firstly, I would like to thank Catarina Moura, for helping and advising me in the experimental work, giving me support every time that things went wrong in the lab, being definitely one of the most important persons during the development of this project. For the availability, sharing scientific rigor, optimism and patience. I would also like to thank you for reading and criticizing this dissertation. Thank you so much!

I would like to thank Prof. Sandra Paiva, for introducing me to this “Scientific World” and for the opportunity to develop this work in these research groups with this project. I want to thank you for showing availability to help in everything that I needed and for the critical review of this dissertation. Thank you for everything.

A very special thanks to Rosana Alves for all constant availability and tips for carrying out this work. I am also grateful for all the support regarding statistical data treatment and for the refreshing ideas about how to look at my results. Thank you.

To all my colleagues at the Molecular Genetics laboratory, for the excellent work environment, for hearing me present my work over and over again and for all the constructive ideas that led to the consultation of this work. Thanks to Björn, Carmen, Cláudia Barata, Cláudia Duarte, Cláudia Pinto, Diogo, Humberto, Paulo and Tatiana.

I could not also forget to thank all the teachers along my academic journey because they gave me essential skills and knowledge's to achieve academic success.

Finally, I would like to show all my gratitude to my friends, boyfriend and family, namely my parents and brother, who always supported me. Thanks for the values transmitted, encouragement, guidance and help me overcoming all the obstacles along this journey.

I would like to dedicate this thesis to all of you!!

We cannot do science alone!!!

STATEMENT OF INTEGRITY

I hereby declare having conducted this academic work with integrity. I confirm that I have not used plagiarism or any form of undue use of information or falsification of results along the process leading to its elaboration.

I further declare that I have fully acknowledged the Code of Ethical Conduct of the University of Minho.

Estudo das condições metabólicas envolvidas na internalização do transportador de monocarboxilato MCT1 em linhas de células humanas cancerígenas

Resumo

O cancro é uma doença complexa que representa um vasto problema mundial devido ao seu nível de incidência e mortalidade, sendo a segunda causa de morte no mundo. Mesmo com a diminuição da mortalidade em muitos países, a incidência desta doença na população continuará a aumentar, o que irá causar sérios problemas, mesmo em países com sistemas de saúde mais avançados. Assim, vários esforços têm sido feitos a fim de identificar novas terapias direcionadas.

Na última década, foi descrito que o transportador de monocarboxilatos MCT1 é altamente expresso em vários tipos de cancro. O MCT1 é um transportador responsável pelo influxo de lactato através da membrana plasmática e, em células cancerígenas, promove o seu metabolismo e a sua rápida proliferação e expansão. Assim, o MCT1 é potencialmente uma molécula alvo que poderá ser usada para fins terapêuticos, bem como um fator de prognóstico útil.

Este projeto teve como objetivo avaliar a expressão e localização do transportador EGFP-MCT1, por microscopia confocal, em células U2OS, editas pela tecnologia CRISPR-Cas9, e crescidas em diferentes condições metabólicas ou na presença de compostos específicos.

Demonstrámos que o transportador EGFP-MCT1 permanece estável na membrana plasmática, em células incubadas num meio sem glucose ou glutamina. Estes resultados evidenciam a relevância de expressar transportadores de nutrientes a um nível endógeno para estudar o seu tráfego intracelular. Adicionalmente, os nossos estudos preliminares sugerem o envolvimento da *via* de sinalização Wnt na internalização do MCT1. Verificámos que a presença de cloreto de lítio (LiCl), um ativador da *via* Wnt, parece levar ao aumento da internalização do MCT1, após 24 h de incubação.

Os resultados obtidos neste estudo pretendem contribuir para um melhor entendimento dos mecanismos moleculares envolvidos na expressão e regulação endocítica de MCT1, e, futuramente, abrir novas possibilidades terapêuticas no combate tumoral.

Palavras-Chave: Cancro, lactato, MCT1, Microscopia de fluorescência, Reprogramação metabólica, Transportadores de monocarboxilatos.

Study of the metabolic conditions involved in monocarboxylate transporter MCT1 internalization in human cancer cell lines

Abstract

Cancer is a complex disease that represents a vast problem worldwide due to its high incidence and mortality, being the second leading cause of death globally. Even with the decrease of mortality in many countries, the incidence of this disease will increase, causing serious problems even in countries where health systems are more advanced. So, efforts have been made in order to identify new-targeted therapies.

In the past decade, it has been reported that the monocarboxylate transporter MCT1 is highly expressed in multiple cancer types. MCT1 is a symporter that is responsible for the influx of lactate across the cell membrane and, in cancer cells, it supplies their metabolism and their rapid proliferation and expansion. This makes it a potential target molecule for therapy as well as a useful prognostic factor.

This project aimed at evaluating the expression and localization of the EGFP-MCT1 transporter, by confocal microscopy, in U2OS cells, edited by the CRISPR-Cas9 technology, and grown under different metabolic conditions or in the presence of specific compounds.

In this work we show that the EGFP-MCT1 transporter remains stable at the plasma membrane, in cells incubated in a medium without glucose or glutamine. These results highlight the relevance of expressing nutrient transporters at an endogenous level to study their intracellular trafficking. Additionally, our preliminary studies suggest the involvement of the Wnt signaling pathway in MCT1 internalization. We found that the presence of lithium chloride (LiCl), an activator of the Wnt pathway, also seems to lead to an increased MCT1 internalization, after 24 h of incubation.

The results obtained in this study will contribute towards a better understanding of the molecular mechanisms involved in the expression and endocytic regulation of MCT1, and open novel therapeutic possibilities in the fight against tumors.

Keywords: Cancer, Fluorescence microscopy, Lactate, MCT1, Metabolic reprogramming, Monocarboxylate transporters.

General Index

Acknowledgements	ii
Resumo	iv
Abstract	v
General Index	vi
Index of figures	viii
Index of tables	xii
Lists of abbreviations and acronyms	xiii
1. Introduction	1
1.1. Hallmarks of Cancer	1
1.2. Metabolic reprogramming in Oncogenesis	2
1.2.1. Warburg effect in cancer cells	3
1.2.2. Molecular mechanisms driving Warburg effect	6
1.3. Significance of lactate transport in cancer	11
1.4. Monocarboxylate transporter (MCTs) family	16
1.4.1. Monocarboxylate transporter 1 (MCT1)	18
1.4.1.1. Regulation of Monocarboxylate transporter 1 (MCT1)	18
1.4.1.2. MCT1 as a therapeutic target in cancer cells	24
1.5. Outline of the thesis	28
2. Materials and Methods.....	29
2.1. Biological Materials.....	29
2.2. Cell culture	29
2.3. Compounds for assessing MCT1 expression.....	29

2.4.	Cell sample preparation and optimization for fluorescence microscopy experiments	30
2.5.	Cell seeding for live-cell imaging.....	30
2.6.	Confocal Fluorescence Microscopy.....	31
2.7.	Image processing and analysis.....	31
2.8.	Statistical analysis	34
3.	Results and Discussion	35
3.1.	Optimization of cell seeding for confocal imaging.....	35
3.2.	Effect of glucose and glutamine deprivation on MCT1 protein expression in U2OS cells.....	36
3.3.	Testing the effect of cycloheximide on MCT1 protein expression in U2OS cells.....	41
3.4.	Testing the effect of lenalidomide on MCT1 protein expression in U2OS cells.....	43
3.5.	Testing the effect of FTY720 on MCT1 protein expression in U2OS cells	45
3.6.	Effect of Protein kinase C (PKC) activator in disruption of MCT1 trafficking transport in U2OS cells	48
3.7.	Testing the effects of a Wnt/ β -catenin pathway activator and an inhibitor on MCT1 protein expression in U2OS cells	51
4.	Final Remarks and Future Perspectives	57
5.	References.....	62
6.	Appendix.....	84

Index of figures

Figure 1 - Hallmarks of cancer.....	2
Figure 2 - Schematic representation of glucose metabolic differences between differentiated tissues (left panel), and normal proliferative tissues and cancer cells (right panel)..	4
Figure 3 - Schematic illustration of the cell-microenvironment interactions associated with the carcinogenesis process.....	5
Figure 4 - Schematic overview of cancer cells metabolism..	6
Figure 5 - Schematic illustration of the molecular mechanisms driving the metabolic reprogramming (Warburg effect) in cancer cells.....	7
Figure 6 - Schematic illustration of the PI3K/AKT/mTOR pathway in cancer cells..	8
Figure 7 - Schematic illustration of the MYC pathway in cancer cells.	10
Figure 8 - Metabolic pathway that leads to the accumulation of lactate and their efflux in cancer cells (continuous lines)..	13
Figure 9 - Impact of lactate, present in tumor microenvironments, on tumor-infiltrating immune cells..	14
Figure 10 - Predicted phylogeny of all MCT members and their correspondent endogenous substrates..	16
Figure 11 - Glycolysis and Lactate efflux in cancer cells..	19
Figure 12 - MCT1 constitutive and regulated pathway by cAMP-dependent internalization in RBE4 cells..	23

Figure 13 - Lonidamine structure and its mechanism for MCT1, MCT2, and MCT4 nonspecific inhibition.....	26
Figure 14 - Key stages of image processing used for the quantification of MCT1 expression.	33
Figure 15 - Fluorescence of U2OS cells at different concentrations (5×10^4 , 7×10^4 , 9×10^4 and 11×10^4 cells/mL) after 0 h and 25 h of incubation time.	35
Figure 16 - Analysis of MCT1 expression in gene-edited U2OS cells after 3 h, 6 h and 9 h of incubation with standard medium (DMEM) and medium A (no glucose and no glutamine) by confocal microscopy imaging (A) and fluorescence quantification (B).	37
Figure 17 - Analysis of MCT1 expression in gene-edited U2OS cells after 3 h, 6 h, and 9 h of incubation with medium B (with glutamine and without glucose) by confocal microscopy imaging (A) and fluorescence quantification (B).	39
Figure 18 - Mechanism of lactate-induced glutamine uptake and metabolism in cancer cells....	40
Figure 19 - Proposed inhibition mechanism of cycloheximide (CHX).....	41
Figure 20 - Analysis of MCT1 expression in gene-edited U2OS cells after 6 h and 24 h of incubation with cycloheximide (CHX) by confocal microscopy imaging (A) and fluorescence quantification (B).	42
Figure 21 - Schematic illustration of the lenalidomide mechanism. (A)	43
Figure 22 - Analysis of MCT1 expression in gene-edited U2OS cells after 6 h and 24 h of incubation with lenalidomide by confocal microscopy imaging (A) and data analysis (B).....	44
Figure 23 - Diagram of endocytic trafficking of transporters disrupted by FTY720.....	46
Figure 24 - Analysis of MCT1 expression in gene-edited U2OS cells after 6 h and 24 h of incubation with FTY720 by confocal microscopy imaging (A) and fluorescence quantification (B).....	47

Figure 25 - Schematic representation of PMA activation of Protein Kinase C (PKC).....	49
Figure 26 - Analysis of MCT1 expression in gene-edited U2OS cells after 6 h and 24 h of incubation with PMA by confocal microscopy imaging (A) and fluoresce quantification (B).....	50
Figure 27 - Schematic representation of the Wnt/ β -catenin pathway and their regulation by an activator, LiCl, and an inhibitor, quercetin, of this network.	52
Figure 28 - Analysis of MCT1 expression after 6 h and 24 h of incubation with LiCl by confocal microscopy imaging (A) and fluorescence quantification (B).....	54
Figure 29 - Analysis of MCT1 expression analysis after 6 h and 24 h of incubation with quercetin by confocal microscopy imaging (A) and fluorescence quantification (B).....	55
Figure 30 - Schematic representation of MCT1 or MCT4 and their regulatory proteins (i.e. CAII, CAIX and CD147) with GFP or mCherry tagged with either GFP or mCherry at the C- or N-termini and their nomenclature.....	60
Figure 31 - Image analysis of MCT1 expression after 3 h, 6 h and 9 h of incubation with medium A (no glucose and no glutamine) by confocal microscopy.	84
Figure 32 - Image analysis of MCT1 expression after 3 h, 6 h and 9 h of incubation with medium B (with glutamine and without glucose) by confocal microscopy.....	85
Figure 33 - Image analysis of MCT1 expression after 6 h and 24 h of incubation with cycloheximide by confocal microscopy.....	86
Figure 34 - Image analysis of MCT1 expression after 6 h and 24 h of incubation with lenalidomide by confocal microscopy.....	86
Figure 35 - Image analysis of MCT1 expression after 6 h and 24 h of incubation with FTY720 by confocal microscopy.....	87

Figure 36 - Image analysis of MCT1 expression after 6 h and 24 h of incubation with PMA by confocal microscopy..... 87

Figure 37 - Image analysis of MCT1 expression after 6 h and 24 h of incubation with LiCl by confocal microscopy..... 88

Figure 38 - Image analysis of MCT1 expression after 6 h and 24 h of incubation with quercetin by confocal microscopy..... 88

Index of tables

Table 1 - Compounds and respective stock concentration (mM) used to study MCT1 protein expression.....	30
Table 2 - Compounds and respective final concentration (nM) used to study MCT1 protein expression.....	31
Table 3 - Mean fluorescence signal strength values for the standard and cells treated with different media (medium A and medium B) for 3 h, 6 h or 9 h (n=2).....	38
Table 4 - Mean fluorescence signal strength values for the standard and cells treated with CHX for 6 h or 24 h (n=2).	43
Table 5 - Mean fluorescence signal strength values for the standard and cells treated with lenalidomide for 6 h or 24 h (n=3).	45
Table 6 - Mean fluorescence signal strength values for for the standard and cells treated with FTY720 for 6 h or 24 h (n=3).....	48
Table 7 - Mean fluorescence signal strength values for the standard and cells treated with PMA for 6 h or 24 h (n=2).	51
Table 8 - Mean fluorescence signal strength values for the standard and cells treated with LiCl for 6 h or 24 h (n=2).	54
Table 9 - Mean fluorescence signal strength values for the standard and cells treated with quercetin for 6 h or 24 h (n=2).	56

Lists of abbreviations and acronyms

ACC - Acetyl-CoA carboxylase

ACL/ ACLY - ATP citrate lyase

ACO - Aconitase

AE1 - Anion exchanger 1

Akt - Protein kinase B

AKT - RAC- α serine/threonine-protein kinase

AMPK - AMP-activated protein kinase

AP-2 - Adaptor Protein 2

APC - Adenomatous polyposis coli

ASCT2 - Alanine-serine-cysteine transporter 2

ATP - Adenosine triphosphate

BCL9 - B-cell chronic lymphocytic leukemia/lymphoma 9 protein

CA - Carbonic anhydrase

Ca²⁺ - Calcium ions

CA9/CAIX - Carbonic anhydrase IX

CA12 - Carbonic anhydrase XII

CAII - Carbonic anhydrase II

CaMK - Ca²⁺/Calcineurin-dependent protein phosphatase

cAMP - Cyclic adenosine monophosphate

β -Cat - β -catenin

CAT1 - Cationic amino acid transporter

CAV - Caveolae

CBP - cAMP response element binding protein (CREB)-binding protein

CCV - Clathrin-coated vesicles

CD147 - Cluster of differentiation 147

CFP - Cyan Fluorescent Protein

CHC - α -cyano-4-hydroxycinnamic acid

ChoK - Choline kinase

CHX - Cycloheximide

CK1 α - Casein kinase 1 α

pCMBS - p-chloromercuribenzenesulfonate

CO₂ - Carbon dioxide

CoA - Coenzyme A

COX - Cytochrome oxidase

CPT - Carnitine palmitoyltransferase

CRBN - Cereblon

CRISPR - Clustered Regulatory Interspaced Short Palindromic Repeat

CS - Citrate synthase

DAG - Diacylglycerol

DBDS - 4,4'-dibenzamidostilbene-2,2'-disulphonate

DCs - Dendritic cells

DIDS - 4,4'-di-isothiocyanostilbene-2,2'-disulphonate

Dkk - Dickkopf

DMEM - Dulbecco's Modified Eagle Medium

DMSO - Dimethyl-sulfoxide

DPBS - Dulbecco's Phosphate-Buffered Saline

Dvl - Disheveled

4E-BP1 - Translational-repressor protein PHAS-1

ECM - Extracellular matrix

EE - Early endosomes

eEF2 - Eukaryotic elongation factor 2

EGF - Epidermal growth factor

EGFP - Enhanced green fluorescent protein

EGFR - Epidermal growth factor receptor

eIF-4E - Eukaryotic translation initiation factor 4E

EMMPRIN - Extracellular matrix metalloproteinase inducer

ER - Endoplasmic reticulum

ERK - Extracellular signal-regulated kinase

F1,6BP - Fructose-1,6-bisphosphate

F2,6BP - Fructose-2,6-bisphosphate

F6P - Fructose-6-phosphate

FAD - Flavin Adenine Dinucleotide

FASN - Fatty-acid synthase

FBS - Fetal Bovine Serum

FH - Fumarate hydratase

FLIM-FRET - Fluorescence Lifetime Imaging Microscopy Förster Resonance Energy Transfer

FPP - Farnesyl pyrophosphate

FRET - Fluorescence Resonance Energy Transfer

FTY720 - Fingolimod hydrochloride

Fz - Frizzled

G1P - Glucose-1-phosphate

G6P - Glucose-6-phosphate

G6PD - Glucose-6-phosphate dehydrogenase

GAPDH - Glyceraldehyde-3-phosphate dehydrogenase

GDP - Guanosine diphosphate

GF - Growth factors

GGPP - Geranylgeranyl pyrophosphate

GLS - Glutaminase

GLS1 - Glutaminase 1

Gluc - Glucose

GLUD - Glutamate dehydrogenase

GLUT - Glucose transporter

GLUT1 - Glucose transporter 1

GOT - Glutamic-oxaloacetic transaminase

GPCRs - G-protein-coupled receptors

GRB2 - Growth factor receptor-bound protein 2

GSH - Glutathione

GSK-3 β - Glycogen synthase kinase 3 β

GTP - Guanosine triphosphate

H⁺ - Hydrogen ion/ proton

H₂O - Water

HDACs - Histone deacetylases

HIF - Hypoxia-inducible factor

HIF-1 - Hypoxia-inducible factor 1

HIF-1 α - Hypoxia-inducible factor 1 α

HIF-1 β - Hypoxia-inducible factor 1 β

HIF-2 α - Hypoxia-inducible factor 2 α

HK - Hexokinase

HK2 - Hexokinase 2

HMG-CoA - 3-hydroxy-3-methylglutaryl coenzyme A

HMGCR - 3-hydroxy-3-methylglutaryl-CoA reductase

HRE - Hypoxia response elements

IGF-1R - Related insulin-like growth factor 1 receptor

IKK α - I κ B kinase α

IKK β - I κ B kinase β

IL-8 - Interleukin 8

InsR - Insulin receptor tyrosine kinase

IP3 - Inositol-1,4,5-triphosphate

IRS1 - Insulin receptor substrate 1

Jen1 – *Saccharomyces cerevisiae* lactate transporter

KEAP - Kelch-like ECH-associated protein 1

Lac - Lactate

LAT1 - L-type amino acid transporter 1

LDH1 - Lactate dehydrogenase 1

LDH5 - Lactate dehydrogenase 5

LDHA - Lactate dehydrogenase A

LE - Late endosomes

LEF - Lymphocyte enhancer factor

Lenalidomide - (3S)-3-(4-Amino-1-oxo-1,3-dihydro-2H-isoindol-2-yl)piperidine-2,6-dione

LiCl - Lithium chloride

LKB1 - Liver kinase B1

LND - Lonidamine

LRP5/6 - Lipoprotein receptor-related protein 5/6

LYS - Lysosomes

MACC1 - Metastasis-associated in colon cancer 1

MAPK - Mitogen-activated protein kinases

MCT1 - Monocarboxylate transporter 1

MCT4 - Monocarboxylate transporter 4

MCTs - Monocarboxylate transporters

MDH - Malate dehydrogenase

MDSCs - Myeloid-derived suppressor cells

ME1 - Malic enzyme 1

MEK - MAPK/ERK kinase

Met - Methionine

MPC - Mitochondrial pyruvate carrier

mTFP1 - Mitochondrial Fission Process 1

mTOR - Mammalian target of rapamycin

mTORC1 - mTOR complex 1

mTORC2 - mTOR complex 2

NADH - Nicotinamide Adenine Dinucleotide

NF - Neurofibromin

NFAT - Nuclear factor of activated T cells

NF- κ B - Nuclear factor- κ B

NHE1 - Na⁺/H⁺ exchanger 1

NK - Natural killer

NRF2 - Nuclear factor (erythroid-derived 2)-like 2

O₂ - Dioxygen

OXPPOS - Oxidative phosphorylation

P - Phosphorylation

p53 - Protein 53

p85 - PIK3 regulatory subunit

p110 - PIK3 catalytic subunit

PDGF-R - Platelet-derived growth factor receptors

PDH - Pyruvate dehydrogenase

PDHK1/ PDK1 - Pyruvate dehydrogenase kinase 1

PDK - Pyruvate dehydrogenase kinase

PDK1 - 3'-phosphoinositidedependent kinase 1

PEP - Phosphoenolpyruvate

PFK - Phosphofructokinase

PGC-1 α - Peroxisome proliferator-activated receptor-gamma coactivator 1- α

PGM - Phosphoglycerate mutase

PHD - Prolyhydroxylases

Phe - Phenylalanine

PHGDH - Phosphoglycerate dehydrogenase

PI3K - Phosphatidylinositol 3-kinase

PI3K-AKT-mTOR - Phosphatidylinositol 3-kinase/Protein Kinase-B/mechanistic target of rapamycin

PIP₂ - Phosphatidylinositol 4,5-bisphosphate;

PIP₃ - Phosphatidylinositol 3,4,5-trisphosphate

PKC - Protein kinase C

PKC α - Protein kinase C - α

PKM2 - Pyruvate kinase M2

PL - Phospholipids

PLC - Phospholipase C

PMA - Phorbol 12-myristate 13-acetate

PP2A - Protein phosphatase 2A

PTEN - Phosphatase and tensin homolog

PYG - Pygopus

Pyr - Pyruvate

Raf - Rapidly accelerated fibrosarcoma

RAS - Rat sarcoma

RE - Recycling endosomes

RFP - Red Fluorescent Protein

ROS - Reactive oxygen species

rpS6 - Ribosomal Protein S6

RTK - Receptor tyrosine kinases

S6K - Ribosomal protein S6 kinase

SCD - Stearoyl-CoA desaturase

SCO2 - Synthesis of cytochrome c oxidase 2

SD - Standard deviation

SDH - Succinate dehydrogenase

siRNAs - Small interfering RNAs

SLC - Solute carrier

SLC 16 - Solute carrier 16 family

TAG - Triacylglycerides

TCA - Tricarboxylic acid cycle

TCF - T-cell factor factor

T_{eff} - Effector T cell

TFRC - Transferrin receptor protein

TGF- β 2 - Transforming growth factor-beta 2

T_H17 - T helper 17 cell

T_H23 - T helper 23 cell

TIGAR - TP53-induced glycolysis and apoptosis regulator

TMs - Transmembrane helices

β -TrCP - β -transducin repeat-containing protein

T_{regs} - Regulatory T cells

TSC - Tuberous sclerosis complex

TSC1/2 - Tuberous sclerosis complex 1/2

Ub - Ubiquitin

UTR - Untranslated region

VDAC - Voltage-dependent anion channel

VEGF - Vascular endothelial growth factor

VHL - Von Hippel-Lindau ubiquitin ligase

Wnt - Wingless-type

YFP - Yellow Fluorescent Protein

1. Introduction

1.1. Hallmarks of Cancer

Cancer is a complex disease that represents a vast problem worldwide due to its level of incidence and mortality. In 2018, 18.1 million people worldwide were diagnosed with cancer, and 9.6 million deaths related to cancer were reported (Ferlay et al., 2019), making cancer the second leading cause of death globally (Global Burden of Disease Cancer Collaboration, 2018). Although cancer mortality is decreasing in many countries, the incidence of cancer in the population is rising, causing serious problems even in countries with more advanced health systems (Global Burden of Disease Cancer Collaboration, 2018). According to the Global Cancer Observatory, in Portugal, 58 199 new cases of cancer were registered (Global Cancer observatory, 2018), with an expected increase to 69 565 new cases in 2040 (Serviço Nacional de Saúde, 2018).

Cancer is a genetic disease that is not caused only by a mutation on a single gene but also by dynamic changes in the genome (Hanahan & Weinberg, 2011; Vogelstein & Kinzler, 2004). Several evidences suggest that tumor formation is a multi-set process that reflects successive genetic changes, culminating in a progressive transformation of normal cells into malignant cells (Hanahan & Weinberg, 2011). These alterations are responsible for tumorigenesis and include somatic mutations in three types of genes, namely oncogenes, tumor-suppressor genes and stability genes (Vogelstein & Kinzler, 2004), leading to changes in regulatory processes that control cell proliferation and homeostasis (Hanahan & Weinberg, 2011).

During the development of human tumors, cells progressively acquire specific biological characteristics, known as hallmarks of cancer (**Figure 1**) (Hanahan & Weinberg, 2011). These hallmarks are critical for emerging cancer cells to become tumorigenic and eventually malignant. The hallmarks of cancer constitute an organizing principle for rationalizing the complexities of neoplastic disease and they are characterized by 1) sustaining proliferative signaling, 2) avoiding growth suppressors, 3) resisting cell death (apoptosis), 4) enabling the replicative immortality, 5) inducing angiogenesis, 6) activating invasion and metastasis, 7) reprogramming cellular energetics, 8) preventing their destruction by the immune system, 9) instability and genomic mutations, and 10) tumor-promoting inflammation (Hanahan & Weinberg, 2011).

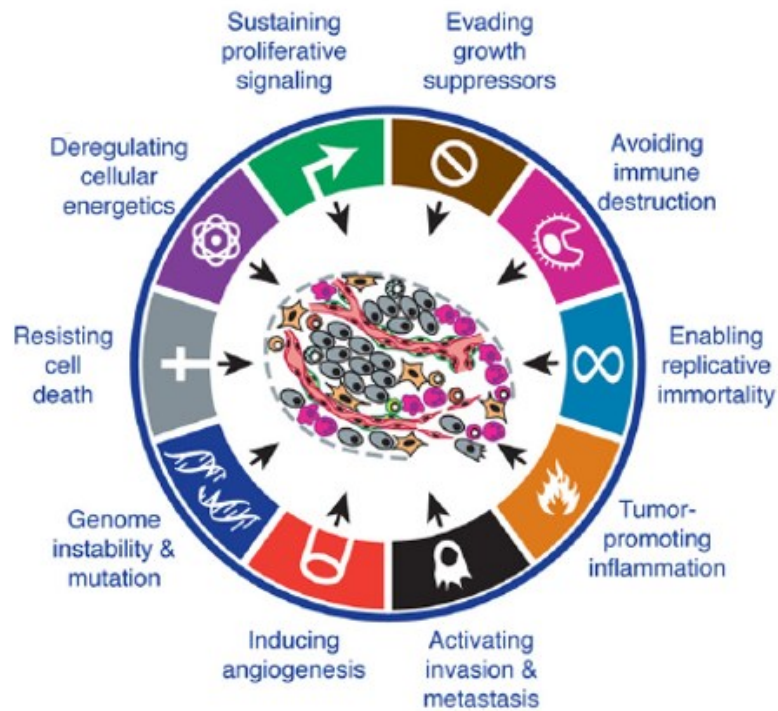


Figure 1 – Hallmarks of cancer. Schematic illustration of the progressive biological abilities acquired by cells during the development of human tumors (adapted from Hanahan and Weinberg 2011).

1.2. Metabolic reprogramming in Oncogenesis

Metabolic reprogramming is a recent term used in cancer metabolism literature to describe conventional metabolic pathways whose activities are enhanced or suppressed in tumor cells in comparison to benign tissues (Deberardinis & Chandel, 2016). Similar to normal cells, the metabolism of cancer cells is essential for survival and proliferation (Vander Heiden et al., 2009). Healthy cells activate different metabolic pathways to produce energy either in the presence or absence of oxygen. In the presence of oxygen, normal cells use glycolysis followed by oxidative phosphorylation (OXPHOS). In the absence of oxygen, healthy cells execute anaerobic glycolysis (Vander Heiden et al., 2009). Unlike normal cells, most cancer cells exhibit high glycolytic metabolism, even in the presence of oxygen, to enhance their malignant phenotype (Kazue et al., 2011).

1.2.1. Warburg effect in cancer cells

In the presence of oxygen, most differentiated tissues are able to metabolize glucose *via* glycolysis followed by complete oxidation of pyruvate to CO₂ (mitochondrial OXPHOS), in order to produce high amounts of ATP molecules (**Figure 2**). 36 ATPs per glucose molecule are produced with minimal production of lactate (Vander Heiden et al., 2009). In the absence of oxygen (anoxia) or under low oxygen conditions (hypoxia), the oxidative phosphorylation is impaired. In order to support mitochondrial OXPHOS, pyruvate is metabolized to lactate by anaerobic glycolysis. Less ATP is produced (2 ATPs per glucose molecule), when compared with oxidative phosphorylation, and a large quantity of lactate is formed *via* lactate fermentation in the cytosol (Vander Heiden et al., 2009).

However, cancer cells are able to convert rapidly the majority of glucose into lactate, even with full mitochondrial activity and in normal oxygen conditions (normoxia) (**Figure 2**) (Vander Heiden et al., 2009; Warburg, 1956). This metabolic reprogramming is known as “Warburg effect” (Deberardinis & Chandel, 2016). This aberrant mechanism of cancer cells is responsible for enhancing glycolysis and allows high production of lactic acid. In fact, cancer cells are able to produce 40 times more lactate than normal cells (Romero-Garcia et al., 2016).

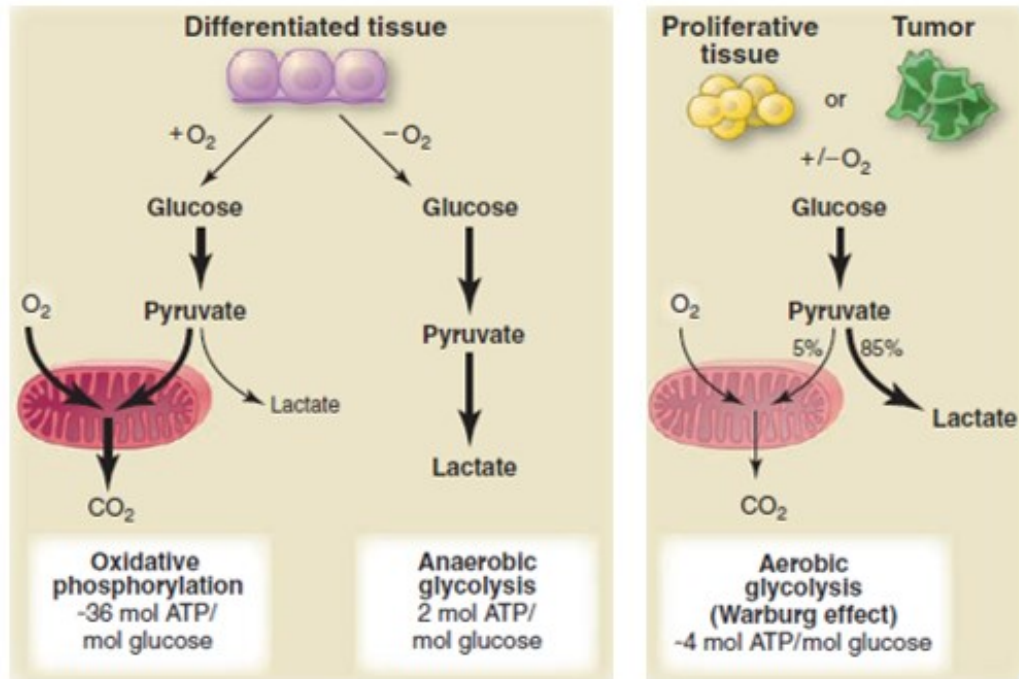


Figure 2 - Schematic representation of glucose metabolic differences between differentiated tissues (left panel), and normal proliferative tissues and cancer cells (right panel). Differentiated tissues determine two different pathways for glucose metabolism. In the presence of oxygen, cells conjugate the glycolytic processes with oxidative phosphorylation. In the absence of oxygen, cells cannot carry out the same process and pyruvate is metabolized to lactate by anaerobic glycolysis. Both normal proliferative and cancer cells convert the majority of glucose into lactate, regardless of whether oxygen is present or not (Warburg effect or aerobic glycolysis), in order to accelerate cell proliferation (Vander Heiden et al., 2009).

The hyper glycolytic phenotype is crucial for the evolutionary sequential development of carcinogenesis from normal tissues to carcinoma *in situ* (Figure 3) (Gatenby & Gillies, 2004). Through persistent aerobic glycolysis, the microenvironment of tumor changes allowing the survival of tumor cells and the death of competing populations, such as normal cells.

The acidification of the tumor microenvironment leads to the degradation of the extracellular matrix, promoting the mobility and invasion of cancer cells. Consequently, cancer cells can access to existing and newly formed blood and lymphatic vascular routes, promoting metastasis and the progression of the carcinoma *in situ* to an invasive state (Gatenby & Gillies, 2004).

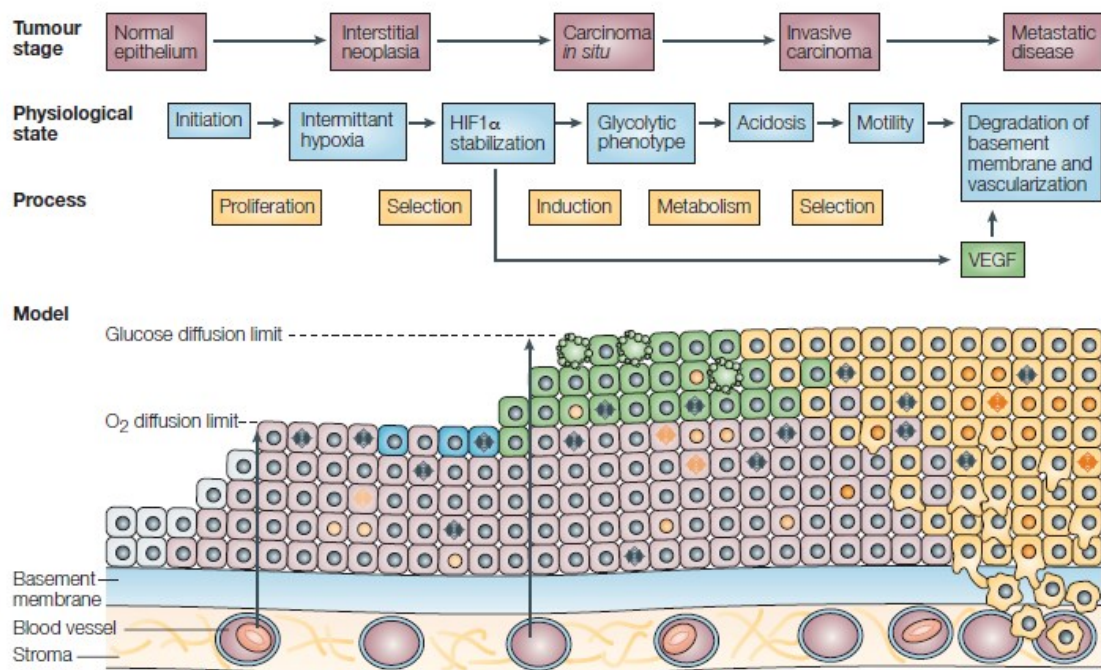


Figure 3 - Schematic illustration of the cell-microenvironment interactions associated with the carcinogenesis process. The carcinogenesis process starts with normal epithelium (grey) and progresses to hyperproliferative cells (pink). After reaching the oxygen diffusion limit, they become hypoxic (blue), which can either lead to cell death (shown with blebbing) or cell survival through glycolytic phenotype adaptation (green). The acidification of the tumor microenvironment induces the extracellular matrix (ECM) degradation which, subsequently, promotes the mobility and invasion of cancer cells (yellow). As cancer progresses, the mutations in cells increase (nuclei shown as light orange for one mutation and dark orange for more mutations) and cells gain access to existing and newly formed blood and lymphatic vascular routes, promoting metastasis and invasiveness (Gatenby & Gillies, 2004).

In cancer cells, malignancy seems to involve the induction of diverse pathways beyond glycolysis, such as glutaminolysis, lipid synthesis, ketone oxidation and serinolysis (**Figure 4**) (Vander Heiden, Cantley, and Thompson 2009). All pathways support core functions like anabolism, catabolism and redox balance, an essential aspect of cancer metabolism (Deberardinis & Chandel, 2016). Cancer cells acquire the ability to generate large amounts of precursors for macromolecule biosynthesis, allowing the accumulation of biomass during cell growth and proliferation (Schulze & Harris, 2012).

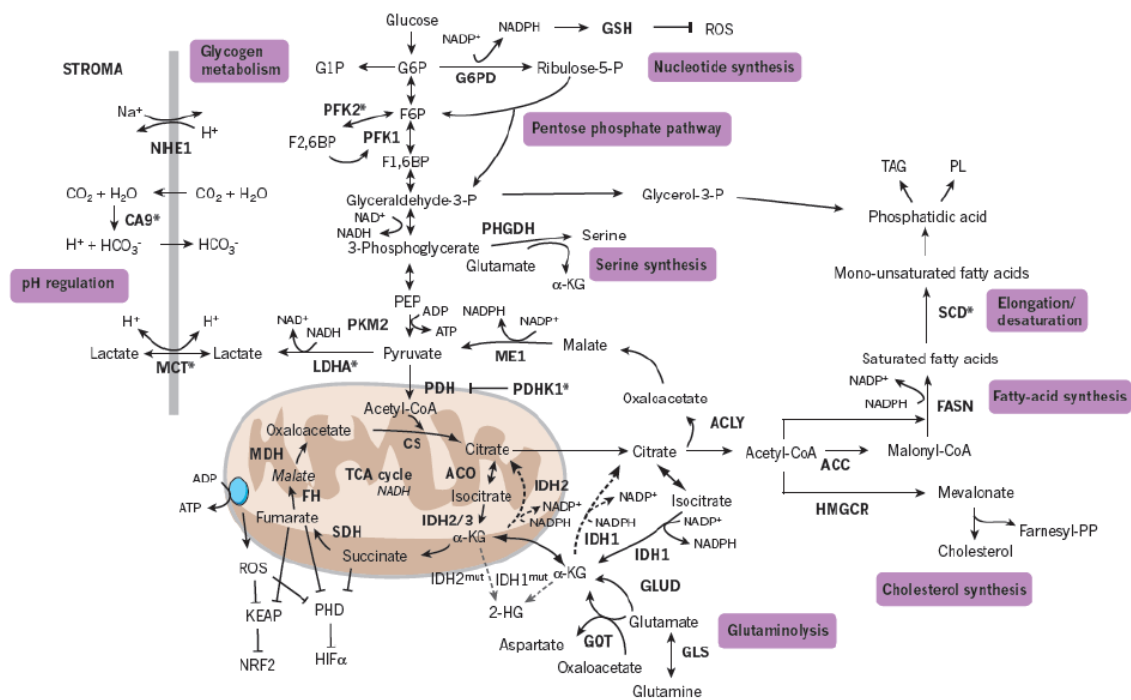


Figure 4 - Schematic overview of cancer cells metabolism. The main metabolic pathways upregulated in cancer cells that contribute to the malignant phenotype and the production of macromolecules in mammalian cells are nucleotide synthesis, the pentose phosphate pathway, serine synthesis, glutaminolysis, cholesterol synthesis, fatty-acid synthesis, and elongation/desaturation. Glycogen synthesis and pH regulation contribute to cellular bioenergetics. The enzymes involved in these pathways are shown in bold, those induced in response to hypoxia are marked with an asterisk. Mutant forms of enzymes that are found in cancer (grey dashed arrow). For abbreviations please see page ix (Schulze & Harris, 2012).

1.2.2. Molecular mechanisms driving Warburg effect

The “Warburg effect” phenomenon also known as “aerobic glycolysis” was described as a metabolic anomaly important for rapid growth and tumor proliferation (Bayley & Devilee, 2012; Kazue et al., 2011; Romero-Garcia et al., 2016). This event is a consequence of complex molecular mechanisms that underlie the metabolic reprogramming of cancer cells (Figure 5) (Kroemer & Pouyssegur, 2008). Several alterations in regulatory processes, such as the deficiency in cellular respiration, oncogenic alterations, and overexpression of glycolytic enzymes and metabolite transporters are characteristic of cancer metabolism (Hirschhaeuser et al., 2011).

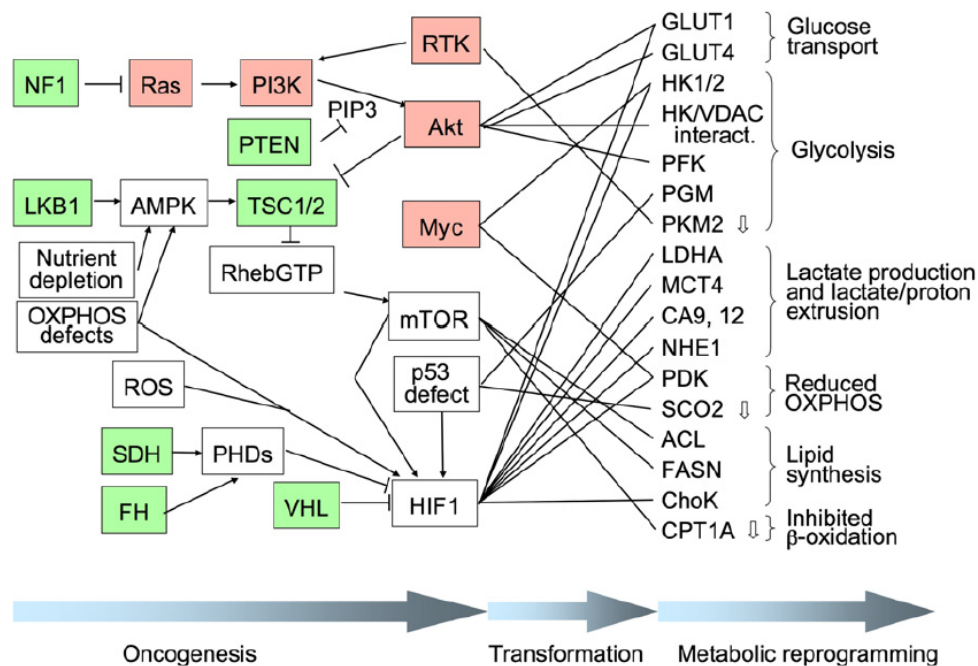


Figure 5 - Schematic illustration of the molecular mechanisms driving the metabolic reprogramming (Warburg effect) in cancer cells. Warburg effect leads to several alterations in regulatory processes, including oncogenic gain-of-function events (pink), loss of tumor suppressors (green) affecting the PI3K/AKT/mTOR/HIF axis, and/or inactivation of the p53 system, well-characterized cancer-associated alterations in metabolism. Note that arrows connecting different proteins do not necessarily indicate direct interactions. For abbreviations please see page ix (Kroemer & Pouyssegur, 2008).

In cancer cells, the proliferative response is also related to the induction of several signaling pathways leading to the aberrant activation of some transcription factors, including hypoxia-inducible factor (HIF) and MYC, and kinases, such as the mammalian target of rapamycin (mTOR) and the phosphatidylinositol 3-kinase (PI3K) (Schulze & Harris, 2012).

The phosphatidylinositol 3-kinase/Protein Kinase-B/mechanistic target of rapamycin (PI3K–AKT–mTOR) pathway is one of the most frequently dysregulated pathways in human malignancies and is implicated in a wide variety of different neoplasms (Dienstmann et al., 2014; Janku et al., 2018; Noorolyai et al., 2019). Activation of this pathway is initiated by receptor tyrosine kinases (RTK) or G-protein–coupled receptors (GPCRs) located at the plasma membrane (Dienstmann et al., 2014), which activate downstream effectors, including mTOR and the protein kinase B (Akt),

thereby promoting the activation of several different other signaling cascades (Figure 6) (Deberardinis & Chandel, 2016; Dienstmann et al., 2014).

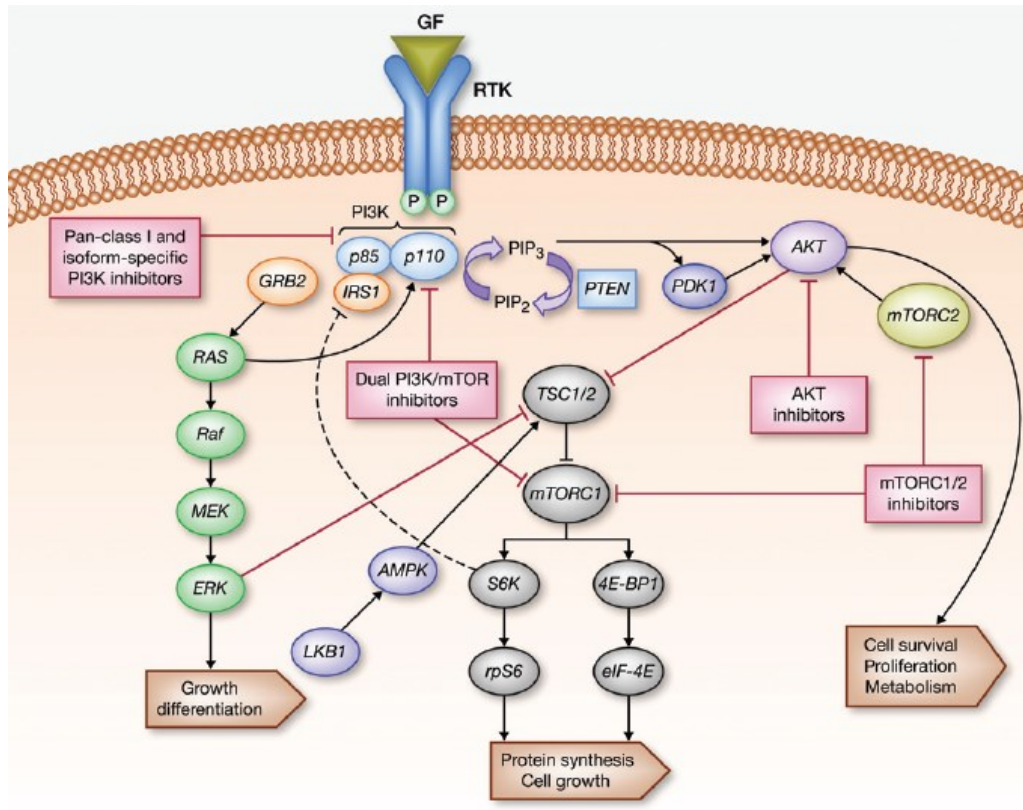


Figure 6 – Schematic illustration of the PI3K/AKT/mTOR pathway in cancer cells. Activation of this pathway initiated by receptor tyrosine kinases (RTK) at the plasma membrane, which leads to the activation of downstream effectors (PI3K, AKT, PDK1, mTORC1, and mTORC2) and inhibition of some regulators (PTEN, TSC complex). Interaction with RAS and AMPK pathways is also displayed. PI3K/AKT/mTOR pathway can also be triggered without the interference of RTK stimulus. For abbreviations please see page ix (Dienstmann et al., 2014).

In cancer cells, the PI3K–AKT–mTOR pathway can still be stimulated by diverse other mechanisms including growth factors, such as the insulin receptor tyrosine kinase (InsR), the related insulin-like growth factor 1 receptor (IGF-1R), the epidermal growth factor (EGF), and the platelet-derived growth factor receptors (PDGF-R). Abnormalities of AKT and RAS, and epigenetic modulators could also cause activation of this pathway (Noorolyai et al., 2019). PI3K-AKT-mTOR network can also be triggered by somatic mutations in specific elements of the signaling pathway,

involving p110a, p110b, p85a, p85b isoform of the PI3K sequence (PIK3CA), PIK3R1, TSC1, TSC2, LKB, and other oncogenes or tumor suppressor genes, such as phosphatase and tensin homolog (*PTE*M) (Dienstmann et al., 2014; Janku et al., 2018; Noorolyai et al., 2019). These mutations lead to the activation of the PI3K-AKT-mTOR network in cancer cells with minimal dependence on extrinsic stimulation by growth factors (Deberardinis & Chandel, 2016).

The PI3K-AKT-mTOR pathway is key for the regulation of main intracellular processes, such as metabolism, motility, growth, proliferation, and differentiation that support the survival, expansion, and dissemination of cancer cells (Dienstmann et al., 2014; Janku et al., 2018).

The MYC pathway is also dysregulated in human cancer cells induced by chromosomal translocations, gene amplification, single-nucleotide polymorphisms and alteration on transcriptional control downstream of β -catenin (Dang et al., 2008; Deberardinis & Chandel, 2016). The activation of this pathway leads to the induction of several genes involved in glycolysis, fatty acid synthesis, glutaminolysis, serine metabolism, and mitochondrial metabolism to support all mechanisms necessary for the proliferation of cancer cells (Deberardinis & Chandel, 2016). Lactate dehydrogenase A (LDHA), glyceraldehyde-3-phosphate dehydrogenase (GAPDH), pyruvate dehydrogenase kinase 1 (PDK1), hexokinase 2 (HK2), glucose transporter 1 (GLUT1), and transferrin receptor protein (TFRC), are targets of the proto-oncogene *MYC* (Dang et al., 2008). When overexpressed, MYC cooperate with HIF-1, changing the metabolism of cells to favor the Warburg effect and the proliferative phenotype of hypoxic cancer cells (**Figure 7**) (Dang et al., 2008; Deberardinis & Chandel, 2016; Schulze & Harris, 2012).

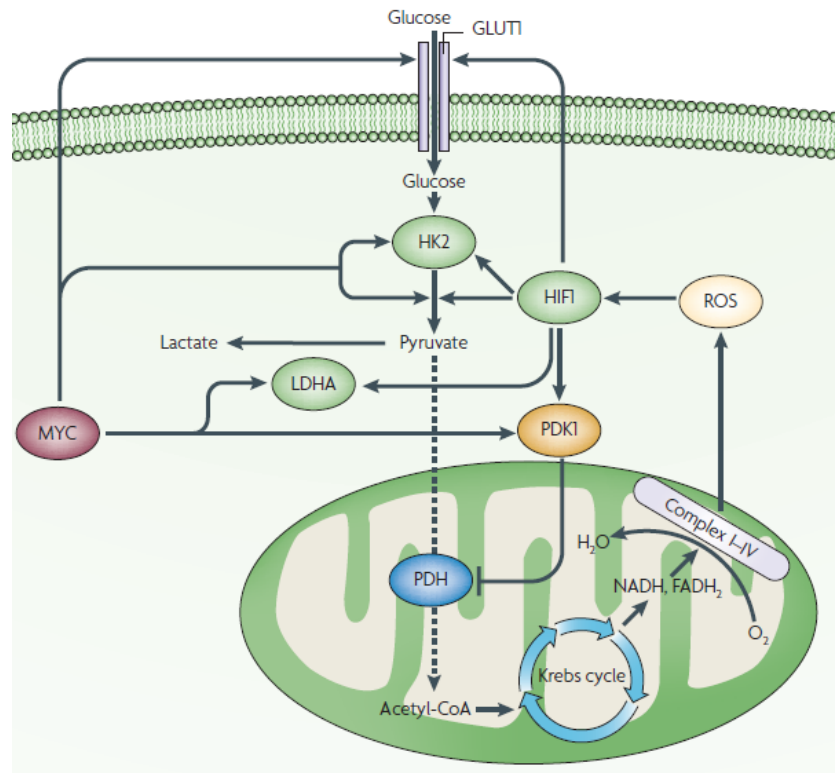


Figure 7 - Schematic illustration of the MYC pathway in cancer cells. Glucose is transported across the plasma membrane by glucose transporter 1 (GLUT1). MYC induces activation of hexokinase 2 (HK2) and pyruvate dehydrogenase kinase 1 (PDK1), increasing lactate levels. MYC independently activates the GLUT1 and lactate dehydrogenase A (LDHA), which further contributes to the Warburg effect and the proliferative phenotype of hypoxic cancer cells. For abbreviations please see page ix (Dang et al., 2008).

The tumor suppressor protein p53 is the most important tumor suppressor in the cell once acts as a genome guardian playing a central role in the cell cycle (Joerger & Fersht, 2016). Upon cellular stress signals, such as DNA damage or oncogenic stress, p53 is activated promoting cell growth arrest, DNA repair, senescence, and cell death, as well as modulating autophagy and cancer metabolism (Zhou et al., 2019). Loss of function of tumor suppressor gene p53, most frequently in human cancers, can regulate cellular metabolism by controlling metabolic genes and increasing the glycolytic flux on cancer cells (Deberardinis & Chandel, 2016; Vander Heiden et al., 2009). In cancer, p53 induces the TP53-induced glycolysis and apoptosis regulator (TIGAR) expression, inhibiting phosphofructokinase and redirecting the glucose toward the pentose phosphate shunt and NADPH production. This adaptative response of cancer cells protects them from oxidative stress (Vander Heiden et al., 2009).

Another tumor suppressor gene involved in the metabolic switch from oxidative phosphorylation towards altered glycolysis of tumor cells is the hypoxia-inducible factor 1 (HIF-1), which is widely associated with cancer progression (Lu et al., 2002). In mammals, HIF-1 is composed by two subunits, hypoxia-inducible factor 1 α (HIF-1 α) and hypoxia-inducible factor 1 β (HIF-1 β) (G. L. Wang et al., 1995). However, it is the expression of HIF-1 α expression that is highly related to most primary and metastatic tumors (Zhong et al., 1999).

HIF-1 α is a major regulator of adaptation to hypoxic stress by regulating genes that encode for proteins involved in glycolysis, glutaminolysis and serinolysis, the three main sources of energy production (Deberardinis et al., 2007; Mazurek et al., 2001a, 2001b). HIF-1 α leads to an enhanced flux of glycolysis in tumor cells and consequently to the accumulation of lactate (Pinheiro et al., 2012). Curiously, HIF-1 α is stabilized by the products of glycolysis, such as lactate and pyruvate, resulting in the accumulation of this master transcription factor (Lu et al., 2002). HIF-1 α also interacts with a few membrane transporters, including GLUT1, to make sure that cells receive an adequate quantity of glucose, and monocarboxylate transporter 4 (MCT4), responsible for the renowned hyper-glycolytic phenotype by secretion and accumulation of lactate extracellularly (Hirschhaeuser et al., 2011; Pinheiro et al., 2012). LDHA is a glycolytic enzyme and also a target for HIF-1 α that allows a continued glycolytic metabolism and production of ATP (Hirschhaeuser et al., 2011; Pinheiro et al., 2012).

Like MYC, HIF-1 α also mediates the induction of other survival genes, including angiogenic growth factors (for example, VEGF), hexokinase II59, and hematopoietic factors (for example, transferrin and erythropoietin) (Gatenby & Gillies, 2004). In addition, when carbonic anhydrase IX (CAIX) and monocarboxylate transporter 1 (MCT1) are upregulated by HIF-1 α , it provides the well-established acid-resistant phenotype (Hirschhaeuser et al., 2011; Pinheiro et al., 2012). HIF1 α can also be stabilized by a range of factors, including cyclooxygenase-2 activity, insulin-like growth factor 2, ERBB2, epidermal growth factor receptor (EGFR), PI3K, heat-shock protein, microtubule status, thioredoxin and histone deacetylase (Gatenby & Gillies, 2004).

1.3. Significance of lactate transport in cancer

In cancer cells, the Warburg effect is responsible for the accumulation of extracellular lactate and, consequently, for the reduction of the pH values to 6,0–6,5, crucial characteristics for the

survival of these cells (Pineiro et al., 2012; Romero-Garcia et al., 2016). The decrease of pH is regulated by different systems at the plasma membrane, namely monocarboxylate transporters (MCTs), Na⁺/H⁺ exchanger 1 (NHE1), CAIX, and anion exchanger 1 (AE1) (Pineiro et al., 2012). Some MCTs transport lactate to the extracellular medium while transport H⁺, performing a double role in the adaptation to hypoxia (Pineiro et al., 2012; Romero-Garcia et al., 2016). Besides the contribution of MCTs to acid-resistance, they are responsible for the hyper-glycolytic phenotype of cancer cells due to the “lactate shuttle” (Romero-Garcia et al., 2016). The symbiotic metabolism between surrounding fibroblasts and non proliferative cancer cells supply proliferative cancer cells with high-energy nutrients, such as lactate and pyruvate (Bovenzi et al., 2015). The lactate shuttle is essential during early tumorigenesis and later during cancer cell metastasis, when blood supply is largely absent (Lisanti et al., 2013)

The accumulation of high levels of lactate in different primary tumor entities was described as key to growth and metastasis of cancer cells (Fischer et al., 2007), and related with the reduction of overall survival of patients (Walenta et al., 1997). The presence of lactate in tumor cells enables them to develop some capacities, including the ability to escape the immunity system, the ability to promote the migration of cells and cell clusters, to establish chemo- and radioresistance, and to form new vessels (**Figure 8**) (Hirschhaeuser et al., 2011; Pineiro et al., 2012; Romero-Garcia et al., 2016).

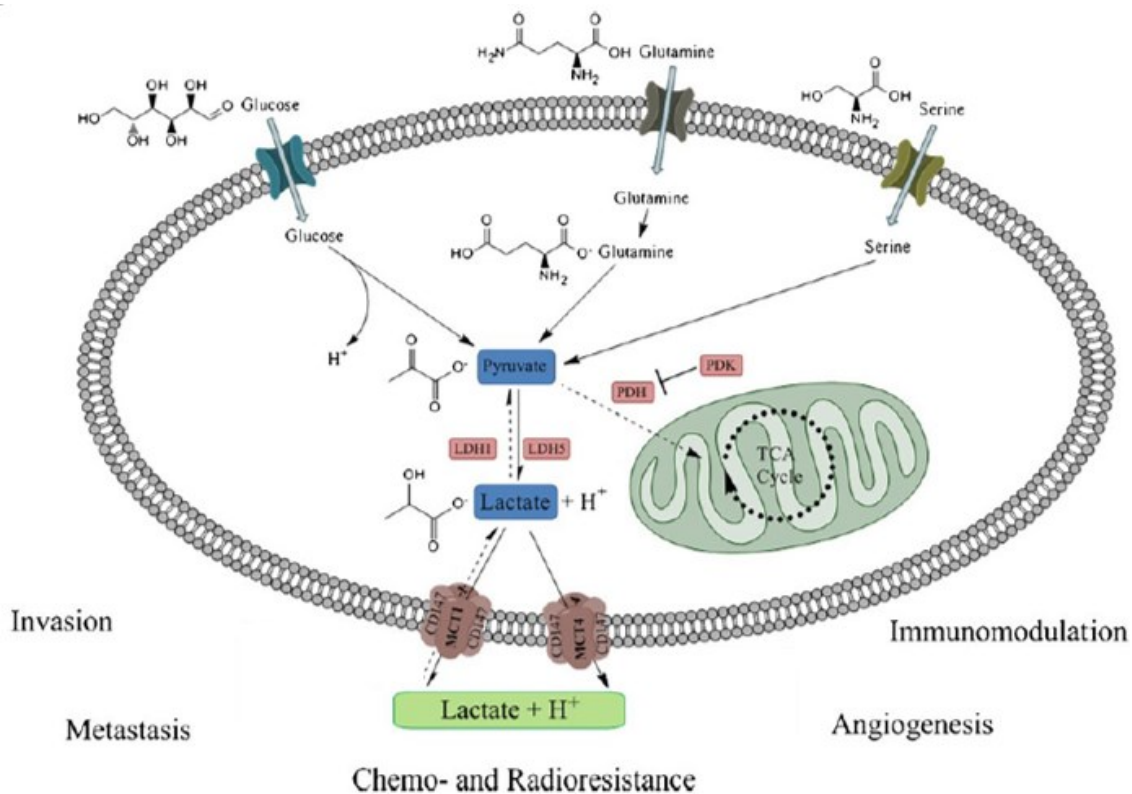


Figure 8 – Metabolic pathway that leads to the accumulation of lactate and their efflux in cancer cells (continuous lines). The accumulation of lactate in tumor cells leads to the development of some capacities including invasion, metastasis, immunomodulation, angiogenesis, and chemo- and radioresistance. Discontinuous lines represent lactate uptake and flow inside oxidative cancer cells (adapted from Pinheiro et al. 2012).

Lactate also plays an important immunoregulatory role in cancer (Romero-Garcia et al., 2016). The inability of the immune system to adequately eliminate aberrant cells is associated with tumor development (Hirschhaeuser et al., 2011). This feature is due to the capacity of cancer cells to upregulate inhibitory molecules, to produce immunosuppressive cytokines, and to downregulate costimulatory molecules (Singer et al., 2011).

The tumor microenvironment is responsible for the alteration of myeloid cells into pathological myeloid-derived suppressor cells (MDSCs), potent immunosuppressive cells (**Figure 9**) (Gabrilovich et al., 2012; Husain et al., 2013). Myeloid cell differentiation does not follow the standard but an alternative pathway that favors the differentiation into pathological MDSCs (Gabrilovich et al., 2012). MDSCs play a key role in both innate and adaptive immunity regulation by inhibiting T cell activation, suppressing natural killer (NK) cell cytotoxicity, supporting the

development of regulatory T cells (T_{reg}) and inhibiting the maturation of dendritic cells (DCs) (Husain et al., 2013).

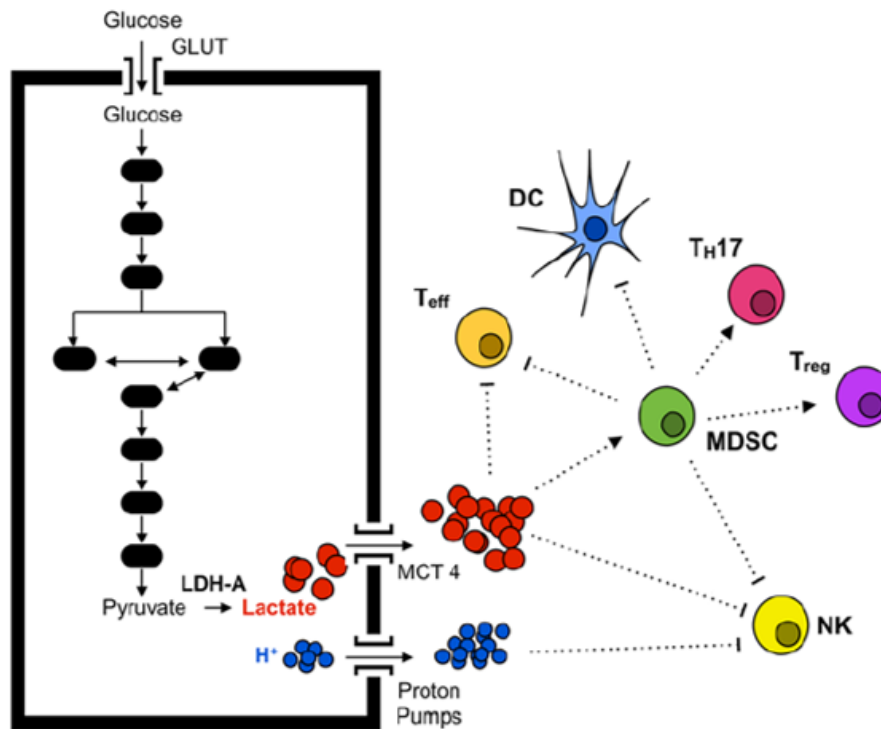


Figure 9 – Impact of lactate, present in tumor microenvironments, on tumor-infiltrating immune cells. Warburg effect is responsible for the accumulation of extracellular lactate and acidification of the tumor microenvironment, crucial for the survival of cancer cells. The increase of lactate secretion results in the accumulation of Myeloid-derived suppressor cells (MDSCs). MDSCs cells inhibit the activity of Natural killer (NK) cells and T lymphocytes, and the maturation of Dendritic cells (DCs). Furthermore, the low pH simultaneously with the high concentration of lactate can have an impact on antitumor immune response, in particular, in the reduction of cytotoxic T cells and in the inactivation of cytokine release from DCs. For abbreviations please see page ix (adapted from Husain, Seth, and Sukhatme 2013).

It has been described that neutrophils, macrophages and DCs are present in tumor microenvironments and, at some point, tumor-infiltrating lymphocytes appear to occur by activation of IL-23/IL17 pathway (Hirschhaeuser et al., 2011; Romero-Garcia et al., 2016). The activation of the IL-23/IL-17 pathway leads to the development of local inflammatory responses toward a

T_H17/T_H23 immune response, favoring the incidence and growth of tumors (Romero-Garcia et al., 2016).

The immune cells use glycolysis as their main energy source *via* glycolysis and produce lactate (Hirschhaeuser et al., 2011; Romero-Garcia et al., 2016). The release of lactate is dependent on the intracellular/extracellular concentration ratio of this molecule (Hirschhaeuser et al., 2011). With the release of high amounts of lactate to the extracellular medium by cancer cells, the immune cells cannot liberate lactate and will have their metabolism disturbed and their functions inhibited (Hirschhaeuser et al., 2011; Romero-Garcia et al., 2016).

The combination of low pH extracellularly and the high intracellular concentration of lactate can also contribute to the reduction of the immune response in the tumor microenvironment, in particular, the decrease of cytotoxic T cells (Fischer et al., 2007; Husain et al., 2013) and NK cells activity, the inhibition of monocytes differentiation into DCs, and the inactivation of cytokine release from DCs (**Figure 9**) (Gottfried et al., 2006; Puig-Kroger et al., 2003). However, T cell suppression is reversible and can be restored by buffering the pH, at physiological values (Fischer et al., 2007; Singer et al., 2011).

Lactate concentrations have been also associated with metastases of diverse cancer cell lines, instead of single-cell migration (Brizel et al., 2001; Goetze et al., 2011; Schwickert et al., 1995; Walenta et al., 1997, 2000). This happens because lactate induces a change in signalization of β -integrins, proteins associated with cell-extracellular matrix adhesion, and activating growth factor-beta 2 (TGF- β 2) (Baumann et al., 2009). Tumor-associated fibroblasts secrete cytokines to remodel the extracellular matrix and provide an environment that promotes the growth and motility of cancer cells (Stern, 2009; Walenta & Mueller-klieser, 2004). Biological activity of lactic acid is also positively related to radioresistance (Sattler et al., 2010) which maybe correlated with its antioxidant properties that can induce or enhance resistance to radiation of anticancer therapies (Groussard et al., 2000). In addition, lactate activates the VEGF/VEGFR2 signaling pathway, in endothelial cells (Beckert et al., 2006; Hunt et al., 2007; Porporato et al., 2012), and stimulates interleukin 8 (IL-8) and, consequently, angiogenesis (Végran et al., 2011).

Some MCTs are involved in the efflux of lactate from cancer cells and, subsequently, are related to the malignant behavior and aggressiveness of cancer cells (Hirschhaeuser et al., 2011; Pinheiro et al., 2012). However, lactate has been recently described as a fundamental key metabolic intermediate in a symbiotic process between glycolytic and oxidative cancer cells

(Sonveaux et al., 2008). The lactate produced by central and hypoxic glycolytic cancer cells is released and consumed by peripheral and oxygenated oxidative cancer cells (Sonveaux et al., 2008). Therefore, lactate can be used as a fuel alternative for oxidative tumor cells, leading to human tumor formation and cancer progression, and to promote survival of hypoxic tumor cells located far from the newly formed blood vessels (Sonveaux et al., 2008).

1.4. Monocarboxylate transporter (MCTs) family

MCTs are present in a wide variety of tissues and are involved in the transport of monocarboxylates such as lactate, pyruvate, ketone bodies (acetoacetate and β -hydroxybutyrate), thyroid hormones, carnitine, aromatic amino acids, and creatine, across the plasma membrane. This makes MCTs essential for the regulation of fundamental cellular processes such as glycolysis, fatty acid homeostasis, as well as other key metabolic pathways (Figure 10) (Fisel et al., 2018; Halestrap, 2012, 2013).

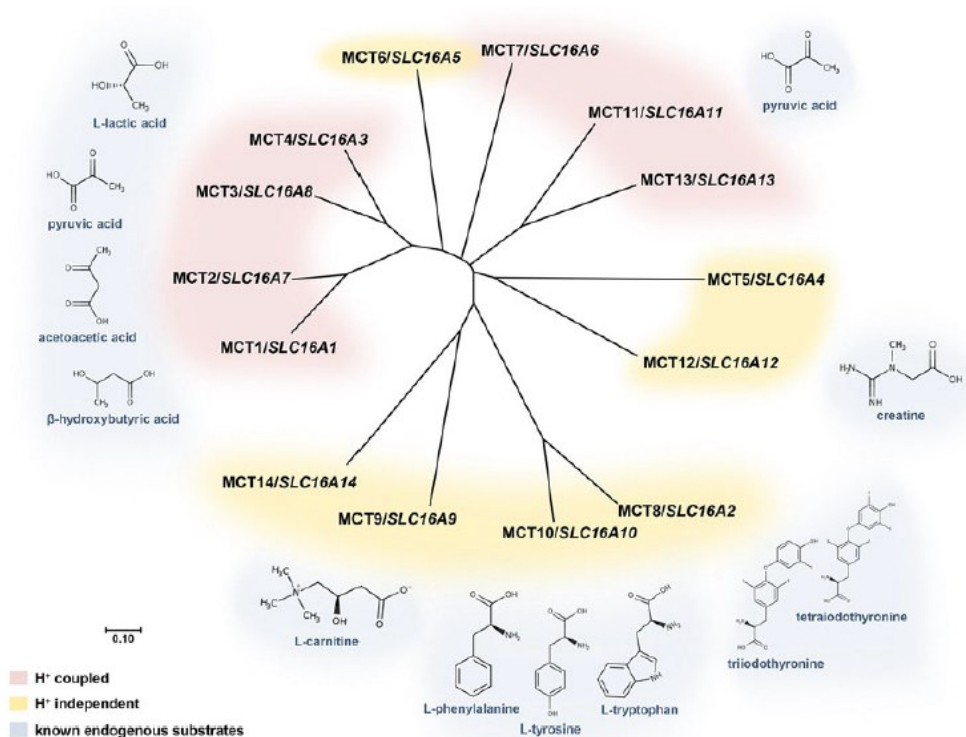


Figure 10 – Predicted phylogeny of all MCT members and their correspondent endogenous substrates. Transporters mediating H⁺ coupled (red) or H⁺ independent (yellow) substrate transport for each MCT are elucidated. In blue are identified the endogenous substrates known for each

transporter. For MCT5–7, MCT13, and MCT14, no substrates have been recognized in humans. For each transporter, both MCT and SLC16 numbers are given. MCT isoform number and SLC16 nomenclature are not the same. SLC16 nomenclature is related to the order in which each cDNA sequence was determined and characterized. The bar indicates the number of substitutions per residue, where 0.1 corresponds to the distance of 10 substitutions per 100 residues (Fisel et al., 2018).

MCTs belong to the solute carrier (SLC) transporter superfamily (Fisel et al., 2018) and are encoded by the *SLC16* gene family which contains conserved sequence motifs in all the 14 human MCT homologs members (Fisel et al., 2018; Halestrap, 2012; Halestrap & Meredith, 2004). Due to the high level of conservation between the different transporters, the MCTs are characterized by the presence of 12 transmembrane helices (TMs) with intracellular N- and C-terminus, and a large cytosolic loop between TM6 and TM7, where the most conserved regions correspond to the TMs domains and the most variable regions match the loops and C-terminus (Halestrap, 2012). In addition, TM1 and TM5 motifs have been characterized as responsible for molecular dynamics and conformational changes of MCTs (Jones & Morris, 2016). The different functional role of these transporters is related to the differences in amino acid sequence as a result of evolutionary divergence (Pinheiro et al., 2012), leading to the formation of different isoforms. Only four of them, MCTs 1–4, have been confirmed to function as proton-symporters of metabolic monocarboxylic acids in mammals (human, mouse, and rat), each one with a distinct substrate and affinities (Halestrap, 2012; Pinheiro et al., 2012) and a high degree of variability among tissue expression levels (Jones & Morris, 2016). In addition, MCT1 and MCT4 have been described as an important key metabolic mechanisms in cancer cells (Wilde et al., 2017). Specifically, MCT1 is overexpressed in OXPHOS cancer cells (elevated lactate influx), while MCT4 is overexpressed in glycolytic cancer cells (elevated lactate efflux) (Doherty & Cleveland, 2013; Semenza, 2008; Wilde et al., 2017).

The role of MCTs in cell homeostasis is extensively described in some tissues (Pinheiro et al., 2012). However, more studies are needed to understand the role of these transporters, as it has been described that many of these MCT isoforms are upregulated in tumor tissues, making them attractive targets and biomarkers for a wide variety of cancers (Jones & Morris, 2016).

1.4.1. Monocarboxylate transporter 1 (MCT1)

MCT1/SLC16A1 is a nonspecific MCT with low/moderate substrate specificity when compared to other MCT family members (Fisel et al., 2018; Pinheiro et al., 2012). MCT1 is a symporter that can uptake or efflux a wider range of monocarboxylates substrates through the plasma membrane (Bröer et al., 1998; Halestrap & Price, 1999), according to the predominant intracellular and extracellular substrate concentrations and the transmembrane pH gradient (Fisel et al., 2018; Halestrap, 2012). MCT1, encoded by the gene *SLC16A1* (Halestrap, 2013), can be found in almost all cell types of the human body, however, it is expressed at low levels in some tissues like β -cells (Pullen et al., 2010; Romero-Garcia et al., 2016). MCT1 carries out its function mostly in heart, skeletal muscle, intestine, liver, kidney, and metastatic cancer cell lines (Halestrap & Price, 1999; Romero-Garcia et al., 2016). This transporter has a high affinity and it is a stereoselective transporter for L-lactate (Bröer et al., 1998; Halestrap, 2012), but not for D-lactate (Halestrap, 2012). MCT1 can also transport pyruvate, short-chain fatty acids (acetate and butyrate), benzoate, propionate, ketone bodies (D, L- β -hydroxybutyrate, and acetoacetate), branched-chain keto-acids (α -ketoisocaproate) formed from transamination of amino acids, and branched oxo-acids with a greater affinity than lactate (Bröer et al., 1998; Cuff et al., 2002; Halestrap, 2012; Halestrap & Meredith, 2004; Kido et al., 2000; Romero-Garcia et al., 2016).

1.4.1.1. Regulation of Monocarboxylate transporter 1 (MCT1)

In cancer cells, MCTs can be subjected to short term, transcriptional or post-transcriptional regulation. In short terms regulation, the activity of MCT1 is modulated by carbonic anhydrase (CA) II and IX (Noor et al., 2018). Both CAs are involved in the interconversion of carbon dioxide and water to bicarbonate and protons, and are responsible for supplying proton-coupled MCT1 (**Figure 11**) (Jones & Morris, 2016; Noor et al., 2018). CAs modulate and enhance MCT1 activity through a “proton-collecting antenna” without participating in the catalytic reaction (Noor et al., 2018). The regulatory noncovalent protein-protein interaction happens between histidine 64 of cytosolic carbonic anhydrase II (CAII) and an intracellular glutamic acid moiety present in MCT1 C-terminus (Noor et al., 2015).

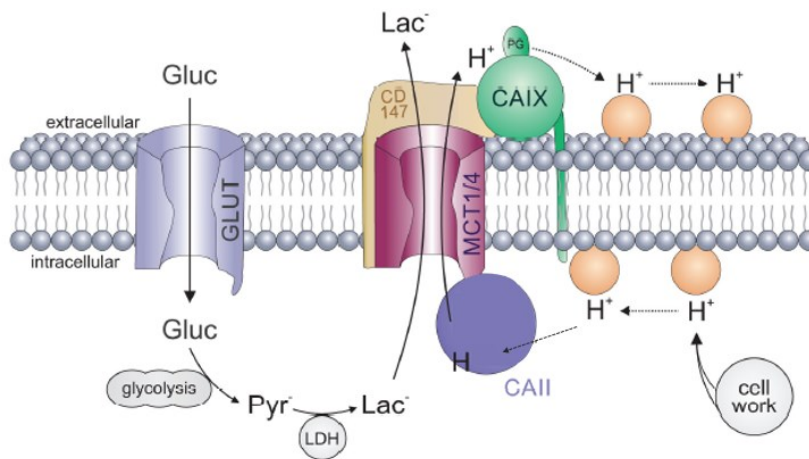


Figure 11 – Glycolysis and Lactate efflux in cancer cells. Carbonic anhydrase II (CAII) is present in intracellular cells and binds to the C-terminal tail of MCT1/4. In hypoxic conditions, carbonic anhydrase IX (CAIX) also binds to MCT1/4 *via* their chaperon CD147 and is responsible for supplying proton-coupled MCT1/4, modulating and enhancing their activity, without participating in the catalytic reaction. Therefore, CAIX acts as a proton antenna, and it is an extremely important mechanism since the diffusion of H⁺ is slow. Firstly, glucose enters the cell through the glucose transporter (GLUT) by facilitated diffusion and it is converted into lactate by anaerobic glycolysis. At the same time, protons are produced by the hydrolysis of ATP. To allow fast extrusion of protons and lactate from the cell, MCTs extract simultaneously both. For abbreviations please see page ix (adapted from Noor et al. 2018).

Regulation and trafficking of MCT1, and also MCT2, MCT3 and MCT4, have been associated with several ancillary proteins (Jones & Morris, 2016). Firstly, a highly glycosylated type I glycoprotein accessory, CD147 (also known as OX-47, HT7, and basigin) (Kirk et al., 2000) has been identified as the most important chaperone protein in the regulation and activity of MCTs and its trafficking to the plasma membrane (Gallagher et al., 2007; Pinheiro, Albergaria, et al., 2010; Pinheiro, Longatto-filho, et al., 2009; Pinheiro, Longatto-Filho, et al., 2009; Pinheiro, Reis, et al., 2010; Wilson et al., 2005). In fact, in the absence of this chaperone, MCT1 cannot appear in the plasma membrane and is accumulated in the Golgi apparatus (Halestrap, 2013). The active form of MCT1 is composed of two CD147 proteins at the cell membrane, which can recruit additional proteins such as cytochrome oxidase (COX) to form supercomplexes (Payen et al., 2019).

Interestingly, CD147 co-expression is essential for proper plasma membrane expression and activity of MCT1 (Jones & Morris, 2016), and CD147 expression is also dependent on MCT1 (Deora et al., 2005). It is possible that CD147 expression may enhance the malignant phenotype of MCT1 (Pineiro et al., 2012). However, the association between both proteins is different among distinct tumors, which might indicate that the regulation of CD147 and MCT1 proteins are different among diverse cancers (Pineiro, Reis, et al., 2010).

CD147, also identified as an extracellular matrix metalloproteinase inducer (EMMPRN), is upregulated in a variety of human cancers and can produce matrix metalloproteinases and vascular endothelial growth factor (VEGF), that may interact with other molecules, such as CD98 (an amino acid transporter), CD44, syndecan-1, γ -secretase, shrew-1, and β -integrin (Gallagher et al., 2009). The interactions can influence diverse cellular networks, suggesting that CD147 may represent a key player in tumor cell invasion and metastasis (Riethdorf et al., 2006).

CD147 may form a “sensory complex” with CD98 and β -integrin to regulate cell physiology and function (Gallagher et al., 2009). It is also capable of interacting with β -integrin in some processes during cell migration, including metastasis and wound healing (Gallagher et al., 2009). The overexpression of CD147 leads to an increase of metastatic potential in some tumors, while the silencing of CD147 in hepatic and ovarian cancer, and lymphoma cell lines leads to a decrease of cell migration (Gallagher et al., 2009).

In tumors, the elevated concentration of extracellular lactate leads to the upregulation of two extracellular matrix proteins responsible for enhancing migration, namely hyaluronan, and type I collagen (Gallagher et al., 2009). CD147 is allowed to stimulate EGFR-Ras-ERK signaling depending on the binding of hyaluronan with CD44 (Grass et al., 2013). The hyaluronan-CD44 interaction contributes to the regulation of MCT1 localization and function (Slomiany et al., 2009) as well as the co-expression of either CD147 or CD44 in the plasma membrane (Pineiro et al., 2012).

CD147 promotes the aggregation of signaling complexes containing CD147, CD44, and EGFR (Grass et al., 2013). It has been described that oncogenic Ras regulates CD147 expression, hyaluronan synthesis, and formation of CD147-CD44-EGFR complexes, creating a positive feedback loop capable of amplifying tumor invasion (Grass et al., 2013). Recently, the MCT chaperone, CD44, has been described in diverse processes related to cancer, namely in cancer progression including cell growth control, matrix adhesion, migration, invasion, cell survival, and chemoresistance (Marhaba & Zoller, 2004; Slomiany et al., 2009).

In skeletal muscle, MCT1 can be transcriptionally regulated by the nuclear factor of activated T cells (NFAT) (Halestrap & Wilson, 2012). NFAT acts by binding to the *MCT1* gene promoter region in consensus NFAT binding sequences, and it is essential to the activation and proliferation of T lymphocytes. The activation process is accompanied by higher levels of MCT1 expression to sustain the extremely high rates of T-cells glycolysis (Halestrap & Wilson, 2012).

During physical exercise, the upregulation of MCT1 can be due to the increased Ca^{2+} /calcineurin-dependent protein phosphatase activity (CaMK), which also leads to the dephosphorylation of the transcription factor NFAT (Halestrap, 2013; Jones & Morris, 2016). In addition, physical exercise leads to the overexpression of MCT1 through a presumed mechanism implicating the activation of the AMP-activated protein kinase (AMPK) and p38 mitogen-activated protein kinases (MAPK) pathway, that triggers the direct activation of downstream regulatory factors, such as peroxisome proliferator-activated receptor-gamma coactivator 1- α (PGC-1 α) (Halestrap & Wilson, 2012; Takimoto et al., 2013).

In cancer cells, MCT1 can be regulated by transcription factors, including p53 and MYC (Halestrap, 2013). Under hypoxic conditions, p53-deficient tumors promote MCT1 expression, allowing the tumor cells to adapt to the metabolic needs by exporting the lactate produced by elevated glycolytic flux (Boidot, 2012) and acquiring therapeutic resistance (Doherty & Cleveland, 2013). Curiously, MYC is enabled to bind the *MCT1* promoter in both normal and cancer cell lines and, as a result, MCT1 inhibition can be a successful strategy to neutralize MYC-driven malignancies (Doherty & Cleveland, 2013).

MCT1 regulation by hypoxic conditions seems to be controversial (Miranda-Gonçalves et al. 2016). Some results indicate that MCT4 expression, but not MCT1, is activated by hypoxia and mediated by HIF-1 α , since MCT4 has hypoxia response elements (HRE) where HIF-1 α can bind (Halestrap, 2013; Ullah et al., 2006). Other studies report that the upregulation of MCT1 expression is mediated by hypoxia in order to support the glycolytic phenotype of cancer cells (Heredia and Wood 2010; Miranda-Gonçalves et al. 2016).

Recently, it has been suggested that HIF-1 α and hypoxia-inducible factor 2 α (HIF-2 α), although have dissimilar roles in different types and stages of the tumor, can be both responsible for the progression of the tumor by regulating targets genes that both have in common (Keith et al., 2011).

Extracellularly acidosis can trigger HIF-2 and consequently *MCT1* transcription (Payen et al., 2019). The HIF-2 mechanism might be involved in MYC and nuclear factor- κ B (NF- κ B) transcriptional activity, where the deregulation of the NF- κ B pathway is associated with oncogenesis (Zhao et al., 2013).

In osteosarcoma cell lines, it was found that the NF- κ B pathway influences the process of glycogen synthase kinase 3 β (GSK-3 β)-mediated regulation of cell survival (Zhao et al., 2013). Other pathways have been described in the *MCT1* regulation, where activation of the Wnt pathway and metastasis-associated in colon cancer 1 (MACC1) signaling leads to induction of *MCT1* transcription (Payen et al., 2019).

MCT1 may also be epigenetically regulated by DNA methylation. For example, DNA methylation can play a role in β -cell-specific *MCT1* silencing (Pullen et al., 2011). In human breast cancer, it was reported that an isolated hypermethylated DNA fragment from 5' upstream region of *MCT1* leads to the silencing of this gene (Asada & Fukutomi, 2003).

A post-transcriptionally mechanism can regulate *MCT1* in several tissues (Halestrap & Price, 1999; Halestrap & Wilson, 2012). *MCT1* post-transcriptional regulation could also involve regulation of its translation through specific sequences and secondary structures in the 5' or 3' untranslated region (UTR) (Halestrap & Wilson, 2012). Since *MCT1* 3'-UTR is very long, it may be related to translational control of *MCT1* expression (Halestrap & Wilson, 2012).

The post-transcriptional mechanism could be associated with overexpression of *MCT1* during the cell cycle, without change *MCT1* mRNA levels (Halestrap & Wilson, 2012). miR-29a, miR-29b, miR-124, and miR-495 are likewise enabled to regulate *MCT1* expression as described as β -cell silencing of *MCT1* gene, by connecting to the binding site present in the *MCT1* 3' UTR (Payen et al., 2019; Pullen et al., 2011). In human triple-negative breast cancer, miR-342-3p directly targets *MCT1*, resulting in a change of lactate and glucose fluxes and disrupting the metabolic homeostasis of tumor cells (Romero-Cordoba et al., 2018). However, the functional role of many miRNAs remains unclear (Romero-Cordoba et al. 2018).

MCT1 levels at the plasma membrane are regulated by cyclic adenosine monophosphate (cAMP)-dependent vesicular trafficking in RBE4 cells (**Figure 12**) (Halestrap & Wilson, 2012; Payen et al., 2019; Uhernik et al., 2014). In rat brain cerebrovascular endothelial cells, cAMP can stimulate and induce the dephosphorylation of *MCT1* and therefore the internalization of the

transporter from the plasma membrane into caveolae (CAV) and early endosomes (EE) (Smith et al., 2012).

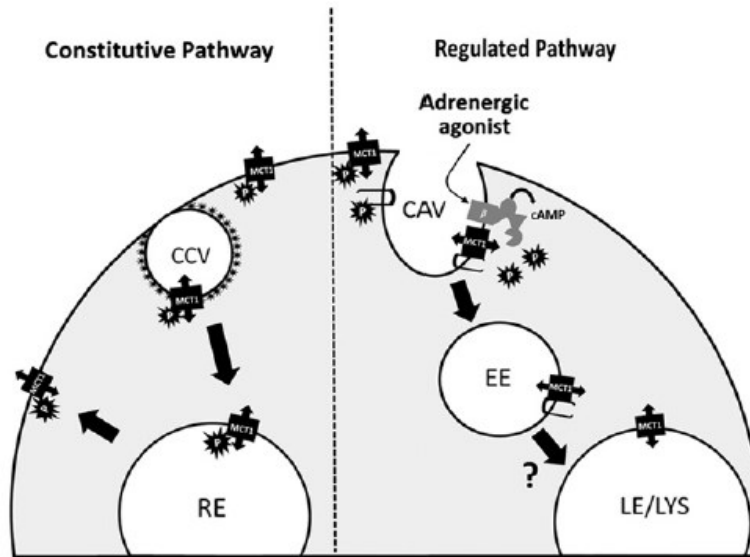


Figure 12 - MCT1 constitutive and regulated pathway by cAMP-dependent internalization in RBE4 cells. In the constitutive pathway, MCT1 internalization occurs by clathrin-coated vesicles (CCV) where it is trafficked to recycling endosomes (RE) for redistribution on the plasma membrane, without the interference of cyclic adenosine monophosphate (cAMP) signaling. In the regulated pathway, the cAMP production leads to activation of a phosphatase which dephosphorylates the MCT1 plasma membrane, promoting internalization of MCT1 from the plasma membrane into caveolae (CAV) and early endosomes (EE). For abbreviations please see page ix (Smith et al., 2012).

MCT expression leads to the upregulation of glycolysis and acid-resistance of cancer cells due to the “lactate shuttle”, leading to the conversion of *in situ* to invasive cancer (Pinheiro, Reis, et al., 2010; Romero-Garcia et al., 2016). MCT1 has been associated with tumor aggressiveness and “stemness” of tumor cells once it been mentioned in several cancers, such as glioma, breast, colorectal, gastric, cervical cancer, and neuroblastoma (Pinheiro et al., 2012; Pinheiro, Reis, et al., 2010; Romero-Garcia et al., 2016). MCT1 has been proposed as a biomarker or prognostic marker for cancer outcome and poor prognosis (Fisel et al., 2018). Therefore, the understanding of the

mechanism of MCT1 regulation can potentially result in a better prognosis and treatment of the disease.

1.4.1.2. MCT1 as a therapeutic target in cancer cells

MCT1 is responsible for cancer metabolic adaptations and has an important effect on the metabolic-symbiosis between different types of cells present in the cancer microenvironment (Sotgia et al., 2013). The metabolic symbiosis system may be responsible for drug-resistance and/or the escape mechanism during antiangiogenic therapy, so targeting this transporter with new effective and nontoxic drugs in cancer therapies will “shut-down” the advantageous symbiosis, making a serious impact in tumor homeostasis (Pineiro et al., 2012; Sotgia et al., 2013). Knowing that MCT1 is overexpressed in some cancer cell lines and that its aberrant expression occurs along with tumor aggressiveness (Fisel et al., 2018), MCT1 inhibition can be used as a potential therapeutic approach in cancer, either to inhibit the effect of lactate, improve the immune system response or decrease the capacity of tumor cells migration (Pineiro et al., 2012).

Inhibition of MCT1 can be performed in a nonspecific way by α -cyano-4-hydroxycinnamic acid (CHC) and its analogs, stilbene disulphonates including 4,4'-di-isothiocyanostilbene-2,2'-disulphonate (DIDS) and 4,4'-dibenzamidostilbene-2,2'-disulphonate (DBDS), phloretin and bioflavonoids such as quercetin, cyanocinnamates, *p*-chloromercuribenzenesulfonate (*p*CMBS), and statins (Fisel et al., 2018; Halestrap, 2012, 2013; Halestrap & Price, 1999; Halestrap & Wilson, 2012).

DIDS can irreversibly bind to MCT1 and MCT2 and disrupt the transporter, while *p*CMBS, an organomercurial reagent, can interrupt MCT-CD147 interaction by directly targeting basigin, and consequently breaking up MCT1, MCT3, and MCT4 expression and activity (Park et al., 2018; Payen et al., 2019). CHC has an antitumor effect by inhibiting lactate uptake into oxygenated cancer cells and indirectly starve hypoxic cancer cells of glucose, disrupting metabolic coupling present in the tumor microenvironment (Bola et al., 2014). In that way, CHC is able to decrease tumor growth, increase the necrosis core associated with the eradication of hypoxic tumor area, and increase the sensitivity of the remaining oxygenated tumor to radiotherapy (Bola et al., 2014; Payen et al., 2019). While effective at inhibiting MCT1 *in vitro*, CHC and DBDS were reported to exhibit substantial off-target effects. CHC can bind and inhibit mitochondrial pyruvate transport and DBDS leads to erythrocyte chloride/bicarbonate exchanger AE1 suppression (Park et al., 2018).

Lipophilic statins, such as cerivastatin, simvastatin, lovastatin, fluvastatin, and atorvastatin, have been described as anticancer medications based on their antiproliferative, proapoptotic and tumoricidal properties in distinct cancer cells by competitive nonspecific MCT inhibition (Fisel et al., 2018; Mehibel et al., 2018). Lovastatin and simvastatin are administered in the inactive lactone form and have the advantage of increasing their lipophilicity and have better access to different tissues, especially to non-hepatic tissues, where they can pass the plasma membrane through passive diffusion and be metabolized to the corresponding active β -hydroxy acid (Kato et al., 2010; Matuszewicz et al., 2015). The remaining are applied in the active form (du Souich et al., 2017).

Statins are a 3-hydroxy-3-methylglutaryl coenzyme A (HMG-CoA) reductase competitive inhibitor used to reduce concentrations of low-density lipoprotein cholesterol (du Souich et al., 2017; Kikutani et al., 2016; Matuszewicz et al., 2015). When the statin is in their active form, β -hydroxy acid, can be biotransformed in hydroxylated metabolites that also contribute to inhibit HMG-CoA (du Souich et al., 2017). In this way, the biosynthesis of mevalonic acid is disrupted as well as the biosynthesis of cholesterol, isoprenoid, ubiquinone, steroids, bile acids, vitamin D, as well as geranylgeranyl pyrophosphate (GGPP) and farnesyl pyrophosphate (FPP) (du Souich et al., 2017; Kato et al., 2010). However, the anticancer activity of statins still remains unclear (Matuszewicz et al., 2015). Other studies describe more cytostatic and cytotoxic effects of statins in malignant and highly metastatic cancer cells than benign and low metastatic cancers when possesses the same origin (Hentosh et al., 2001). Statins affect cell-cycle regulatory proteins in G1 and S phase in a dose and time-dependent manner (Matuszewicz et al., 2015). Lipophilic statins can be used to sensitize cancer cells to different chemotherapies without affecting normal cells, improving overall survival in patients (Kato et al., 2010).

Another chemotherapeutic agent is lonidamine (LND) which was described to be responsible for potent and nonspecific inhibition of MCT1, MCT2, and MCT4, sensitizing tumor cells and enhancing treatments (Fisel et al., 2018; Nancolas et al., 2016). LND has as an advantage the selective activity against different tumors without affecting normal tissues (Nath et al., 2016). In human melanoma xenografts, LND inhibits the mitochondrial pyruvate carrier (MPC) and suppresses MCT1 by an unknown mechanism (**Figure 13**) (Nancolas et al., 2016; Nath et al., 2016). However, it has been described that the inhibition of respiration involves reduced mitochondrial uptake of pyruvate *via* MPC, as well as inhibition of the mitochondrial electron-transport chain at Complex II and perhaps also Complex I (Nath et al., 2016). LND can drive to the

accumulation of reactive oxygen species (ROS) through Complex II (Nath et al., 2016). Consequently, LND leads to an increase of intracellular L-lactate, a reduction of the intracellular pH, and a decrease of nucleoside triphosphate levels, leading to the inhibition of MCT1 (Nancolas et al., 2016; Nath et al., 2016).

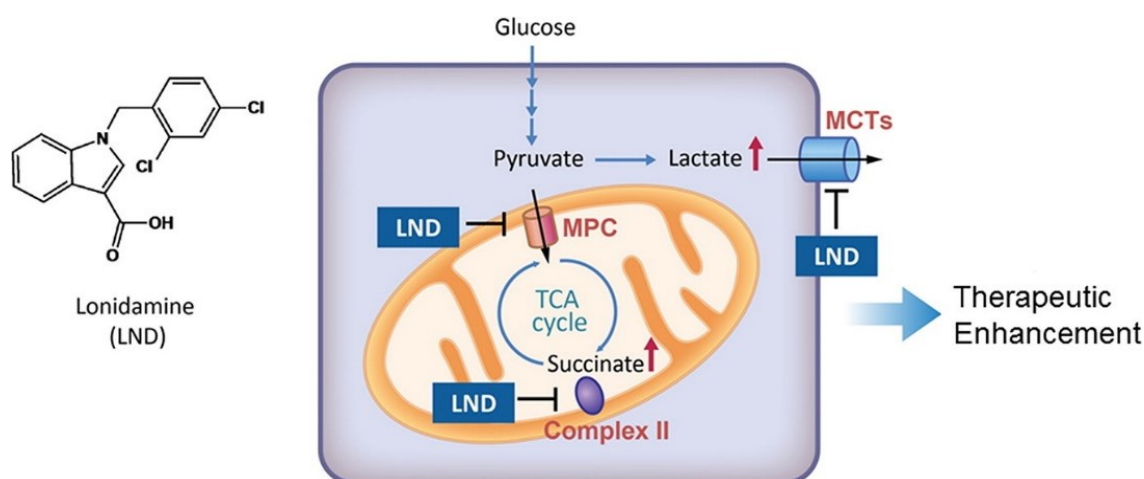


Figure 13 – Lonidamine structure and its mechanism for MCT1, MCT2, and MCT4 nonspecific inhibition. Lonidamine (LND) is responsible for the inhibition of mitochondrial pyruvate carriers (MPC) and complex II, increasing the intracellular levels of L-lactate and decreasing intracellular pH and nucleoside triphosphate levels, leading to the inhibition of MCT1 (Nath et al., 2016).

Nonspecific MCT inhibition has been demonstrated to exert therapeutic effects, but these compounds cannot determine the individual role of MCT isoforms or particularly inhibit one specific altered MCT in a pathophysiological pathway (Fisel et al., 2018). Nonspecific MCT inhibitors do not present a high clinical prospect in cancer (Payen et al., 2019). It is crucial to create new specific inhibitors of MCT1 and test their efficacy in preclinical studies (Fisel et al., 2018).

The interest in MCT1 inhibitors increased in 2007 with a new class of immunomodulatory drugs (Bueno et al., 2007). AR-C117977 and AR-C122982 are potent MCT1 and MCT2 inhibitors that can act through direct binding to intracellularly TM domains 7-10 (Park et al., 2018). The MCT1 suppression can affect the function of B lymphocytes *in vitro* and *in vivo* and cause immunosuppression *via* inhibition of T lymphocyte proliferation (Paul et al., 2017). However, AR-

C117977 and AR-C122982 present some disadvantages as they cannot inhibit cytokine production or the expression of early leukocyte activation markers *in vitro*, and had high lipophilicity, very low solubility, poor oral bioavailability with short plasma half-lives, limiting their clinical value (Bueno et al., 2007; Pahlman et al., 2013; Park et al., 2018). In order to overcome these barriers, other compounds were synthesized based on the above mentioned compounds. AR-C155858 and its derivative, AZD3965 (Polanski et al., 2014), are specific and extremely high-affinity inhibitors of MCT1 over MCT2 (6-fold greater specificity), developed by AstraZeneca. These inhibitors are able to inhibit T lymphocyte activation and proliferation, by blocking lactate efflux, and also MCT1 while having an immunosuppressive effect (Bola et al., 2014; Fisel et al., 2018; Halestrap, 2013; Ovens et al., 2010; Payen et al., 2019). The inhibition of MCT1 by AZD3965 was shown to be time-dependent, suggesting that maybe the compound enters the cell before binding to the same region than AR-C117977 and AR-C122982. At this moment, AZD3965 is at phase I/II in preclinical tests for treating patients with some types of advanced cancers (Fisel et al., 2018; Park et al., 2018). AZD3965 has been shown to be most effective against cancer cells expressing high levels of MCT1 in hypoxia with simultaneous low expression of MCT4, once high levels of MCT4 expression are correlated with resistance of the drug (Jones & Morris, 2016; Park et al., 2018).

BAY-8002 was described as a novel potent and selective inhibitor of MCT1-dependent bidirectional lactate transport (Quanz et al., 2018). BAY-8002 and AZD3965, despite the distinct structure, both act in a similar way, binding to the same or overlapping sites, and suppressing MCT1 and MCT2 activity, which decreases tumor growth but not tumor regression (Payen et al., 2019; Quanz et al., 2018). However, BAY-8002 is more selective for MCT1 than MCT2 (Payen et al., 2019).

An alternative strategy to specifically target MCT1 consists in the use of small interfering RNAs (siRNAs) loaded in PEGylated chitosan nanoparticles (Corbet et al., 2015; Payen et al., 2019). Chitosan is a natural polymer that is non-toxic, non-immunogenic, biodegradable, and biocompatible. When combined with nanoparticles, it can be used as a platform for delivery siRNA into tumors through electrostatic interactions, increasing the efficacy of cell binding (Corbet et al., 2015).

MCT1 and MCT4 present a similar function which can result in a compensatory pathway, increasing chemosensitivity and radiosensitivity, but not tumor cell death (Fisel et al., 2018; Quanz et al., 2018). Even with the simultaneous inhibition of MCT1 and MCT4, cancer cells can induce a

metabolic shift toward oxidative phosphorylation and survival (Fisel et al., 2018). So, the utilization of a rational drug combination that includes MCT1 and MCT4 inhibitors and blockers of oxidative phosphorylation is fundamental to disrupt metabolic homeostasis of cancer cells, leading to tumor cell death (Fisel et al., 2018).

1.5. Outline of the thesis

MCTs are present in a wide variety of tissues and are involved in the transport of diverse monocarboxylates across the plasma membrane. MCTs belong to the SLC16 transporter family and, so far, 14 homolog members have been identified, being all essential for the regulation of fundamental cellular processes. MCT1 is a well characterized member that functions as a proton-symporter of metabolic monocarboxylic acids in mammals. While MCT1 enables the uptake of lactate, facilitating to upregulation of glycolysis, it also enables the transport of H⁺, contributing to the preservation of intracellular pH of cancer cells. MCT1 plays a dual role in the maintenance of the metabolic phenotype in tumor cells. MCT1 has also been associated with angiogenesis and cancer migration, invasion, and metastasis. Therefore, MCT1 is a potential target molecule for cancer therapy as well as a useful prognostic factor.

Little is known regarding the conditions that lead to removal of MCT1 from the plasma membrane. This project aims at studying the expression and localization of MCT1, by confocal microscopy. We will use a U2OS cancer cell line harboring MCT1 fused at the N-terminal with the EGFP protein, by CRISPR-Cas9. Cells will be grown in media with or without glucose and/or glutamine and in the presence or absence of distinct compounds namely cycloheximide, lenalidomide, FTY720, PMA, lithium chloride, and quercetin. These conditions were selected based on previous reports stating that they influence MCT1 or other nutrients transporters expression at the plasma membrane.

2. Materials and Methods

2.1. Biological Materials

We used U2OS cells harboring MCT1 fused with the enhanced green fluorescent protein (EGFP-MCT1) in both alleles, at the N-terminal, using Clustered Regulatory Interspaced Short Palindromic Repeat (CRISPR)-Cas9 technology. These cells were previously generated by our group (Gómez-Varela et al., 2020).

2.2. Cell culture

U2OS cells were thawed using a 37°C water bath and cultured in Dulbecco's Modified Eagle Medium (DMEM; Lonza and Gibco), supplemented with 10% (v/v) Fetal Bovine Serum (FBS; Gibco), and 10.000 U/mL Penicillin and 10.000 µg/mL Streptomycin (Merck). The medium DMEM, containing 4.5 g/L of glucose and L-glutamine, was used as standard.

The adherent cell line was always grown in monolayer culture at 37°C in a humidified incubator with 5% CO₂. U2OS cells were periodically tested for *Mycoplasma* by PCR.

2.3. Compounds for assessing MCT1 expression

Cells were treated, when indicated, with phorbol 12-myristate 13-acetate (PMA; Sigma-Aldrich ref P1585-1MG), cycloheximide (CHX; Sigma-Aldrich ref C7698-1G), fingolimod hydrochloride (FTY720; Sigma-Aldrich ref SML0700), lithium chloride (LiCl; Sigma-Aldrich ref L-0505), (3S)-3-(4-Amino-1-oxo-1,3-dihydro-2H-isoindol-2-yl)piperidine-2,6-dione (lenalidomide; Santa Cruz Biotechnology ref sc-218656), and quercetin dihydrate (EMD Millipore ref 551600). FTY720 was dissolved in water and stored at -20°C; LiCl was dissolved in water and stored at room temperature; the remaining compounds (CHX, lenalidomide, PMA and quercetin) were dissolved in DMSO and stored at -20°C. For these compounds, 1% of DMSO was added to the medium as a control. The stock concentration of compounds are presented in **Table 1**.

Table 1 - Compounds and respective stock concentration (mM) used to study MCT1 protein expression.

Compounds	Concentrations (mM)
cycloheximide	3.55×10^2
FTY720	5.82×10^2
lenalidomide	1×10^1
LiCl	1×10^3
PMA	1
quercetin	8×10^1

The cell culture media used in this study were either DMEM (4.5 g/L of glucose and L-glutamine) as a standard condition, or medium A (no glucose, no glutamine and no phenol red; Alfacene) and medium B (no glucose and no sodium pyruvate, supplemented with glutamine; Alfacene), all stored at 4°C.

2.4. Cell sample preparation and optimization for fluorescence microscopy experiments

For the confocal fluorescence microscopy imaging, cells at 80-90% confluence were washed with Dulbecco's Phosphate-Buffered Saline (DPBS; Gibco), detached with Trypsin (Corning) and re-suspended in fresh complete medium (DMEM). To optimize the cell density for fluorescence microscopy experiments, gene-edited U202 cells were seeded into a μ -Slide 8 well plate ibiTreat (Ibidi) at different concentrations, namely 5×10^4 , 7×10^4 , 9×10^4 and 11×10^4 cells/mL. These cell densities were selected based on a concentration range recommended by the manufacturer's instructions. Cells were incubated for 24 h at 37°C, 5% CO₂, and imaged with a confocal fluorescence microscope at time 0 h and 25 h later.

2.5. Cell seeding for live-cell imaging

After re-suspension in fresh complete medium, cells were seeded into ibiTreat μ -Slide 8 well chambers, with a cell density of 5×10^4 cells/mL, per well. After 24 h of incubation, cell medium was removed and cells were washed with DPBS. 300 μ L of either standard DMEM, medium A, or medium B, and the corresponding compounds, were added to each well. The final concentration

of compounds used to study MCT1 protein expression are presented in **Table 2**. Fluorescence microscopy was performed after 6 h and 24 h of incubation.

Table 2 - Compounds and respective final concentration (nM) used to study MCT1 protein expression.

Compounds	Concentrations (nM)
cycloheximide	3.55×10^5
FTY720	5.82×10^2
lenalidomide	1×10^1
LiCl	2×10^7
PMA	1×10^3
quercetin	8×10^4

2.6. Confocal Fluorescence Microscopy

Live-cell imaging with U2OS cells was performed with a Zeiss LSM 780 inverted confocal microscope after 24 h of incubation of U2OS cells. EGFP-MCT1 was excited using an Argon laser at 488 nm and detected between 493–598 nm. To avoid photobleaching, and consequently the phototoxicity of cells, the intensity of lamp was set at 15% of power laser. The pinhole size was set to 1 Airy units, the detector gain to 700, the digital offset to 0 and the digital gain to 1.0. Microscopic images were acquired with an oil immersion 40×(1.3 NA) objective (EC Plan-Neofluar®) and using the Zeiss ZEN digital imaging software.

2.7. Image processing and analysis

Fluorescence intensity of all images was acquired in Z-stacks (8-bit, 1024x1024 pixels, lsm files). All images were processed and analyzed using FIJI software (Schindelin et al., 2012), as briefly explained in **Figure 14**. For optimization experiments, each z-stack image was acquired at 0 h and 25 h. For MCT1 expression analysis, acquisition was performed at 6 h and 24 h, using the *sum slices* tool in order to visualize the sum of each intensity pixel in all cells.

For MCT1 expression representative images acquired by confocal microscopy, all images were acquired by subtraction of just one stack (representative of the middle of the cell) and colored in green.

For confocal imaging data analysis (**Appendix**), each z-stack image was combined into two equal sum slices z-stack image, where one of them was used as the original image (**Figure 14A**) and the other one was adjusted with a *median filter* tool (**Figure 14B**) to smooth the image and remove thin-structured objects (Yang, 2016). The *Image calculator* tool was used to subtract the second filtered image from the original, to remove background and to enable the appearance of small features, corresponding to the pixels with the highest intensity of the original image (**Figure 14C**). The noise level of the images was reduced using the *thresholding* tool, with identical settings for all images. This approach can remove some texture introduced by the previous median filter that was not present in the original image, once the filter size was significant (Yang, 2016). Another *median filter* was used to reduce residuals of autofluorescence background from images (Powell et al., 2019) by replacing each pixel with the median of the neighboring pixel values (Bankhead, 2014). The quantification of MCT1 fluorescence intensity was normalized by dividing the fluorescence intensity per number of cells in each image. The number of cells was determined using the *cell counter* plugin and only cells with a visible nucleus were considered.

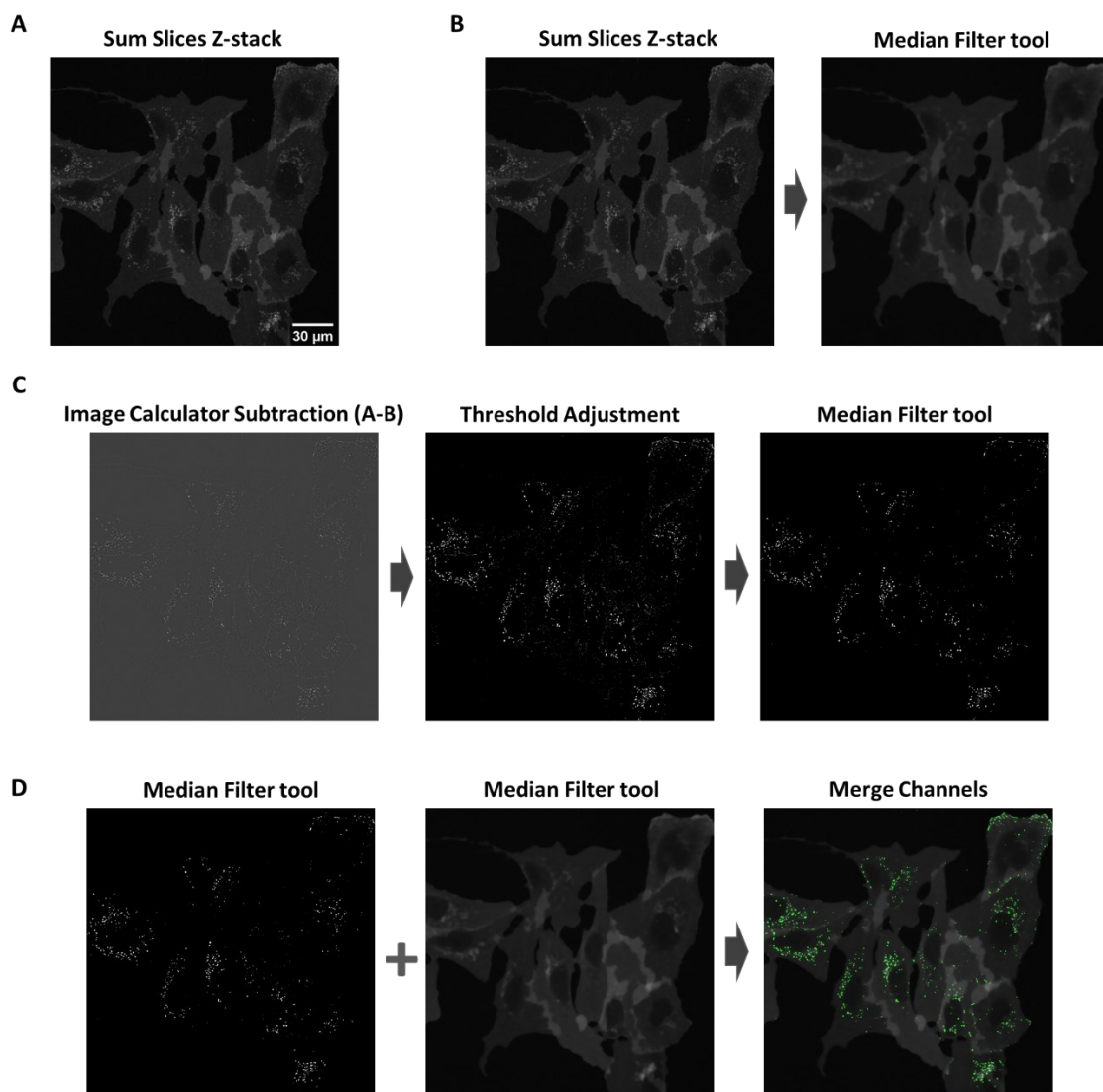


Figure 14 – Key stages of image processing used for the quantification of MCT1 expression. Each z-stack image acquired after 6 h and 24 h of cell incubation was combined into two equal sum slices z-stack image: **(A)** the original image and **(B)** the original image adjusted with a *median filter* tool. **(C)** The *Image calculator* tool was used to subtract the adjusted image from the original. The results of subtracted images were adjusted using the *thresholding* tool and processed by a *median filter*, before quantifying the fluorescent intensity of each image. **(D)** The *merge channels* plugin was used to combine images acquired after the different *median filter* tool (step B and C) to enhance the visualization of the MCT1 (green) in the cell (grey). This step was just used in the confocal microscopy analysis.

All images were processed in the same way with all tools, except with the *thresholding* tool once images from different sets were acquired with a different laser intensity. So, in order to not

acquire more or less information than the original image, *thresholding* was higher for the images acquired with more laser intensity, and smaller for the images acquired with less laser intensity. However, all images acquired on the same day were processed with the same *thresholding* as they were exposed to the same laser intensity, enabling the statistical analyzes of the data.

For the analysis of MCT1 expression by confocal microscopy imaging, the images processed with the median filter were combined with the *merge channel plugin* to improve the visualization of MCT1 (green) in the cells (grey) (**Figure 14D**).

2.8. Statistical analysis

GraphPad Prism 8 software (GraphPad Prism Software Inc., San Diego, CA, USA) was used for statistical analysis. The experiments with FTY720 and lenalidomide were repeated 3 times independently while other experiments, including assays with cycloheximide, PMA, LiCl, quercetin, medium A and medium B were repeated 2 times independently. Fluorescent intensity values were tested with a two-way ANOVA. Statistical significance between groups was analyzed by Tuckey post hoc test and was considered to be statistically significant at $P \leq 0.05$. Results shown on graphs represent the mean \pm standard deviation (mean \pm SD).

3. Results and Discussion

3.1. Optimization of cell seeding for confocal imaging

To optimize the optimal cell density for microscopy, gene-edited U2O2 cells were seeded into a μ -Slide 8 well plate ibiTreat (Ibidi) at different concentrations (5×10^4 , 7×10^4 , 9×10^4 and 11×10^4 cells/mL). Cells were observed with the confocal fluorescence microscope after 0 h and 25 h of incubation (Figure 15).

As shown in Figure 15, all cell densities were suitable for quantitative image analysis at different time-points. At 0 h, cells were separated enough to enable the visualization of MCT1 transporter and to simplify the cell counting, improving data analysis. However, after 25 h, at 9×10^4 cells/mL and 11×10^4 cells/mL cell densities, the acquired images were saturated, leading to inaccurate quantification in live-cell imaging (Bankhead, 2014). From all the tested concentrations, 5×10^4 cells/mL was found to be the optimal cell concentration for confocal imaging because of the quality of images and to facilitate the counting of the cell number, which is required for the fluorescent intensity quantification studies.

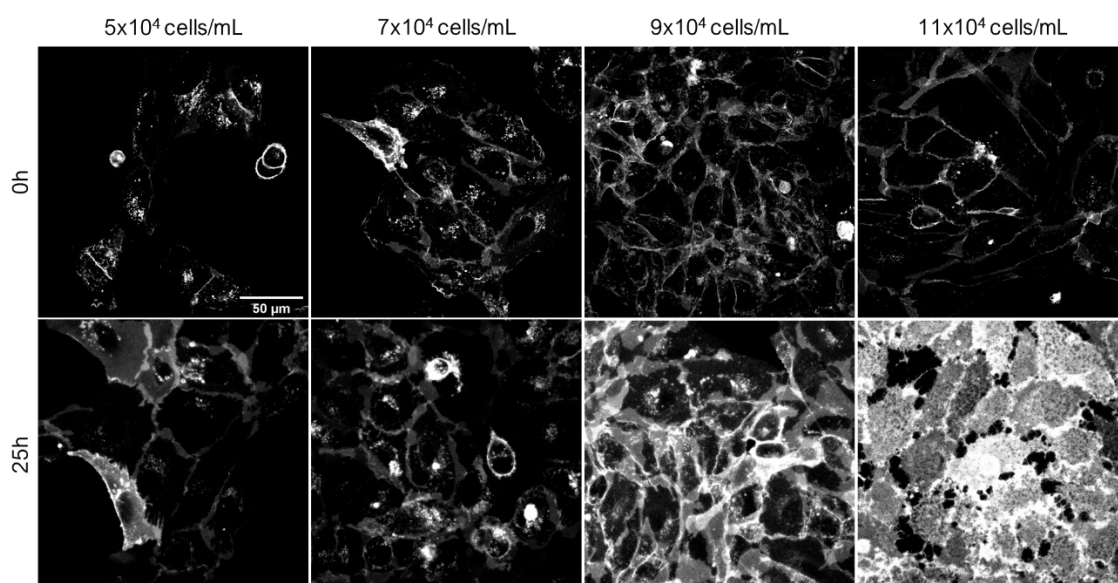


Figure 15 - Fluorescence of U2OS cells at different concentrations (5×10^4 , 7×10^4 , 9×10^4 and 11×10^4 cells/mL) after 0 h and 25 h of incubation. 5×10^4 cells/mL was chosen as an optimal cell concentration for confocal imaging. Scale bar corresponds to 50 μ m.

3.2. Effect of glucose and glutamine deprivation on MCT1 protein expression in U2OS cells

Cancer cells consume high levels of glucose and convert them rapidly into lactate (Vander Heiden et al., 2009; Warburg et al., 1927). This has been described as a key feature of their metabolism, promoting growth, survival, proliferation, long-term maintenance, as well as a reduction of overall survival in cancer patients (Liberti & Locasale, 2016; Walenta et al., 1997). As mentioned in the introduction section, MCT1 has been reported to be overexpressed in several cancer cell lines. In order to analyze MCT1 expression in the U2OS cell line, cells were grown in distinct media (medium A and medium B) containing different components.

Firstly, cells were exposed either to medium A (no glucose and no glutamine) or to the standard DMEM control medium and observed by confocal microscopy, every 3 h for a period of 9 h (**Figure 16A**). It was possible to detect a fluorescent signal, localized at the plasma membrane, in all conditions analyzed. After 3 h of incubation, the level of MCT1 expression was higher in cells incubated with DMEM than when cells were incubated in medium A. The expression of MCT1 increases over time in Medium A, and after 9 h no difference is found between the conditions tested and MCT1 fluorescence is clearly observed at the plasma membrane. Fluorescence signal strength levels (**Figure 16B**) remain similar after 6 h and 9 h of incubation. Mean fluorescence signal strength values for cells incubated with DMEM (standard) and medium A after 3 h, 6 h and 9 h of incubation are presented in **Table 3**.

These results are in contrast to what has been reported when MCT1 was ectopically expressed in SiHa cells lysates under glucose- and glutamine-deprivation for 48 h (Saedeleer et al., 2014). However, in our work MCT1 is expressed under the control of its native promoter, and we observe that cells treated with medium A seem to recover MCT1 expression after 9 h of incubation (**Figure 16A**).

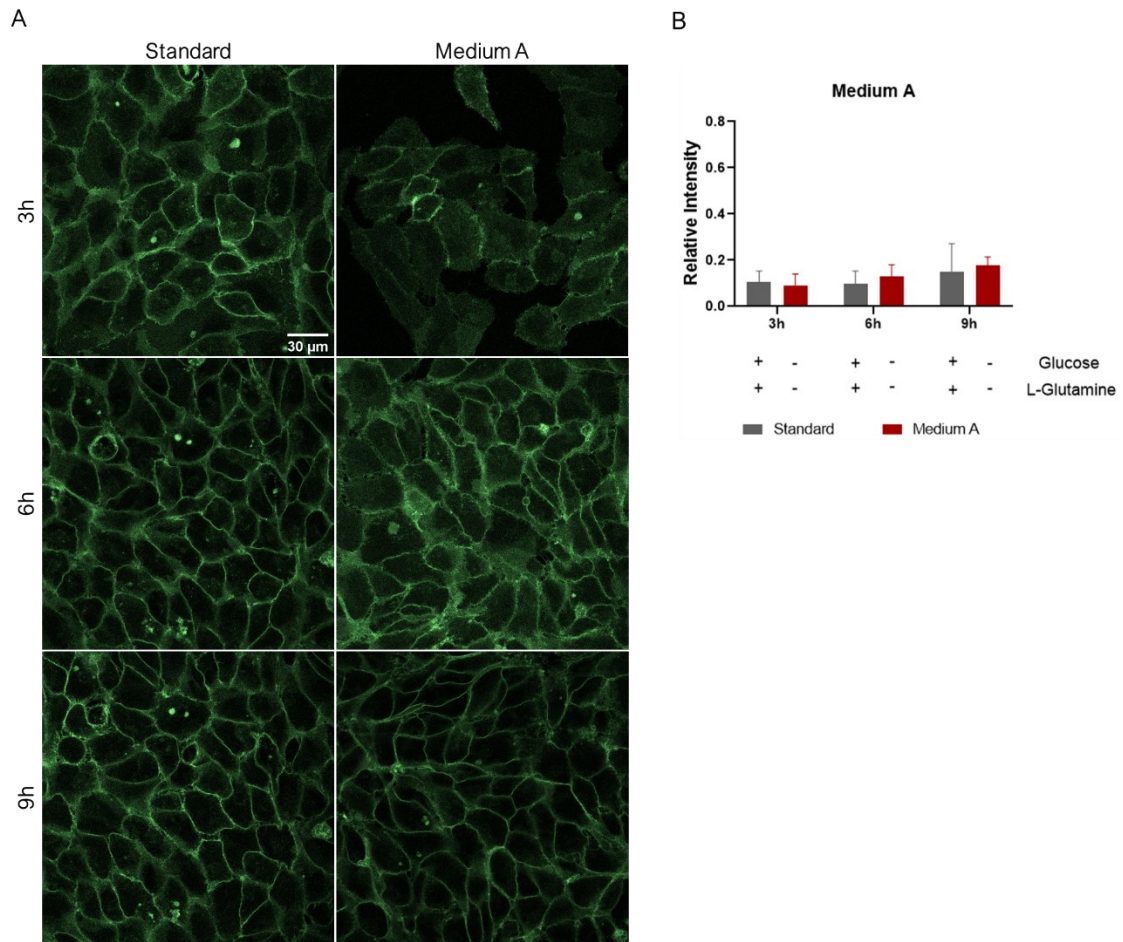


Figure 16 – Analysis of MCT1 expression in gene-edited U2OS cells after 3 h, 6 h and 9 h of incubation with standard medium (DMEM) and medium A (no glucose and no glutamine) by confocal microscopy imaging (A) and fluorescence quantification (B). Images are representative of two independent experiments. Scale bar corresponds to 30 μm . The quantification of fluorescence signal strength was normalized by dividing the total fluorescence intensity per number of cells in each image acquired using confocal microscopy imaging. Error bars represent SD.

Table 3 - Mean fluorescence signal strength values for the standard and cells treated with different media (medium A and medium B) for 3 h, 6 h or 9 h (n=2).

Incubation time	Mean fluorescence signal strength values		
	Standard	Medium A	Medium B
3 h	0.0861 ± 0.0434	0.0454 ± 0.0204	0.1098 ± 0.0467
6 h	0.0859 ± 0.0635	0.0899 ± 0.0791	0.0741 ± 0.0347
9 h	0.0942 ± 0.0495	0.0993 ± 0.0630	0.1416 ± 0.0468

In the last decades, transient transfection has been continually used to study proteins and their involvement in cellular processes (Gibson et al., 2013; Moriya, 2015). However, this results in artificial overexpression of proteins, leading to complex consequences as the function of diverse proteins is interconnected (Moriya, 2015). Overexpression of proteins can lead to cell toxicity, dysregulation of the gene dosage balance which affects protein folding and complex assembly, accumulation of complex aggregates, downstream regulation, biological pathway modulation, and severe abnormal changes in phenotypes (Bolognesi & Lehner, 2018; Gibson et al., 2013; Moriya, 2015). In addition, overexpressed GFP-tagged proteins may result in ectopic cellular localizations and/or be involved in non-native interactions (Bolognesi & Lehner, 2018; Gibson et al., 2013).

Regulatory molecules such as transcription factors and signaling molecules can be modulated by alterations in the external/internal cellular conditions (Moriya, 2015). MCT1 is highly regulated by transcription factors that when activated/inactivated can promote/reduce the expression of MCT1 (Halestrap, 2013; Jones & Morris, 2016; Payen et al., 2019). So, it is possible that the variations in the external/internal cellular conditions led to altered MCT1 regulation and trafficking in cells overexpressing the transporter, as presented by Saedeleer and colleagues.

We also compared the expression of MCT1 after cells were incubated either with medium B (no glucose and glutamine) or with the standard control (DMEM). Few differences were found after cells were observed by confocal microscopy (**Figure 17A**). MCT1 was clearly localized at the plasma membrane, in all time points analyzed and for both conditions. This is in accordance with the fluorescence signal strength levels obtained (**Figure 17B**). Mean fluorescence signal strength values for the standard and cells treated with medium B after 3 h, 6 h and 9 h of incubation are presented in **Table 3**.

The results reported in the literature seem to be controversial as it has been described that MCT1 protein expression increased in transfected SiHa cells lysates 48 h after glucose-deprivation (Saedeleer et al., 2014). However, it was also described that MCT1 protein expression was equal in HBMEC cells lysates 24 h after glucose-deprivation (Miranda-Gonçalves et al., 2017). Cells treated with medium B also seem to slightly recover MCT1 expression after 9 h of incubation (Figure 17A).

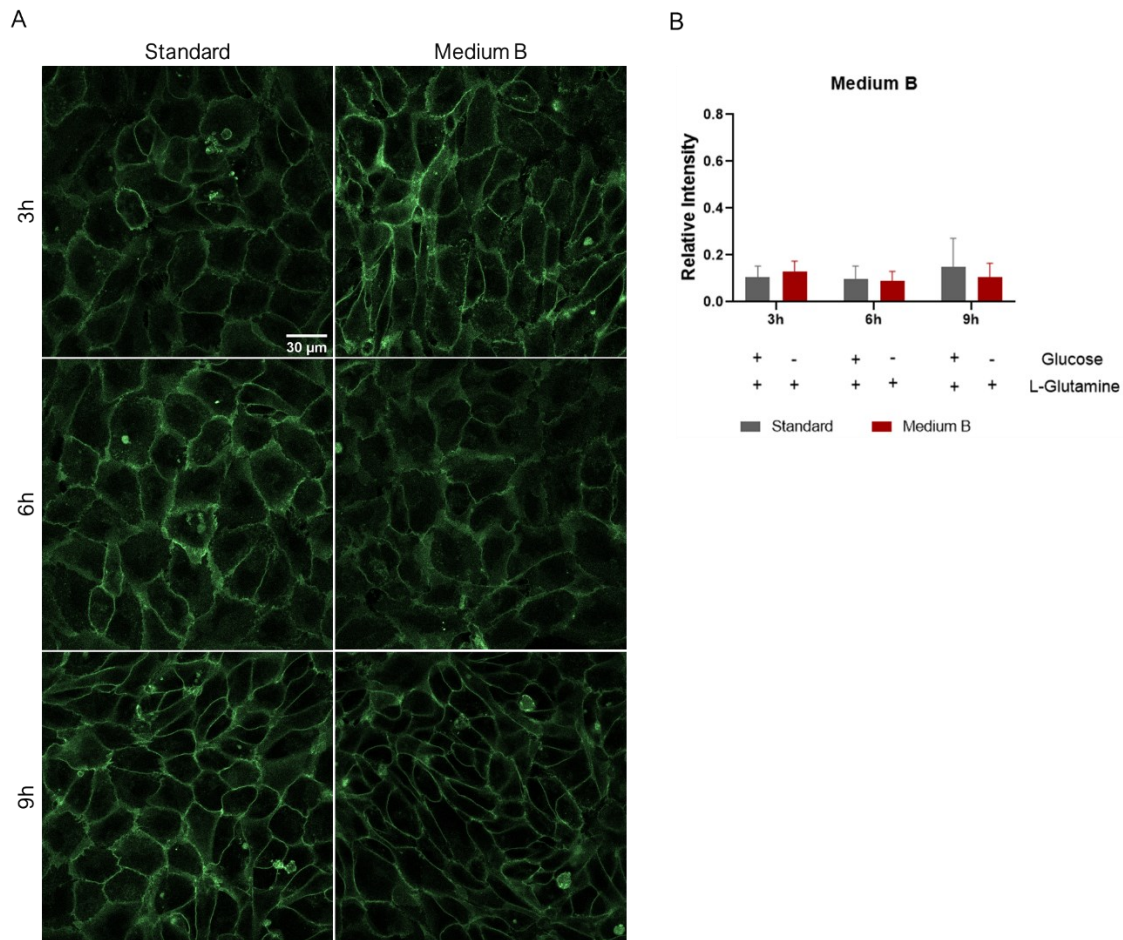


Figure 17 – Analysis of MCT1 expression in gene-edited U2OS cells after 3 h, 6 h, and 9 h of incubation with medium B (with glutamine and without glucose) by confocal microscopy imaging (A) and fluorescence quantification (B). Images are representative of two independent experiments. Scale bar corresponds to 30 μ m. The quantification of fluorescence signal strength was normalized by dividing the total fluorescence intensity per number of cells in each image acquired using confocal microscopy imaging. Error bars represent SD.

In *in vivo* tumors, the lactate present in the microenvironment strongly activates the glutaminolysis machinery in an MCT1-dependent manner (Figure 18) (Pérez-Escuredo et al., 2016). This involves the uptake of lactate by MCT1 and its oxidation to pyruvate by lactate dehydrogenase 1 (LDH1). In the cytosol, pyruvate mediates lactate signaling by inhibiting the prolylhydroxylases (PHD) and consequently stabilizing HIF-2 α protein. HIF-2 α stabilizes c-Myc protein expression into the nucleus of the cell, leading to the transcription of target genes, such as *ASCT2*, that is responsible for glutamine uptake into the cells (Pérez-Escuredo et al., 2016). Our results show that, in the conditions tested, EGFP-MCT1 is stably maintained at the plasma membrane, both in the presence or absence of glucose or glutamine.

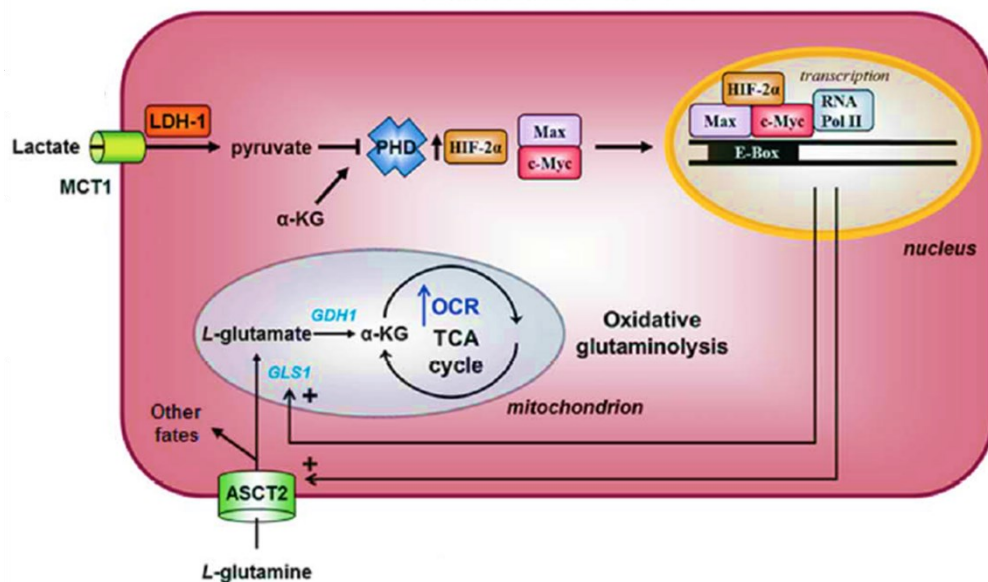


Figure 18 – Mechanism of lactate-induced glutamine uptake and metabolism in cancer cells.

Lactate enters into the cell by MCT1-facilitated transport and its oxidized to pyruvate in the cytosol by lactate dehydrogenase 1 (LDH1). Pyruvate inhibits the prolylhydroxylases (PHD), resulting in the stabilization of HIF-2 α protein. HIF-2 α protein stabilizes c-Myc protein expression (or c-Myc-Max complexes) in the nucleus. c-Myc promotes the transcription of target genes, such as *ASCT2*, a transmembrane transporter responsible for the uptake of glutamine to inside the cell. Glutamine can stay in the cytosol or in the mitochondria, where it is converted to glutamate by glutaminase 1 (GLS1) (adapted from Pérez-Escuredo et al. 2016).

From this point on, we proposed to test the effect of specific compounds in the expression and localization of MCT1, namely cycloheximide, lenalidomide, FTY720, PMA, LiCl and quercetin.

However, after the experiments described in this section, we had difficulties to establish the conditions for control experiments. In the above mentioned experiments, we see a clear localization of MCT1 at the plasma membrane when cells are incubated for 3 h in DMEM medium (control) and a negligible GFP cytoplasmatic signal is observed. This is in contrast to what was found in the experiments that will be described in the following sections, where we observe internal fluorescence already in the control experiments. Still, we will present the results obtained and the reasoning behind testing the selected compounds, as well as the expected results.

3.3. Testing the effect of cycloheximide on MCT1 protein expression in U2OS cells

Cycloheximide (CHX) is a eukaryotic protein synthesis inhibitor that acts by reversibly binding to the ribosomal E-site and inhibits the attachment of eukaryotic elongation factor 2 (eEF2), responsible for the elongation phase of eukaryotic translocation (**Figure 19**) (Schneider-Poetsch et al., 2010; Sharma et al., 2019). However, the exact binding site for CHX remains unknown and it is unclear if CHX acts directly or indirectly with eEF2 (Schneider-Poetsch et al., 2010). Surprisingly, even in high concentrations, CHX allows one complete translocation cycle from their initial position on mRNA before interrupting elongation, leading to the accumulation of ribosomes in the start codon (Schneider-Poetsch et al., 2010; Sharma et al., 2019).

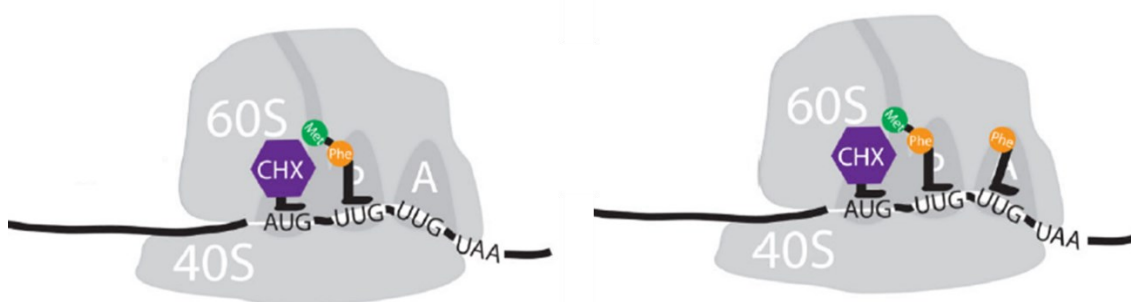


Figure 19 - Proposed inhibition mechanism of cycloheximide (CHX). CHX binds the ribosomal E-site and inhibits eukaryotic translocation by preventing the attachment of eukaryotic elongation factor 2. However, the attachment of CHX leads to the skewing of the deacylated tRNA binding to the E-site allowing one complete translocation round from their initial position on mRNA before interrupting elongation. This leads to the accumulation of ribosomes in the start codon. For abbreviations please see page ix (Schneider-Poetsch et al., 2010).

The acquired fluorescence live-cells images show a slight decrease in MCT1 expression at the plasma membrane when cells are treated with CHX, when compared to the standard, more pronounced after 24 h of incubation (**Figure 20A**). Comparable results were obtained by Talaia and colleagues where CHX triggered Jen1 protein internalization (Talaia et al., 2017). Jen1 is a lactate transporter well characterized in *Saccharomyces cerevisiae*.

Analysis of fluorescence signal strength (**Figure 20B**) suggested a decrease of fluorescence signal strength in cells treated with CHX compared with the standard, after 6 h and 24 h of incubation. The fluorescence signal strength response to treatment with CHX showed analogous results from previously published results, where after 24 h of incubation with this compound and in glucose medium, the MCT1 protein expression decreased in transfected SiHa cells lysates (Saedeleer et al., 2014). Mean fluorescence signal strength values for the standard and cells treated with CHX after 6 h and 24 h of incubation are presented in **Table 4**.

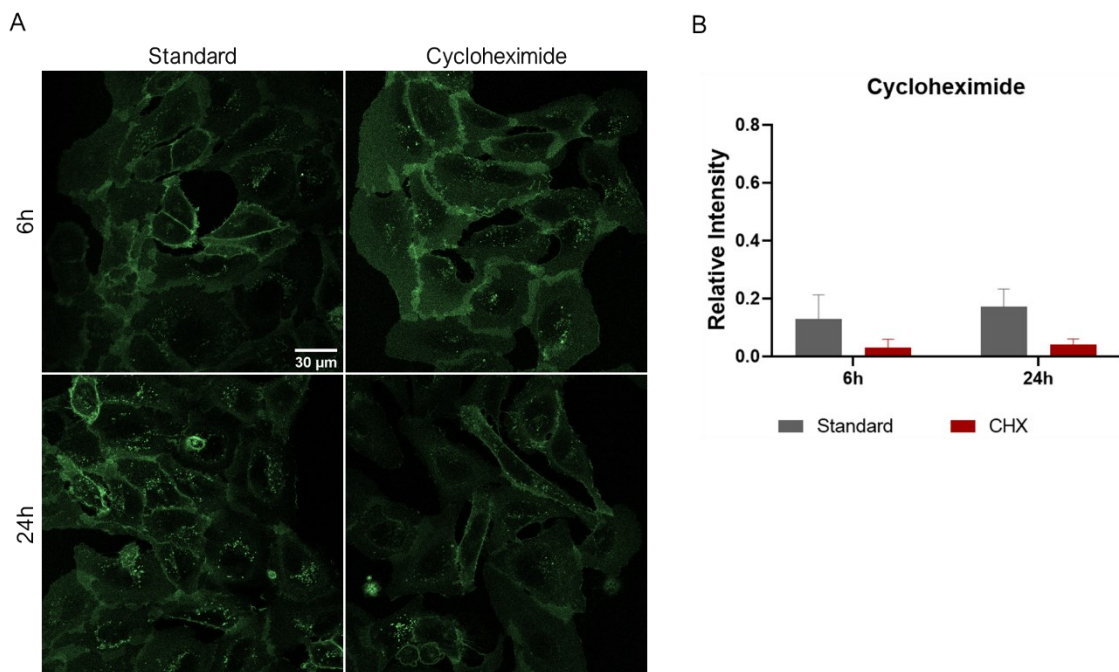


Figure 20 – Analysis of MCT1 expression in gene-edited U2OS cells after 6 h and 24 h of incubation with cycloheximide (CHX) by confocal microscopy imaging (A) and fluorescence quantification (B). U2OS cells were treated with 3.55×10^5 nM CHX. Images are representative of two independent experiments. Scale bar corresponds to 30 μm. The quantification of fluorescence signal strength was normalized by dividing the total fluorescence intensity per number of cells in each image acquired using confocal microscopy imaging. Error bars represent SD.

Table 4 - Mean fluorescence signal strength values for the standard and cells treated with CHX for 6 h or 24 h (n=2).

Incubation time	Mean fluorescence signal strength values	
	Standard	CHX
6 h	0.1298 ± 0.0829	0.0317 ± 0.0277
24 h	0.1707 ± 0.0621	0.0415 ± 0.0191

3.4. Testing the effect of lenalidomide on MCT1 protein expression in U2OS cells

Recently, an activity for an immunomodulatory drug, lenalidomide, was reported on hematological malignancies and distinct solid tumor types (Eichner et al., 2016). Lenalidomide treatment leads to destabilization of cereblon preventing its binding to CD147 and MCT1 proteins, disturbing the correct folding and maturation of CD147 and MCT1 proteins, and inactivating the CD147–MCT1 transmembrane complex (**Figure 21**) (Eichner et al., 2016).

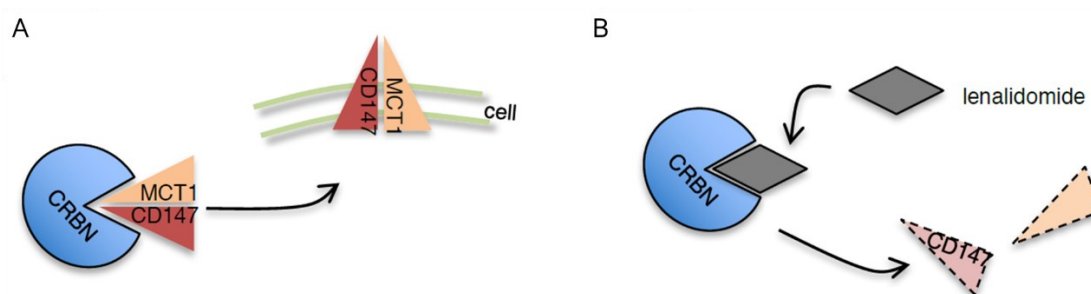


Figure 21 – Schematic illustration of the lenalidomide mechanism. (A) Cereblon (CRBN) functions as a chaperon for CD147-MCT1 association and proper localization in the cell membrane. (B) Lenalidomide binds competitively to CRBN and abrogates CD147–MCT1 transmembrane complex assembly and correct localization (adapted from Heider 2018).

To analyze the effect of lenalidomide on MCT1 expression, cells were visualized by confocal microscopy after 6 h and 24 h of incubation with this compound (**Figure 22A**). After 6 h of incubation, we observe a more clear labeling of the plasma membrane in non-treated cells. This is in accordance with what is described in the literature, where lenalidomide leads to the decrease of MCT1 expression (Eichner et al., 2016; Heider, 2018). It was also reported an increase of MCT1 internalization and its accumulation in the endoplasmic reticulum (ER), in transfected MM1S cells treated with lenalidomide, in a dose and time-dependent manner (Eichner et al., 2016).

In addition to conventional analysis, we calculated the fluorescence signal strength by data analysis (**Figure 22B**). As shown, no significant difference in the fluorescence signal strength was detected between cells treated with lenalidomide when compared with the standard, after 6 h and 24 h of incubation ($p=0.9017$ and $p=0.9945$, respectively). Mean fluorescence signal strength values for the standard and cells treated with lenalidomide for 6 h and 24 h are presented in **Table 5**.

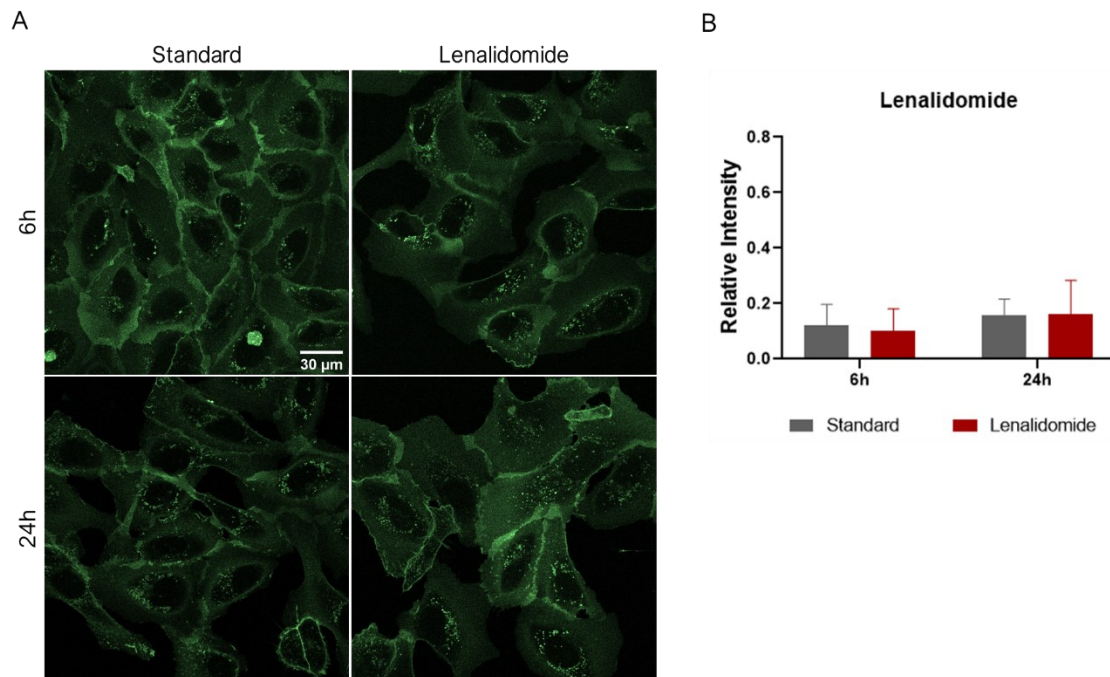


Figure 22 – Analysis of MCT1 expression in gene-edited U2OS cells after 6 h and 24 h of incubation with lenalidomide by confocal microscopy imaging (A) and data analysis (B). U2OS cells were treated with 10 nM lenalidomide. Images are representative of three independent experiments. Scale bar corresponds to 30 μm. The quantification of fluorescence signal strength was normalized by dividing the total fluorescence intensity per number of cells of each image acquired using confocal microscopy imaging. Error bars represent SD. No significant differences were determined.

Table 5 - Mean fluorescence signal strength values for the standard and cells treated with lenalidomide for 6 h or 24 h (n=3).

Time Incubation	Mean fluorescence signal strength values	
	Standard	Lenalidomide
6 h	0.1213 ± 0.0756	0.1022 ± 0.0796
24 h	0.1569 ± 0.0593	0.1623 ± 0.1209

The fact that the decrease in protein expression in our work is not so evident might lay on the fact that distinct cell lines were used in the above-mentioned studies. On the other hand, CRBN is essential for lenalidomide activity, however, the complete molecular and biochemical mechanisms for this immunomodulatory drug resistance remain unknown (Sebastian et al., 2017). In cell lines resistant to lenalidomide, the expression of CRBN protein is greatly reduced (Gandhi et al., 2014; Zhu et al., 2019), some signaling pathways are dysregulated, such as Wnt/ β -catenin, MEK/ERK, or STAT3 pathways, and a higher antioxidative capacity is found (Mogollón et al., 2019; Nass & Efferth, 2018; Sebastian et al., 2017).

Lenalidomide mediates the activation of the Wnt/ β -catenin pathway by suppressing casein kinase 1 α expression while enhancing glycogen synthase kinase 3 α / β phosphorylation, enzymes that function as regulators of signal transduction pathways (Bjorklund et al., 2011; Mogollón et al., 2019). The immunomodulatory drug can disrupt CRBN-E3 ubiquitin ligase complex, responsible for the ubiquitination of diverse cellular proteins, and accumulate β -catenin in the cytoplasm that when translocated to the nucleus caused overexpression of various pro-survival and anti-apoptotic factors increasing cell survival, such as c-Myc protein, and cyclin D1 (Bjorklund et al., 2011; Nass & Efferth, 2018).

It is possible that U2OS cells are less sensitive to lenalidomide. So, more studies need to be performed in order to elucidate this hypothesis. Studies with supplementary lenalidomide doses need to be done to clarify if lenalidomide was used at a non-toxic concentration. On the other hand, since lenalidomide acts in a time-dependent manner, longer incubation periods should be tested.

3.5. Testing the effect of FTY720 on MCT1 protein expression in U2OS cells

FTY720 is a water-soluble sphingolipid synthetic molecule which, can trigger nutrient transporter proteins downregulation, reduce cell surface expression of transporters and access to

nutrients, and induce a starvation-like response in both yeast and mammalian cells (Barthelemy et al., 2017; Finicle et al., 2018; Rosales et al., 2011). When dephosphorylated, FTY720 enters through the plasma membrane and perhaps alters the lipidic microenvironment and structure and activity of plasma membrane proteins, including transporters (**Figure 23**) (Barthelemy et al., 2017). The synthetic molecule disrupts the endocytic trafficking of transporters, including transporters of the following substrates: glucose (such as GLUT1), pyruvate, lactate and acetate (such as MCT1 and MCT4), glutamine (such as ASCT2), leucine (such as LAT1), and cationic amino acid (such as CAT1) (Barthelemy et al., 2017; Finicle et al., 2018).

FTY720 acts by inhibiting phosphatidylinositol 3-phosphate 5-kinase, leading to the accumulation of large endosomes with intraluminal vesicles, to inhibition of autophagosome formation and autophagosome-lysosome fusion (Barthelemy et al., 2017). However, the mechanism of action of this compound is not totally understood. It has been described that FTY720 may function *via* regulation of mTOR complex 1 (mTORC1) and stimulation of protein phosphatase 2A (PP2A), inducing the downregulation of transporters (Barthelemy et al., 2017).

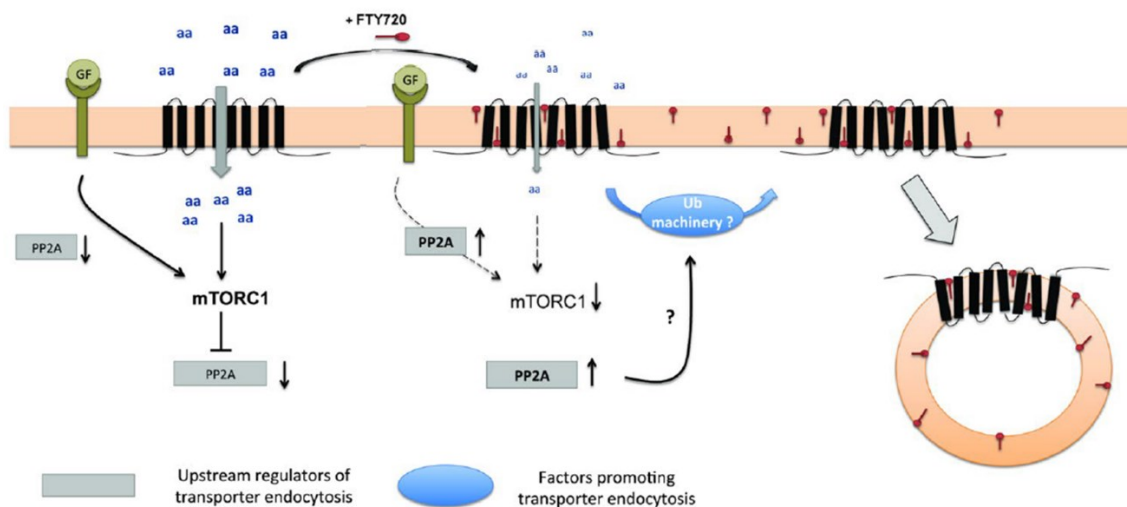


Figure 23 – Diagram of endocytic trafficking of transporters disrupted by FTY720. In mammalian cells, the mechanism of action of this compound is not totally understood. However, dephosphorylation of FTY720 leads to the insertion of these molecules into the plasma membrane, causing a decrease of the intrinsic nutrient transporter’s activity, and consequently nutrient uptake, and inhibition of the TORC1 kinase complex. The reduced mTOR complex 1 (mTORC1) signaling contributes to the stimulation of mechanism involving a Protein Phosphatase 2A (PP2A) which can activate a machinery, possibly dependent on ubiquitin, and promote the endocytosis of nutrient transporters. For abbreviations please check page ix (adapted from Barthelemy et al. 2017).

In images acquired by confocal microscopy analysis (**Figure 24A**), we observed a higher number of internal fluorescent punctuate structures in treated cells when compared to control cells, after 6 h of incubation. Barthelemy *et al.* reported that 6 h of FTY720 treatment was sufficient to promote endocytosis of the LAT1/SLC7A5, a bidirectional L-Type amino acid transporter, very important in leucine uptake, in transfected HeLa cells (Barthelemy et al., 2017). In addition, the SH-BC-893, a highly effective and non-toxic FTY720 analog widely used in many model systems (Rosales et al., 2011), led to the internalization and vascularization of GLUT1/SLC2A1 transporter in HeLa cells after 6 h of incubation, mimicking the effect of glucose starvation as FTY720 (S. M. Kim et al., 2016). It was also reported that FTY720 led to the downregulation of GLUT1 and accumulation in vesicles in the cytoplasm in HeLa and DU145 cells, after 15 h of incubation, and in FL5.12 cells, after 24 h of incubation (Rosales et al., 2011).

The fluorescence signal strength was obtained by data analysis (**Figure 24B**) and no significant differences were found between cells treated with FTY720 when compared to the standard, independently of the incubation time ($p=0.9852$ and $p=0.7099$, after 6 h and 24 h of incubation, respectively). Mean fluorescence signal strength values for the standard and cells treated with FTY720 after 6 h and 24 h of incubation are presented in **Table 6**.

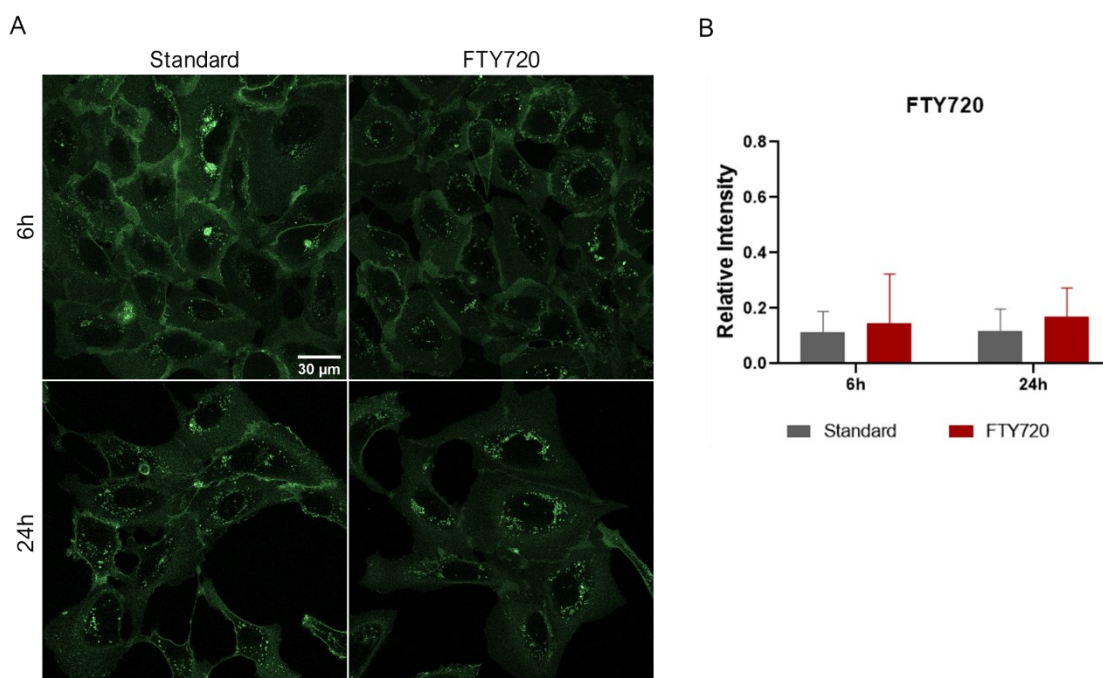


Figure 24 – Analysis of MCT1 expression in gene-edited U2OS cells after 6 h and 24 h of incubation with FTY720 by confocal microscopy imaging (A) and fluorescence quantification (B). U2OS cells were treated with 5.82×10^2 nM FTY720. Images are representative of three independent

experiments. Scale bar corresponds to 30 μm . The quantification of fluorescence signal strength was normalized by dividing the total fluorescence intensity per number of cells of each image acquired using confocal microscopy imaging. Error bar represents SD. No significant differences were determined.

Table 6 - Mean fluorescence signal strength values for the standard and cells treated with FTY720 for 6 h or 24 h (n=3).

Incubation time	Mean fluorescence signal strength values	
	Standard	FTY720
6 h	0.1157 \pm 0.0725	0.1447 \pm 0.1782
24 h	0.1182 \pm 0.0791	0.1695 \pm 0.1042

The concentration of FTY720 used in this study (0.58 μM) was lower than employed in the literature (5 μM). In the future, additional FTY720 concentrations should be studied.

3.6. Effect of Protein kinase C (PKC) activator in disruption of MCT1 trafficking transport in U2OS cells

Protein kinase C (PKC) belongs to a serine/threonine kinases family and can be divided into dissimilar isoforms broadly conserved in eukaryotes (Koivunen et al., 2005; Rosse et al., 2010). Through several different transcription factors, including ERK, JNK, and NF- κ B (Leonard et al., 2015), PKC acts in diverse intracellular signaling processes in physiological and pathological conditions (Isakov, 2018), including tumor formation, proliferation, differentiation, and invasion, and chemoresistance (Katsuya Narumi et al., 2012; Otake et al., 2013).

Activation of this network is mediated by G-protein coupled receptor or receptor tyrosine kinase activation and posteriorly generation of inositol-1,4,5-triphosphate (IP3) and diacylglycerol (DAG) (**Figure 25**) (Matias et al., 2016). DAG activates and translocates PKC to cell membranes while IP3 releases calcium from ER which potentiates PKC activation (Matias et al., 2016). Internalization and translocation of PKC occurs from the plasma membrane to a perinuclear subset of RAB11-positive recycling endosomes by dependent caveolae- and clathrin-mediated endocytosis (M. Liu et al., 2017). Activation of PKC is strictly dependent on a posttranslational maturation process involving a series of phosphorylation steps that culminate in the regulation of gene

expression, cell-cycle progression, cell migration, proliferation and differentiation, cell survival, and apoptosis (Isakov, 2018). However, the downstream pathway of this signaling cascade involved in the regulation of MCT1 expression remains poorly understood (K. Narumi et al., 2010). To understand the role of PKC in the expression and function of mammalian lactate transporter MCT1, we analyzed the PMA, a PKC activator in U2OS human cell lines (K. Narumi et al., 2010).

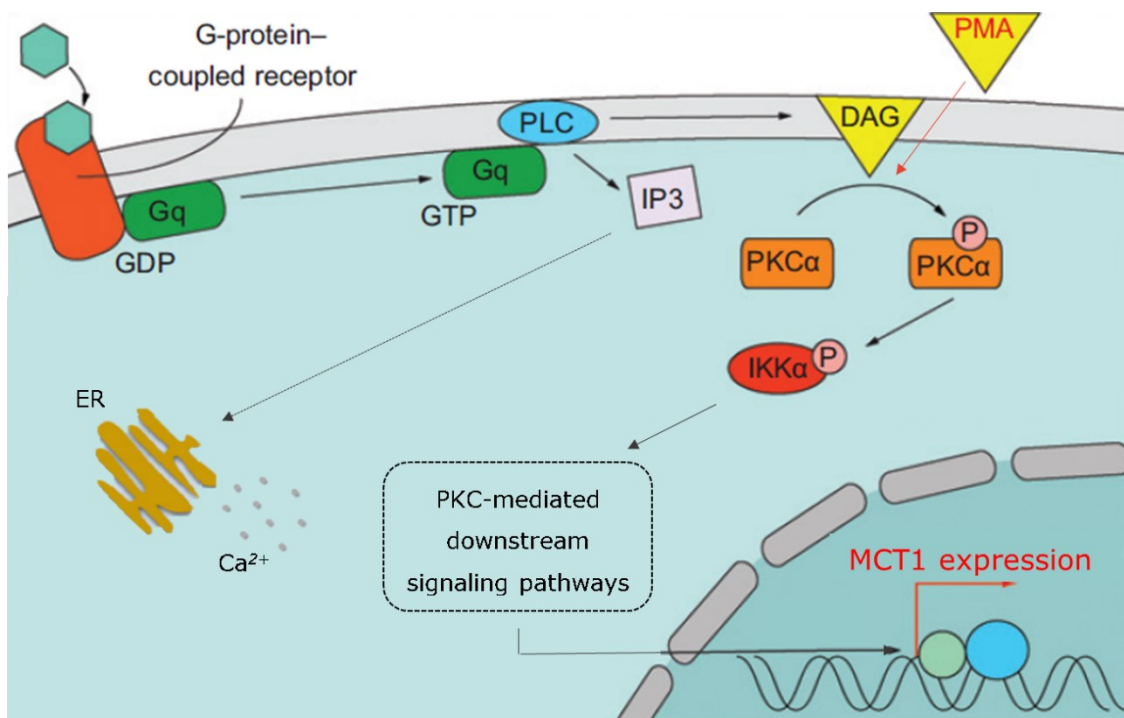


Figure 25 - Schematic representation of PMA activation of Protein Kinase C (PKC). Canonical PKC signaling pathway is mediated by G-protein coupled receptor or receptor tyrosine kinase activation and posteriorly generation of inositol-1,4,5-triphosphate (IP3) and diacylglycerol (DAG) from cell membrane phospholipids. DAG activates and translocates PKC to cell membranes while IP3 releases calcium (Ca²⁺) from the endoplasmic reticulum (ER) which potentiates PKC activation. Then, activated PKC phosphorylates its specific substrates on serine/threonine residues. PMA, a PKC activator, competes with DAG for the same binding site similarly leading to PKC activation. For abbreviations please check page ix (adapted from Leonard et al. 2015).

PMA leads to PKC activation by competing with DAG for the same binding site (**Figure 25**) (M. Liu et al., 2017; Matias et al., 2016).

The impact of PMA treatment in MCT1 expression in U2OS cells was analyzed by confocal microscopy (**Figure 26A**). When cells were treated with PMA there was not such distinct labeling of

the plasma membrane, after 6 h of incubation, in comparison with control cells. After 24h of incubation with PMA, we observed a slight increase in internal cytoplasmatic fluorescence. Similar results were reported by Sorokin *et al.*, where PMA led to the decrease of DAT expression at the plasma membrane and to its subsequent internalization, after 0.5 h of incubation, in transfected HeLa cells.

The fluorescence signal strengths between cells treated with PMA and the standard was similar in both time points (**Figure 26B**). Mean fluorescence signal strength values for the standard and cells treated with PMA after 6 h and 24 h of incubation are presented in **Table 7**.

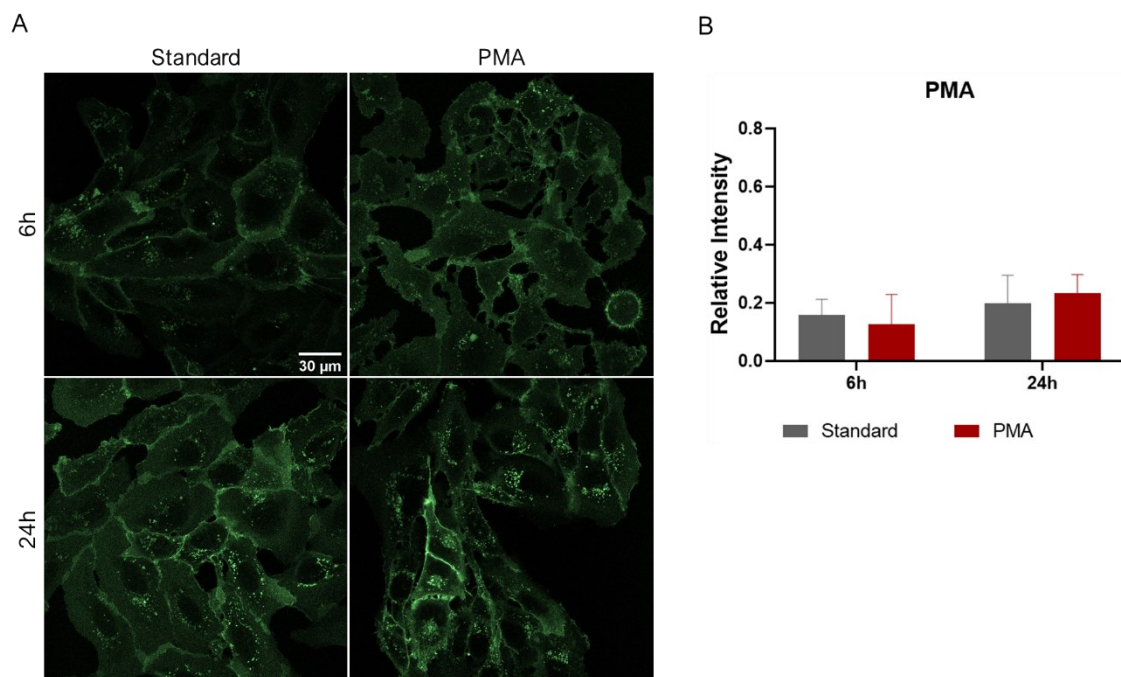


Figure 26 – Analysis of MCT1 expression in gene-edited U2OS cells after 6 h and 24 h of incubation with PMA by confocal microscopy imaging (A) and fluorescence quantification (B). U2OS cells were treated with 1×10^3 nM PMA. Images are representative of two independent experiments. Scale bar corresponds to 30 μm. The quantification of fluorescence signal strength was normalized by dividing the total fluorescence intensity per number of cells in each image acquired using confocal microscopy imaging. Error bars represent SD.

Table 7 - Mean fluorescence signal strength values for the standard and cells treated with PMA for 6 h or 24 h (n=2).

Incubation time	Mean fluorescence signal strength values	
	Standard	PMA
6 h	0.1584 ± 0.0542	0.1257 ± 0.1032
24 h	0.1998 ± 0.0955	0.2321 ± 0.0656

The results acquired are the opposite of what is described in the literature, where the expression level of *MCT1* mRNA and MCT1 protein increased in transfected RD cells lysates after 24 h of incubation with PMA (K. Narumi et al., 2010). Similar outcomes were achieved in Caco-2 cells lysates, where an increase in MCT1 protein expression was observed after 24 h of incubation (Alrefai et al., 2004). In these reports the authors analyzed protein expression by western-blotting and no fluorescence microscopy analysis was carried out.

It has also been described that the expression levels of *MCT4* mRNA, encoding a similar mammalian transporter that mediates the efflux of lactate and that is highly expressed in cancer cells, were enhanced in response to PMA in a time-dependent manner. The expression levels of *MCT4* mRNA increased over time in a period of 24 h in transfected RD cells lysates (Katsuya Narumi et al., 2012). However, the increase in MCT4 protein expression was only detected after 24 h of incubation (Katsuya Narumi et al., 2012).

In addition, it has been described that PMA can increase insulin-independent glucose transporter *GLUT1* mRNA, after 6 h and 12 h of incubation, and *GLUT3* mRNA levels, after 6 h and 24 h of incubation, in RD cells lysates (Otake et al., 2013). Yet, several studies have demonstrated a poor correlation between mRNA and protein expression levels in different human cancer cells (Chen et al., 2002; Koussounadis et al., 2015; Lichtinghagen et al., 2002; Pascal et al., 2008; Shankavaram et al., 2007). Our studies need to be repeated and complemented with western blot analysis.

3.7. Testing the effects of a Wnt/ β -catenin pathway activator and an inhibitor on MCT1 protein expression in U2OS cells

The canonical Wnt/ β -catenin signaling pathway plays an important role in developmental processes, such as cell growth and differentiation. However, the aberrant and constitutive activation

of this signaling pathway has been tightly associated with tumorigenesis of various types of human cancers (Yao et al., 2011). To understand the role of this pathway in the expression and function of MCT1 protein, we studied the effects of LiCl and quercetin, a Wnt/ β -catenin activator and inhibitor, respectively, in the U2OS human cell line.

LiCl inhibits glycogen synthase kinase 3 β protein (GSK-3 β), a negative regulator of the Wnt signaling pathway *in vivo* (Figure 27) (Hedgepeth et al., 1997; Phiel & Klein, 2001). LiCl prevents the formation of a multiprotein complex with GSK-3 β and other proteins, including the adenomatous polyposis coli protein (APC), axin, PP2A, dishevelled (dsh), and β -catenin (Phiel & Klein, 2001). The activation of this signaling pathway blocks the phosphorylation of β -catenin, a market for ubiquitination and degradation *via* the proteasome pathway, allowing the accumulation of this protein in the cytoplasm and its subsequent translocation to the nucleus. This leads to the transcription of Wnt target genes that play a key role in the regulation of cell proliferation (Phiel & Klein, 2001).

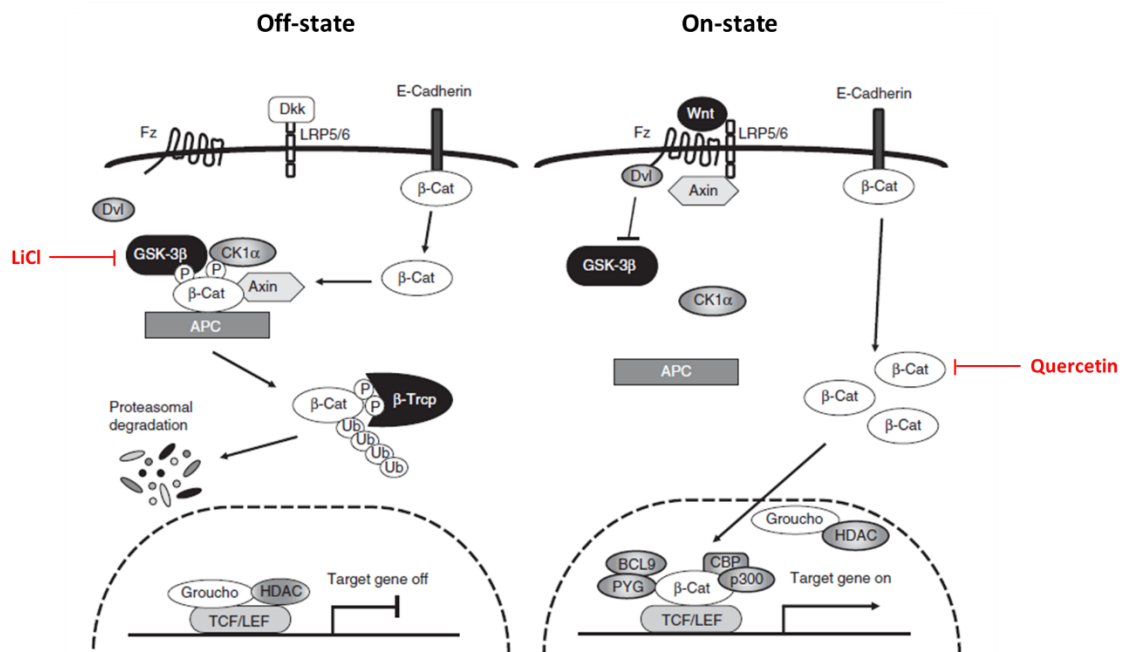


Figure 27 - Schematic representation of the Wnt/ β -catenin pathway and their regulation by an activator, LiCl, and an inhibitor, quercetin, of this network. Dickkopf (Dkk) interacts with low-density lipoprotein receptor-related protein 5/6 (LRP5/6) to inhibit the binding of Wnt ligands. In the absence of Wnt/ β -catenin signaling, “Wnt off” state (Left panel), free cytoplasmic β -catenin is phosphorylated by a complex assembly by casein kinase 1 α (CK1 α), glycogen synthase kinase-3 β (GSK3 β), adenomatous polyposis coli (APC), and Axin and recognized by β -transducin repeat-

containing protein (β -TrCP). β -catenin is subsequently ubiquitinated, which targets it for degradation *via* the proteasome pathway. Interactions between the Wnt ligand and the Fz/LRP receptor trigger Wnt signal transduction, as seen in the 'Wnt on' state (Right panel). Phosphorylation of β -catenin is interrupted, allowing the accumulation of this protein in the cytoplasm and consequently translocation to the nucleus, where forms a complex with TCF/LEF and activates the transcription of Wnt target genes. LiCl, by inhibition of GSK-3 β protein, blocks the formation of a multiprotein complex with GSK-3 β and other proteins (APC, axin, PP2A, dsh, and β -catenin), leading to the accumulation of β -catenin in the cytoplasm. The migration of β -catenin to the nucleus is the key to the transcription of Wnt target genes. Quercetin reduces the stabilization of the β -catenin and consequently inhibits the Wnt pathway. For abbreviations please check page ix (adapted from Yao, Ashihara, and Maekawa 2011).

In live-cells confocal imaging (**Figure 28A**), we observed that treatment with LiCl resulted in a similar expression of MCT1 when compared to control cells after 6 h of incubation. An increase in MCT1 expression and internal EGFP-MCT1 signal was found in cells treated with LiCl over the standard after 24 h of incubation. It has been described that MCT1 expression was dramatically increased in transfected RBE4 cells after 24 h of incubation with LiCl, but the level of *MCT1* mRNA was not affected (Z. Liu et al., 2016).

Analysis of data acquired from confocal microscopy imaging (**Figure 28B**) show a similar fluorescence signal strength in cells treated with LiCl over the standard after 6 h and 24 h of incubation. Mean fluorescence signal strength values for the standard and cells treated with LiCl for 6 h and 24 h are presented in **Table 8**.

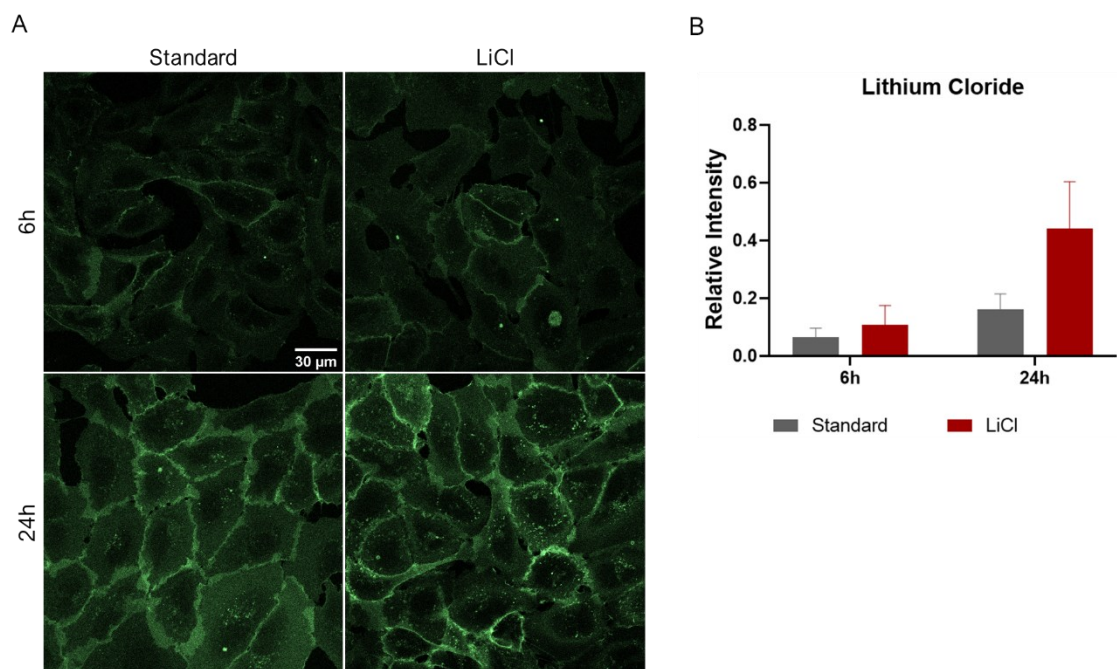


Figure 28 – Analysis of MCT1 expression after 6 h and 24 h of incubation with LiCl by confocal microscopy imaging (A) and fluorescence quantification (B). U2OS cells were treated with 2×10^7 nM LiCl. Images are representative of two independent experiments. Scale bar corresponds to 30 μm. The quantification of fluorescence signal strength was normalized by dividing the fluorescence intensity per number of cells of each image acquired using confocal microscopy imaging. Error bars represent SD.

Table 8 - Mean fluorescence signal strength values for the standard and cells treated with LiCl for 6 h or 24 h (n=2).

Incubation time	Mean fluorescence signal strength values	
	Standard	LiCl
6 h	0.0665 ± 0.0300	0.1084 ± 0.0665
24 h	0.1606 ± 0.0544	0.4401 ± 0.1636

Quercetin is a naturally produced flavonoid (McKay et al., 2015) which has been widely studied for its antioxidative, anti-inflammatory, antiallergic, antiviral, and anticarcinogenic properties (H. Kim et al., 2013; Q. Wang & Morris, 2007). Quercetin goes into the cells *via* GLUT1, 3, and 4 (Gomes, 2014) and leads to the inhibition of the Wnt pathway, by reducing the stabilization of the β-catenin protein (H. Kim et al., 2013), and to blocking diverse efflux transporters, including

the membrane transport of lactate (**Figure 27**) (Q. Wang & Morris, 2007). However, the interaction between flavonoids and plasma membrane transporters is not totally categorized (Shim et al., 2007). This flavonoid applies diverse biological activities in diverse cancer cell models (H. Kim et al., 2013).

The level of MCT1 expression seems lower in treated cells after 6 h of incubation but no differences were found between treated and non-treated cells, after 24 h of exposure with quercetin (**Figure 29A**).

Analysis of fluorescence signal strength (**Figure 29B**) detected a decrease, after 6 h of incubation, and a similar fluorescence signal strength in cells treated with quercetin over the standard, after 24 h of incubation. Due to the high standard deviation acquired for cells treated with quercetin these results need to be confirmed with additional biological replicates. Mean fluorescence signal strength values for the standard and cells treated with quercetin after 6 h and 24 h of incubation are presented in **Table 9**.

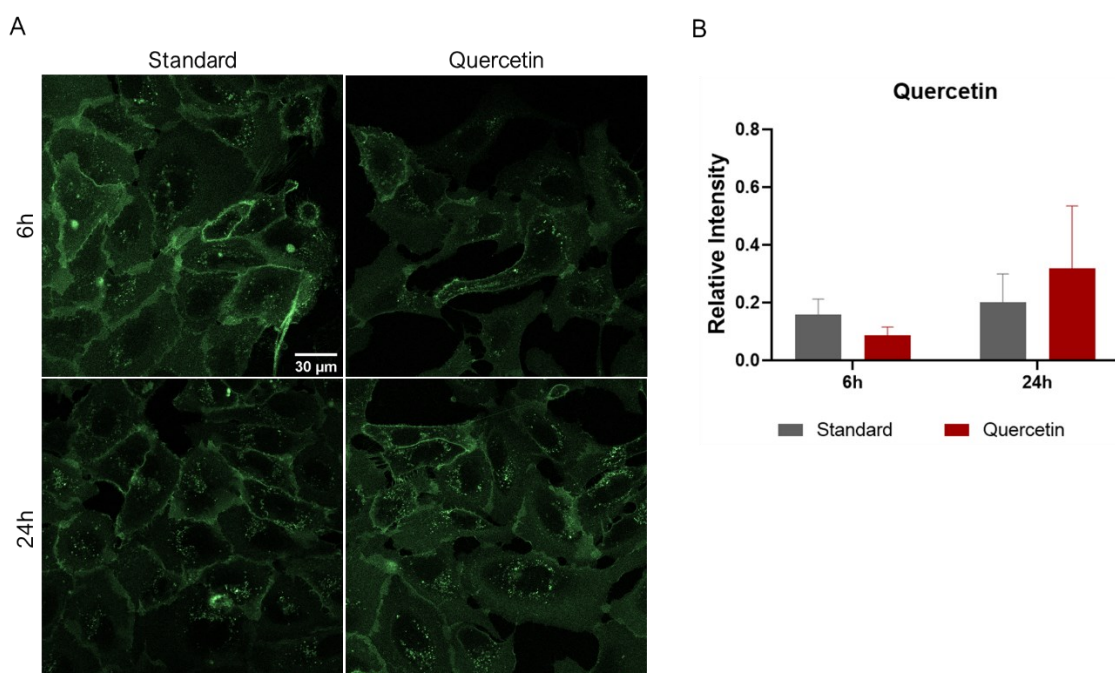


Figure 29 – Analysis of MCT1 expression analysis after 6 h and 24 h of incubation with quercetin by confocal microscopy imaging (A) and fluorescence quantification (B). U2OS cells were treated with 8×10^4 nM quercetin. Images are representative of two independent experiments. Scale bar corresponds to 30 μm. The quantification of fluorescence signal strength was normalized by dividing the fluorescence intensity per number of cells of each image acquired using confocal microscopy imaging. Error bars represent SD.

Table 9 - Mean fluorescence signal strength values for the standard and cells treated with quercetin for 6 h or 24 h (n=2).

Time Incubation	Mean fluorescence signal strength values	
	Standard	Quercetin
6 h	0.1584 ± 0.0542	0.0861 ± 0.0296
24 h	0.1998 ± 0.0955	0.3196 ± 0.2153

It was suggested that quercetin changes glucose metabolism by inhibiting MCT1 activity (Morris & Felmlee, 2008; Payen et al., 2019; Reyes-Farias & Carrasco-Pozo, 2019). Quercetin has been demonstrated to inhibit MCT1- mediated L-lactate uptake (Bröer et al., 1999). However, Izumi *et al.*, found that after 72 h of quercetin incubation (5 µM), cell invasion activity was reduced without affecting the expression of MCT1 protein in human lung cancer A110L cells lysates (Izumi et al., 2011).

Quercetin is a non-specific MCT1 inhibitor that can inhibit other cell targets (Amorim et al., 2015). Le Floch *et al.* demonstrated that specific MCT1 inhibitor by AR-C155858 in Ras-transformed fibroblasts led to the suppression of lactate export, glycolytic rates, and tumor growth (Le Floch et al., 2011). However, with the reestablished of MCT4 expression, cells became resistant to MCT1 inhibition and an increase of tumorigenicity was observed (Le Floch et al., 2011). The MCT1/MCT4 shuttle between normoxic/oxidative and hypoxic/glycolytic cancer cells can be the explanation for the results acquired after 24 h of incubation with quercetin.

4. Final Remarks and Future Perspectives

In cancer cells, the accumulation of high levels of lactate in the extracellular medium due to the Warburg effect and, consequently, the reduction of extracellular pH, are essential conditions for the growth and metastasis of these cells. MCTs are involved in the influx and efflux of lactate from cancer cells and are related to the malignant behavior and aggressiveness of these cells. The overexpression of MCT1 has been identified in several types of cancer as a marker for poor prognosis. The aim of the present work was to analyze the effect of specific metabolic conditions and compounds in MCT1 protein expression and localization, in genetically edited human cancer cell lines.

In this work we could not determine a clear metabolic condition triggering MCT1 internalization. When cells were incubated in media A or B, MCT1 was clearly stabilized at the plasma membrane, contrary to what is reported in the literature. The potential internalization seems to be overtaken by a strong recycling of the protein. In cancer cells, MCT1 can be subjected to various types of regulation (Payen et al., 2019). MCT1 expression levels at the plasma membrane can be regulated by two distinct physiological conditions: a constitutive pathway or a cAMP-dependent pathway. By a constitutive pathway, MCT1 is highly recycled involving clathrin-coated vesicles (CCV) (Smith et al., 2012). MCT1 contains a motif in its C-terminus that allows interactions with adaptor protein 2 (AP-2) complexes and, consequently, promotes the internalization of the transporter by CCV to recycling endosomes (RE) for redistribution at the plasma membrane (Smith et al., 2012; Staruschenko et al., 2005). Because of this mechanism, MCT1 is always in constant movement in the cell, where the velocity of its transport depends on the relationship between the size and the velocity of cells (Uhernik et al., 2014). The CCV mechanism allows the visualization of some MCT1 concentrated points in the cytoplasm without any previous metabolic induction, which is what we find in most conditions tested. Our data highlights the fact that many studies reported in the literature should be revised using cell lines expressing proteins at their endogenous levels.

The work described in this thesis, regarding the analysis of the effects of specific compounds on MCT1 protein expression and trafficking, should be repeated and complemented with further analyzes. Most compounds were only tested twice, due to the pandemic situation that halted all laboratory work for several months. Still, we believe that we gained experience in working with

these compounds and we believe to have at least one promising candidate for further analysis. In our preliminary studies it seems that lithium chloride (LiCl), an activator of the Wnt pathway, results in an increase in MCT1 internalization, after 24 h of incubation.

In the future, we hope to fully characterize the mechanisms underlying the endocytic trafficking and downregulation of MCT1, determining whether a clathrin-dependent or independent process is involved. We also hope to identify the signaling pathways that are associated with MCT1 regulated endocytosis. Moreover, all studies should be complemented with western blot analysis, a semiquantitative analysis of protein expression typically used in this field (Gorr & Vogel, 2015).

Bioimaging, acquired by fluorescence microscopy, is a fundamental technique for tracking and monitoring important biological processes, fundamental biomolecular interactions, and visualizing different cellular and subcellular components, providing higher and more complemented information (Cordina et al., 2018; Payen et al., 2019). However, bioimaging technology has some barriers, such as the autofluorescence of cells and no standardization of image acquisition and processing (Pang et al., 2012). Autofluorescence of cells can happen due to some endogenous fluorescent cell metabolism molecules such as morinamide adenine dinucleotide (NADH), riboflavin and flavin adenine dinucleotide (FAD) coenzymes (Andersson et al., 1998; Aubin, 1979; Hennings et al., 2009; Pang et al., 2012). Autofluorescence of cells cannot be removed with a non-toxic approach (Payen et al., 2019; Van de Lest et al., 1995), which consequently can affect the quantification of fluorescent targeting specific cellular components (Cordina et al., 2018). A new approach to study MCT1 expression using confocal microscopy needs to be evaluated to reduce the autofluorescence and to upgrade the quantification of MCT1 expression. Van de Lest *et al.* proposed a technique that involves the acquisition of two images, one acquired at 480 nm representing both fluorescence and autofluorescence and a second image acquired at 380 nm representing only autofluorescence. The autofluorescence free image was the result of subtraction of the second image from the first one (Van de Lest et al., 1995). However, this method involved a reference image obtained at a different excitation wavelength, which cannot correspond necessarily to the true autofluorescence (Pang et al., 2012). Without a standardization procedure for the acquisition and processing of images acquired with autofluorescence contamination, the quantification of the biomarker signal expression can be often confounded with the autofluorescence of cells and originate false positives (Payen et al., 2019). Even with the optimization of fluorescent microscopy parameters, such as excitation wavelengths, excitation power, microscope apertures, and buffers (Van de Lest et al., 1995), studies involved the

standardization of image acquisition, considering the determination of the best dark pixel intensity, illumination pattern correction, and photobleaching determination need to be performed in order to minimize the autofluorescence of cells (Payen et al., 2019).

MCT1 has been mainly described to be functionally active at the plasma membrane, but also at the mitochondrial and peroxisomal membranes (Payen et al., 2019). MCT1 can be also expressed in the nucleus in low-grade tumors (Pinheiro et al., 2014). Consequently, complementary studies should be done to clarify the role of MCT1 at different cellular locations.

Studies regarding MCT4 expression in the U2OS cell line should also be performed as there seems to be a high correlation between MCT1 and MCT4 expression (MCT1-MCT4 shuttle). A simultaneous analysis of MCT1 and MCT4 expression would promote the understanding of the symbiotic relationship between these transporters. MCT1 degradation can lead to the inhibition of compensatory pathways responsible for the chemo- and radioresistance of cancer cells, opening new targeted therapies (Fisel et al., 2018; Quanz et al., 2018). Also, to better study the interactions of these carriers with other molecules, different biochemical techniques could be used to collect large data sets for molecular interactions and discover the existence of protein complexes in cells (Wilson et al., 2009).

Fluorescence resonance energy transfer (FRET) is a powerful technique with improved spatial (angstrom) and temporal (nanosecond) resolution, distance, range, and sensitivity (Sekar & Periasamy, 2003). FRET has been useful for monitoring several developmentally regulated events in single cells, tissues, and organ cells (De Los Santos et al., 2015). FRET is particularly useful for studying the distance between two distinct sites on a macromolecule, the distance between two fluorophore-tagged proteins and molecular interactions in alive cells (De Los Santos et al., 2015). This mechanism involves the transference of nonradiative energy from a donor fluorophore, in an excited electronic state, to a nearby acceptor chromophore through intermolecular long-range dipole-dipole interactions between the pair of molecules (De Los Santos et al., 2015; Sekar & Periasamy, 2003). The donor molecule is excited and emits energy that is absorbed by the acceptor and loses energy *via* heat or fluorescent emission, called sensitized emission (Sekar & Periasamy, 2003).

Currently, the most commonly used FRET pairs are cyan fluorescent protein (CFP)-yellow fluorescent protein (YFP) variants, mitochondrial fission process 1 (mTFP1)-YFP variants, and GFP-red fluorescent protein (RFP) variants (De Los Santos et al., 2015; Diaspro et al., 2006).

GFP is a bright, stable, non-toxic fluorophore (White & Stelzer, 1999) usually used for molecular and cellular biology studies as a fluorescent marker to study the structural dynamics and proton transfer process in a living cell (Kaur, 2018; Weiss, 2004). However, when green-red FRET pairs are used, the red fluorescent proteins can present low brightness. So, the GFP-mCherry FRET pair is used in fluorescence lifetime imaging microscopy Förster resonance energy transfer (FLIM-FRET) as it exhibits a decent dynamic range due to the relatively high fluorescence lifetime of GFP and relatively large spectral overlap. This could make this technique a better candidate to study the protein dynamics of these carriers (Bajar et al., 2016). FLIM-FRET approach could be a positive added value to future experiments.

In order to perform this technique, plasmids harboring *MCT1* or *MCT4* genes with GFP or mCherry at their 3'- or 5'- ends, need to be designed and constructed by the classical DNA cloning method. After transfection, cells would be able to express MCT1 or MCT4 proteins tagged with either GFP or mCherry at the C- or N-termini (Figure 30) (Wilson et al., 2002).

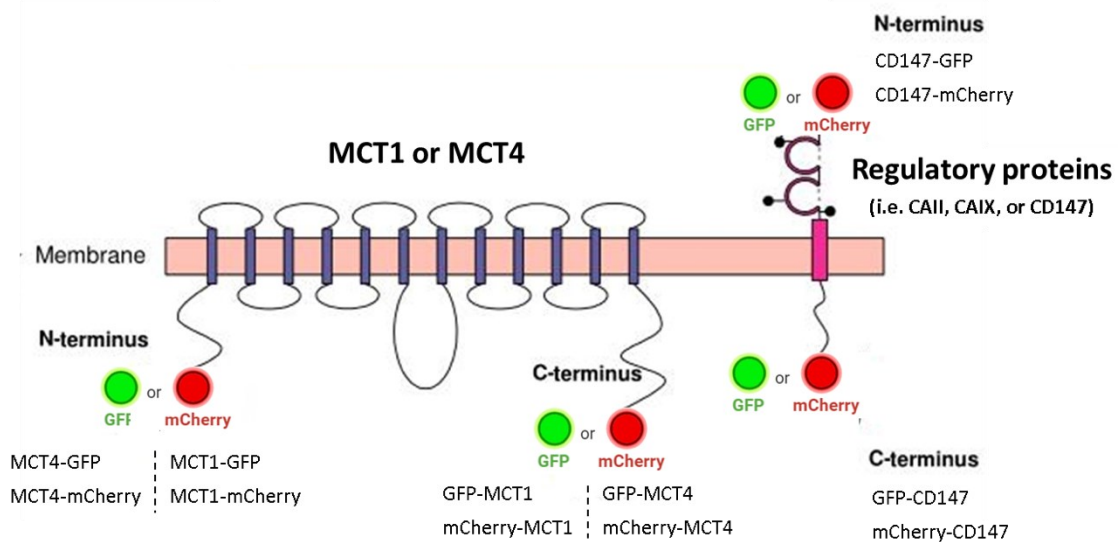


Figure 30 - Schematic representation of MCT1 or MCT4 and their regulatory proteins (i.e. CAII, CAIX and CD147) with GFP or mCherry tagged with either GFP or mCherry at the C- or N-termini and their nomenclature. For abbreviations please check page ix (adapted from Wilson et al., 2002).

FRET analysis would have the potential to possible interactions that may occur between MCT1 and MCT4. Additionally, the plasmids constructions could be used for colocalization studies. The FLIM-FRET technique would also allow the study of the interactions between MCT1 or MCT4 with proteins involved in the regulation of these carriers, such as CAII, CAIX, or CD147. However, these analyzes would require that the above-mentioned strategy for plasmids construction should be followed. In this case the generation of plasmids harboring the regulatory proteins CAII, CAIX, or CD147 with GFP or mCherry at the C- or N- termini would need to be carried out (**Figure 30**) (Wilson et al., 2002).

The study of protein interactions between MCT1 or MCT4 will result in a better understanding of the mechanisms underlying the regulation and endocytic trafficking of both carriers and, therefore, will contribute to develop potential novel therapies.

5. References

- Alrefai, W. A., Tyagi, S., Gill, R., Saksena, S., Hadjiagapiou, C., Mansour, F., Ramaswamy, K., & Dudeja, P. K. (2004). Regulation of butyrate uptake in Caco-2 cells by phorbol 12-myristate 13-acetate. *American Journal of Physiology-Gastrointestinal and Liver Physiology*, *286*(2), G197–G203. doi:10.1152/ajpgi.00144.2003
- Amorim, R., Pinheiro, C., Miranda-Gonçalves, V., Pereira, H., Moyer, M. P., Preto, A., & Baltazar, F. (2015). Monocarboxylate transport inhibition potentiates the cytotoxic effect of 5-fluorouracil in colorectal cancer cells. *Cancer Letters*, *365*(1), 68–78. doi:10.1016/j.canlet.2015.05.015
- Andersson, H., Baechi, T., Hoechl, M., & Richter, C. (1998). Autofluorescence of living cells. *Journal of Microscopy*, *191*(1), 1–7. doi:10.1046/j.1365-2818.1998.00347.x
- Asada, K., & Fukutomi, T. (2003). Reduced Expression of GNA11 and Silencing of MCT1 in Human Breast. *Oncology*, *64*(4), 380–388. doi:10.1159/000070297
- Aubin, J. E. (1979). Autofluorescence of Viable Cultured Mammalian Cells. *The Journal of Histochemistry and Cytochemistry*, *27*(1), 36–43. doi:10.1177/27.1.220325
- Bajar, B. T., Wang, E. S., Zhang, S., Lin, M. Z., & Chu, J. (2016). A Guide to Fluorescent Protein FRET Pairs. *Sensors (Basel, Switzerland)*, *16*(9). doi:10.3390/s16091488
- Bankhead, P. (2014). *Analyzing fluorescence microscopy images with ImageJ*.
- Barthelemy, C., Barry, A. O., Twyffels, L., & André, B. (2017). FTY720-induced endocytosis of yeast and human amino acid transporters is preceded by reduction of their inherent activity and TORC1 inhibition. *Scientific Reports*, *7*(13816), 1–16. doi:10.1038/s41598-017-14124-2
- Baumann, F., Leukel, P., Doerfelt, A., Beier, C. P., Dettmer, K., Oefner, P. J., Kastenberger, M., Kreutz, M., Nickl-jockschat, T., Bogdahn, U., Bosserhoff, A., & Hau, P. (2009). Lactate promotes glioma migration by TGF-beta2-dependent regulation of matrix metalloproteinase-2. *Neuro-Oncology*, *11*(4), 368–380. doi:10.1215/15228517-2008-106
- Bayley, J., & Devilee, P. (2012). The Warburg effect in 2012. *Current Opinion in Oncology*, *24*(1), 62–67. doi:10.1097/CCO.0b013e32834deb9e

- Beckert, S., Farrahi, F., Aslam, R. S., Scheuenstuhl, H., Hussain, M. Z., & Hunt, T. K. (2006). Lactate stimulates endothelial cell migration. *Wound Repair and Regeneration*, *14*(3), 321–324. doi:10.1111/j.1743-6109.2006.00127.x
- Bjorklund, C. C., Ma, W., Wang, Z. Q., Davis, R. E., Kuhn, D. J., Kornblau, S. M., Wang, M., Shah, J. J., & Orłowski, R. Z. (2011). Evidence of a role for activation of Wnt/ β -catenin signaling in the resistance of plasma cells to lenalidomide. *Journal of Biological Chemistry*, *286*(13), 11009–11020. doi:10.1074/jbc.M110.180208
- Boidot, R. (2012). Regulation of Monocarboxylate Transporter MCT1 Expression by p53 Mediates Inward and Outward Lactate Fluxes in Tumors. *Cancer Research*, *72*(4), 939–949. doi:10.1158/0008-5472.CAN-11-2474
- Bola, B. M., Chadwick, A. L., Michopoulos, F., Blount, K. G., Telfer, B. A., Williams, K. J., Smith, P. D., Critchlow, S. E., & Stratford, I. J. (2014). Inhibition of Monocarboxylate Transporter-1 (MCT1) by AZD3965 Enhances Radiosensitivity by Reducing Lactate Transport. *Molecular Cancer Therapeutics*, *13*(12), 2805–2816. doi:10.1158/1535-7163.MCT-13-1091
- Bolognesi, B., & Lehner, B. (2018). Protein Overexpression: Reaching the limit. *eLife*, *7*, 1–3. doi:10.7554/eLife.34595
- Bovenzi, C. D., Hamilton, J., Tassone, P., Johnson, J., Cognetti, D. M., Luginbuhl, A., Keane, W. M., Zhan, T., Tuluc, M., Bar-ad, V., Martinez-outschoorn, U., & Curry, J. M. (2015). Prognostic Indications of Elevated MCT4 and CD147 across Cancer Types: A Meta-Analysis. *BioMed Research International*, *2015*, 242437–14. doi:10.1155/2015/242437
- Brizel, D. M., Schroeder, T., Scher, R. L., Walenta, S., Clough, R. W., Dewhirst, M., & Mueller-Lieser, W. (2001). Elevated Tumor Lactate Concentrations Predict For An Increased Risk Of Metastases In Head-And-Neck Cancer. *International Journal of Radiation Oncology, Biology, Physics*, *51*(2), 349–353. doi:10.1016/s0360-3016(01)01630-3
- Bröer, S., Bröer, A., Schneider, H. P., Stegen, C., Halestrap, A. P., & Deitmer, J. W. (1999). Characterization of the high-affinity monocarboxylate transporter MCT2 in *Xenopus laevis* oocytes. *Biochemical Journal*, *341*(3), 529–535. doi:10.1042/0264-6021:3410529
- Bröer, S., Schneider, H., Bro, A., Rahman, B., Hamprecht, B., & Deitmer, J. W. (1998). Characterization of the monocarboxylate transporter 1 expressed in *Xenopus laevis* oocytes

- by changes in cytosolic pH. *Biochemical Journal*, 333(Pt 1), 167–174. doi:10.1042/bj3330167
- Bueno, V., Binet, I., Steger, U., Bundick, R., Ferguson, D., & Murray, C. (2007). The Specific Monocarboxylate Transporter (MCT1) Prolongs Allograft Survival in the Mouse. *Transplantation*, 84(9), 1204–1207. doi:10.1097/01.tp.0000287543.91765.41
- Chen, G., Gharib, T. G., Huang, C. C., Taylor, J. M. G., Misek, D. E., Kardia, S. L. R., Giordano, T. J., Iannettoni, M. D., Orringer, M. B., Hanash, S. M., & Beer, D. G. (2002). Discordant protein and mRNA expression in lung adenocarcinomas. *Molecular & Cellular Proteomics*, 1(4), 304–313. doi:10.1074/mcp.M200008-MCP200
- Corbet, C., Pourcelle, V., Marchand-brynaert, J., Pourcelle, V., & Marchand-brynaert, J. (2015). Delivery of siRNA targeting tumor metabolism using non-covalent PEGylated chitosan nanoparticles: Identification of an optimal combination of ligand structure, linker and grafting method. *Journal of Controlled Release*, 223, 53–63. doi:10.1016/j.jconrel.2015.12.020
- Cordina, N. M., Sayyadi, N., Parker, L. M., Everest-Dass, A., Brown, L. J., & Packer, N. H. (2018). Reduced background autofluorescence for cell imaging using nanodiamonds and lanthanide chelates. *Scientific Reports*, 8(4521), 1–14. doi:10.1038/s41598-018-22702-1
- Cuff, M. A., Lambert, D. W., & Shirazi-beechey, S. P. (2002). Substrate-induced regulation of the human colonic monocarboxylate transporter, MCT1. *Journal of Physiology*, 539(Pt 2), 361–371. doi:10.1013/jphysiol.2001.014241
- Dang, C. V., Kim, J., Gao, P., & Yuste, J. (2008). The interplay between MYC and HIF in cancer. *Nature Reviews Cancer*, 8(1), 51–56. doi:10.1038/nrc2274
- De Los Santos, C., Chang, C. W., Mycek, M. A., & Cardullo, R. A. (2015). FRAP, FLIM, and FRET: Detection and analysis of cellular dynamics on a molecular scale using fluorescence microscopy. *Molecular Reproduction and Development*, 82, 587–604. doi:10.1002/mrd.22501
- Deberardinis, R. J., & Chandel, N. S. (2016). Fundamentals of cancer metabolism. *Oncology*, 2(5), 1–18. doi:10.1126/sciadv.1600200
- Deberardinis, R. J., Mancuso, A., Daikhin, E., Nissim, I., Yudkoff, M., Wehrli, S., & Thompson, C. B. (2007). Beyond aerobic glycolysis: Transformed cells can engage in glutamine metabolism

- that exceeds the requirement for protein and nucleotide synthesis. *Proceedings of the National Academy of Sciences of the United States of America*, *104*(49), 19345–19350. doi:10.1073/pnas.0709747104
- Deora, A. A., Philp, N., Hu, J., Bok, D., & Rodriguez-boulan, E. (2005). Mechanisms regulating tissue-specific polarity of monocarboxylate transporters and their chaperone CD147 in kidney and retinal epithelia. *Proceedings of the National Academy of Sciences of the United States of America*, *102*(45), 16245–16250. doi:10.1073/pnas.0504419102
- Diaspro, A., Chirico, G., Usai, C., Ramoino, P., & Dobrucki, J. (2006). Photobleaching. In *Handbook of Biological Confocal Microscopy* (pp. 690–702). doi:10.1007/978-0-387-45524-2_39
- Dienstmann, R., Rodon, J., Serra, V., & Tabernero, J. (2014). Picking the Point of Inhibition : A Comparative Review of PI3K/AKT/mTOR Pathway Inhibitors. *Molecular Cancer Therapeutics*, *13*(5), 1021–1032. doi:10.1158/1535-7163.MCT-13-0639
- Doherty, J. R., & Cleveland, J. L. (2013). Targeting lactate metabolism for cancer therapeutics. *The Journal of Clinical Investigation*, *123*(9), 3685–3692. doi:10.1172/JCI69741.transcription
- du Souich, P. du, Roederer, G., & Dufour, R. (2017). Pharmacology & Therapeutics Myotoxicity of statins : Mechanism of action. *Pharmacology and Therapeutics*, *175*, 1–16. doi:10.1016/j.pharmthera.2017.02.029
- Eichner, R., Heider, M., Fernández-Sáiz, V., Van Bebber, F., Garz, A. K., Lemeer, S., Rudelius, M., Targosz, B. S., Jacobs, L., Knorn, A. M., Slawska, J., Platzbecker, U., Germing, U., Langer, C., Knop, S., Einsele, H., Peschel, C., Haass, C., Keller, U., ... Bassermann, F. (2016). Immunomodulatory drugs disrupt the cereblon-CD147-MCT1 axis to exert antitumor activity and teratogenicity. *Nature Medicine*, *22*(7), 735–743. doi:10.1038/nm.4128
- Ferlay, J., Colombet, M., Soerjomataram, I., Mathers, C., Parkin, D. M., Piñeros, M., Znaor, A., & Bray, F. (2019). Estimating the global cancer incidence and mortality in 2018 : GLOBOCAN sources and methods. *International Journal of Cancer*, *144*(8), 1941–1953. doi:10.1002/ijc.31937
- Finicle, B. T., Ramirez, M. U., Liu, G., Selwan, E. M., McCracken, A. N., Yu, J., Joo, Y., Nguyen, J., Ou, K., Roy, S. G., Mendoza, V. D., Corrales, D. V., & Edinger, A. L. (2018). Sphingolipids inhibit endosomal recycling of nutrient transporters by inactivating ARF6. *Journal of Cell*

Science, 131(12), 1–15. doi:10.1242/jcs.213314

Fischer, K., Hoffmann, P., Voelkl, S., Meidenbauer, N., Ammer, J., Edinger, M., Gottfried, E., Schwarz, S., Rothe, G., Hoves, S., Renner, K., Timischl, B., Mackensen, A., Kunz-schughart, L., Andreesen, R., Krause, S. W., & Kreutz, M. (2007). Inhibitory effect of tumor cell-derived lactic acid on human T cells. *Blood*, 109(9), 3812–3820. doi:10.1182/blood-2006-07-035972

Fisel, P., Schaeffeler, E., & Schwab, M. (2018). Clinical and Functional Relevance of the Monocarboxylate Transporter Family in Disease Pathophysiology and Drug Therapy. *Clinical and Translational Science*, 11(4), 352–364. doi:10.1111/cts.12551

Gabrilovich, D. I., Ostrand-rosenberg, S., & Bronte, V. (2012). Coordinated regulation of myeloid cells by tumours. *Nature Reviews Immunology*, 12(4), 253–268. doi:10.1038/nri3175

Gallagher, S. M., Castorino, J. J., & Philp, N. J. (2009). Interaction of monocarboxylate transporter 4 with beta1-integrin and its role in cell migration. *American Journal of Physiology-Cell Physiology*, 296(3), C414–C421. doi:10.1152/ajpcell.00430.2008.

Gallagher, S. M., Castorino, J. J., Wang, D., & Philp, N. J. (2007). Monocarboxylate Transporter 4 Regulates Maturation and Trafficking of CD147 to the Plasma Membrane in the Metastatic Breast Cancer Cell Line MDA-MB-231. *Cancer Research*, 67(9), 4182–4190. doi:10.1158/0008-5472.CAN-06-3184

Gandhi, A. K., Mendy, D., Waldman, M., Chen, G., Rychak, E., Miller, K., Gaidarova, S., Ren, Y., Wang, M., Breider, M., Carmel, G., Mahmoudi, A., Jackson, P., Abbasian, M., Cathers, B. E., Schafer, P. H., Daniel, T. O., Lopez-Girona, A., Thakurta, A., & Chopra, R. (2014). Measuring cereblon as a biomarker of response or resistance to lenalidomide and pomalidomide requires use of standardized reagents and understanding of gene complexity. *British Journal of Haematology*, 164(2), 233–244. doi:10.1111/bjh.12622

Gatenby, R. A., & Gillies, R. J. (2004). Why Do Cancers Have High Aerobic Glycolysis? *Nature Reviews Cancer*, 4(11), 891–899. doi:10.1038/nrc1478

Gibson, T. J., Seiler, M., & Veitia, R. A. (2013). The transience of transient overexpression. *Nature Methods*, 10(8), 715–721. doi:10.1038/nmeth.2534

Global Burden of Disease Cancer Collaboration. (2018). Global, Regional, and National Cancer

- Incidence, Mortality, Years of Life Lost, Years Lived With Disability, and Disability-Adjusted Life-Years for 29 Cancer Groups, 1990 to 2016: A Systematic Analysis for the Global Burden of Disease Study. *JAMA Oncology*, 5(12), 1749–1768. doi:10.1001/jamaoncol.2018.2706
- Global Cancer observatory. (2018). *Estimated age-standardized incidence rates (World) in 2018, all cancers, both sexes, all ages*. https://Gco.larc.fr/Today/Online-Analysis-Map?V=2018&mode=population&mode_population=continents&population=900&populations=900&key=asr&sex=0&cancer=39&type=0&statistic=5&prevalence=0&population_group=0&ages_group%5B%5D=0&ages_group%5B%5D=17&nb_items=5&gro.
- Goetze, K., Walenta, S., Ksiazkiewicz, M., Kunz-schughart, L. A., & Mueller-kliesser, W. (2011). Lactate enhances motility of tumor cells and inhibits monocyte migration and cytokine release. *International Journal Of Oncology*, 39(2), 453–463. doi:10.3892/ijo.2011.1055
- Gomes, N. I. A. P. (2014). *Role of Monocarboxylate Transporters in Prostate Carcinoma*.
- Gómez-Varela, A. I., Stamov, D. R., Miranda, A., Alves, R., Barata-antunes, C., Dambournet, D., Drubin, D. G., Paiva, S., & Beule, P. A. A. De. (2020). Simultaneous co-localized super-resolution fluorescence microscopy and atomic force microscopy : combined SIM and AFM platform for the life sciences. *Scientific Reports*, 10(1122), 1–10. doi:10.1038/s41598-020-57885-z
- Gorr, T. A., & Vogel, J. (2015). Western blotting revisited: Critical perusal of underappreciated technical issues. *Proteomics - Clinical Applications*, 9(3–4), 396–405. doi:10.1002/prca.201400118
- Gottfried, E., Kunz-schughart, L. A., Ebner, S., Mueller-kliesser, W., Hoves, S., Andreesen, R., Mackensen, A., & Kreutz, M. (2006). Tumor-derived lactic acid modulates dendritic cell activation and antigen expression. *Blood*, 107(5), 2013–2022. doi:10.1182/blood-2005-05-1795
- Grass, G. D., Tolliver, L. B., Momka, B., & Toole, B. P. (2013). CD147, CD44 , and the Epidermal Growth Factor Receptor (EGFR) Signaling Pathway Cooperate to Regulate Breast Epithelial Cell Invasiveness. *The Journal Of Biological Chemistry*, 288(36), 26089–26104. doi:10.1074/jbc.M113.497685
- Groussard, C., Morel, I., Chevanne, M., Monnier, M., Cillard, J., Delamarche, A., Morel, I., Chev-

- M., Monnier, M., & Cillard, J. (2000). Free radical scavenging and antioxidant effects of lactate ion: an in vitro study. *Journal of Applied Physiology*, *89*(1), 169–175. doi:10.1152/jap.2000.89.1.169
- Halestrap, A. P. (2012). The Monocarboxylate Transporter Family—Structure and Functional Characterization. *IUBMB Life*, *64*(1), 1–9. doi:10.1002/iub.573
- Halestrap, A. P. (2013). The SLC16 gene family—Structure, role and regulation in health and disease. *Molecular Aspects of Medicine*, *34*(2–3), 337–349. doi:10.1016/j.mam.2012.05.003
- Halestrap, A. P., & Meredith, D. (2004). The SLC16 gene family — from monocarboxylate transporters (MCTs) to aromatic amino acid transporters and beyond. *Pflügers Archiv - European Journal of Physiology*, *447*(5), 619–628. doi:10.1007/s00424-003-1067-2
- Halestrap, A. P., & Price, N. T. (1999). The proton-linked monocarboxylate transporter (MCT) family: structure, function and regulation. *Biochemical Journal*, *343*(Pt 2), 281–299. doi:10.1042/bj3430281
- Halestrap, A. P., & Wilson, M. C. (2012). The Monocarboxylate Transporter Family — Role and Regulation. *IUBMB Life*, *64*(2), 109–119. doi:10.1002/iub.572
- Hanahan, D., & Weinberg, R. A. (2011). Hallmarks of Cancer : The Next Generation. *Cell*, *144*(5), 646–674. doi:10.1016/j.cell.2011.02.013
- Hedgepeth, C. M., Conrad, L. J., Zhang, J., Huang, H. C., Lee, V. M. Y., & Klein, P. S. (1997). Activation of the Wnt signaling pathway: A molecular mechanism for lithium action. *Developmental Biology*, *185*(1), 82–91. doi:10.1006/dbio.1997.8552
- Heider, M. (2018). *IMiDs mediate their anti-myeloma activity via destabilization of the CD147/MCT1 complex.*
- Hennings, L., Kaufmann, Y., Griffin, R., Siegel, E., Novak, P., Corry, P., Moros, E. G., & Shafirstein, G. (2009). Dead or alive? Autofluorescence distinguishes heat-fixed from viable cells. *International Journal of Hyperthermia*, *25*(5), 355–363. doi:10.1080/02656730902964357
- Hentosh, P., Yuh, S. H., Elson, C. E., & Pef, D. M. (2001). Sterol-Independent Regulation of 3-

- Hydroxy-3-methylglutaryl Coenzyme A Reductase in Tumor Cells. *Molecular Carcinogenesis*, 32(3), 154–166. doi:10.1002/mc.1074
- Heredia, F. P. De, & Wood, I. S. (2010). Hypoxia stimulates lactate release and modulates monocarboxylate transporter (MCT1, MCT2, and MCT4) expression in human adipocytes. *Pflügers Archiv - European Journal of Physiology*, 459(3), 509–518. doi:10.1007/s00424-009-0750-3
- Hirschhaeuser, F., Sattler, U. G. A., & Mueller-kliesser, W. (2011). Lactate: A Metabolic Key Player in Cancer. *American Association for Cancer Research*, 71(22), 6921–6926. doi:10.1158/0008-5472.CAN-11-1457
- Hunt, T. K., Aslam, R. S., Beckert, S., Wagner, S., Ghani, Q. P., Hussain, M. Z., Roy, S., & Al, H. E. T. (2007). Forum Original Research Communication. *Antioxidants & Redox Signaling*, 9(8), 1115–1124. doi:10.1089/ars.2007.1674
- Husain, Z., Seth, P., & Sukhatme, V. P. (2013). Tumor-derived lactate and myeloid-derived suppressor cells Linking metabolism to cancer immunology. *Oncolmmunology*, 2(11), e26383-1-e26383-3. doi:10.4161/onci.26383
- Isakov, N. (2018). Protein kinase C (PKC) isoforms in cancer, tumor promotion and tumor suppression. *Seminars in Cancer Biology*, 48, 36–52. doi:10.1016/j.semcan.2017.04.012
- Izumi, H., Takahashi, M., Uramoto, H., Nakayama, Y., Oyama, T., Wang, K. Y., Sasaguri, Y., Nishizawa, S., & Kohno, K. (2011). Monocarboxylate transporters 1 and 4 are involved in the invasion activity of human lung cancer cells. *Cancer Science*, 102(5), 1007–1013. doi:10.1111/j.1349-7006.2011.01908.x
- Janku, F., Yap, T. A., & Meric-bernstam, F. (2018). Targeting the PI3K pathway in cancer: are we making headway? *Clinical Oncology*, 15(5), 273–291. doi:10.1038/nrclinonc.2018.28
- Joerger, A. C., & Fersht, A. R. (2016). The p53 Pathway: Origins, Inactivation in Cancer, and Emerging Therapeutic Approaches. *Annual Review of Biochemistry*, 85(1), 375–404. doi:10.1146/annurev-biochem-060815-014710
- Jones, R. S., & Morris, M. E. (2016). Monocarboxylate Transporters: therapeutic targets and prognostic factors in disease. *Clinical Pharmacology & Therapeutics*, 100(5), 454–463.

doi:10.1002/cpt.418

- Kato, S., Smalley, S., Sadarangani, A., Chen-Lin, K., Oliva, B., Brañes, J., Carvajal, J., Gejman, R., Owen, G. I., & Cuello, M. (2010). Lipophilic but not hydrophilic statins selectively induce cell death in gynaecological cancers expressing high levels of HMGCoA reductase. *Journal of Cellular and Molecular Medicine*, *14*(5), 1180–1193. doi:10.1111/j.1582-4934.2009.00771.x
- Kaur, J. (2018). Green fluorescent protein chromophore versus isolated chromophore and its derivatives in organic solvents: A novel thought to engineer GFP for the rational design of organic solvent biosensor. *Research Reports*, *2*, e1–e14. doi:10.9777/rr.2018.10335
- Kazue, S., Marie, N., Mieko, S., & Shinjo, O. (2011). Metabolism and Brain Cancer. *Clinics*, *66*(S1), 33–43. doi:10.1590/S1807-59322011001300005
- Keith, B., Johnson, R. S., & Simon, M. C. (2011). HIF1 α and HIF2 α : sibling rivalry in hypoxic tumour growth and progression. *Nature Reviews Cancer*, *12*(1), 9–22. doi:10.1038/nrc3183
- Kido, Y., Tamai, I., Okamoto, M., Suzuki, F., & Tsuji, A. (2000). Functional Clarification of MCT1-Mediated Transport of Monocarboxylic Acids at the Blood- Brain Barrier Using In Vitro Cultured Cells and In Vivo BUI Studies. *Pharmaceutical Research*, *17*(1), 55–62. doi:10.1023/A:1007518525161
- Kikutani, Y., Kobayashi, M., Konishi, T., Sasaki, S., Narumi, K., Furugen, A., Takahashi, N., & Iseki, K. (2016). Involvement of Monocarboxylate Transporter 4 Expression in Statin-Induced Cytotoxicity. *Journal of Pharmaceutical Sciences*, *105*(4), 1544–1549. doi:10.1016/j.xphs.2016.01.014
- Kim, H., Seo, E. M., Sharma, A. R., Ganbold, B., Park, J., Sharma, G., Kang, Y. H., Song, D. K., Lee, S. S., & Nam, J. S. (2013). Regulation of Wnt signaling activity for growth suppression induced by quercetin in 4T1 murine mammary cancer cells. *International Journal of Oncology*, *43*(4), 1319–1325. doi:10.3892/ijo.2013.2036
- Kim, S. M., Roy, S. G., Chen, B., Nguyen, T. M., Mcmonigle, R. J., Mccracken, A. N., Zhang, Y., Kofuji, S., Hou, J., Selwan, E., Finicle, B. T., Nguyen, T. T., Ravi, A., Ramirez, M. U., Wiher, T., Guenther, G. G., Kono, M., Sasaki, A. T., Weisman, L. S., ... Edinger, A. L. (2016). Targeting cancer metabolism by simultaneously disrupting parallel nutrient access pathways.

- The Journal of Clinical Investigation*, 126(11), 4088–4102. doi:10.1172/JCI87148.for
- Kirk, P., Wilson, M. C., Heddle, C., Brown, M. H., Barclay, A. N., & Halestrap, A. P. (2000). CD147 is tightly associated with lactate transporters MCT1 and MCT4 and facilitates their cell surface expression. *The EMBO Journal*, 19(15), 3896–3904. doi:10.1093/emboj/19.15.3896
- Koivunen, J., Aaltonen, V., & Peltonen, J. (2005). Protein kinase C (PKC) family in cancer progression. *Cancer Letters*, 235(2006), 1–10. doi:10.1016/j.canlet.2005.03.033
- Koussounadis, A., Langdon, S. P., Um, I. H., Harrison, D. J., & Smith, V. A. (2015). Relationship between differentially expressed mRNA and mRNA-protein correlations in a xenograft model system. *Scientific Reports*, 5(10775), 1–9. doi:10.1038/srep10775
- Kroemer, G., & Pouyssegur, J. (2008). Tumor Cell Metabolism : Cancer’s Achilles’ Heel. *Cancer Cell*, 13(6), 472–482. doi:10.1016/j.ccr.2008.05.005
- Le Floch, R., Chiche, J., Marchiq, I., Naïken, T., Ilk, K., Murray, C. M., Critchlow, S. E., Roux, D., Simon, M. P., & Pouyssegur, J. (2011). CD147 subunit of lactate/H⁺ symporters MCT1 and hypoxia-inducible MCT4 is critical for energetics and growth of glycolytic tumors. *Proceedings of the National Academy of Sciences of the United States of America*, 108(40), 16663–16668. doi:10.1073/pnas.1106123108
- Leonard, B., McCann, J. L., Starrett, G. J., Kosyakovsky, L., Luengas, E. M., Molan, A. M., Burns, M. B., McDougle, R. M., Parker, P. J., Brown, W. L., & Harris, R. S. (2015). The PKC/NF-κB signaling pathway induces APOBEC3B expression in multiple human cancers. *Cancer Research*, 75(21), 4538–4547. doi:10.1158/0008-5472.CAN-15-2171-T
- Liberti, M. V., & Locasale, J. W. (2016). The Warburg Effect: How Does it Benefit Cancer Cells? *Trends in Biochemical Sciences*, 41(3), 211–218. doi:10.1016/j.tibs.2015.12.001
- Lichtinghagen, R., Musholt, P. B., Lein, M., Römer, A., Rudolph, B., Kristiansen, G., Hauptmann, S., Schnorr, D., Loening, S. A., & Jung, K. (2002). Different mRNA and protein expression of matrix metalloproteinases 2 and 9 and tissue inhibitor of metalloproteinases 1 in benign and malignant prostate tissue. *European Urology*, 42(4), 398–406. doi:10.1016/S0302-2838(02)00324-X
- Lisanti, M. P., Martinez-outschoorn, U. E., & Sotgia, F. (2013). Oncogenes induce the cancer associated fibroblast phenotype: Metabolic symbiosis and “fibroblast addiction” are new

- therapeutic targets for drug discovery. *Cell Cycle*, *12*(17), 2723–2732. doi:10.4161/cc.25695
- Liu, M., Clarke, C. J., Salama, M. F., Choi, Y. J., Obeid, L. M., & Hannun, Y. A. (2017). Co-ordinated activation of classical and novel PKC isoforms is required for PMA-induced mTORC1 activation. *Plos One*, *12*(9), 1–16. doi:10.1371/journal.pone.0184818
- Liu, Z., Sneve, M., Haroldson, T. A., Smith, J. P., & Drewes, L. R. (2016). Regulation of monocarboxylic acid transporter 1 trafficking by the canonical Wnt/ β -catenin pathway in rat brain endothelial cells requires cross-talk with notch signaling. *Journal of Biological Chemistry*, *291*(15), 8059–8069. doi:10.1074/jbc.M115.710277
- Lu, H., Forbes, R. A., & Verma, A. (2002). Hypoxia-inducible Factor 1 Activation by Aerobic Glycolysis Implicates the Warburg Effect in Carcinogenesis*. *The Journal Of Biological Chemistry*, *277*(26), 23111–23115. doi:10.1074/jbc.M202487200
- Marhaba, R., & Zoller, M. (2004). CD44 in cancer progression: Adhesion, migration and growth regulation. *Journal of Molecular Histology*, *35*(3), 211–231. doi:10.1023/B:HIJO.0000032354.94213.69
- Matias, D., Bessa, C., Fátima Simões, M., Reis, C. P., Saraiva, L., & Rijo, P. (2016). Natural Products as Lead Protein Kinase C Modulators for Cancer Therapy. In *Studies in Natural Products Chemistry* (Vol. 50). doi:10.1016/B978-0-444-63749-9.00002-5
- Matuszewicz, L., Meissner, J., & Toporkiewicz, M. (2015). The effect of statins on cancer cells – review. *Tumor Biology*, *36*(7), 4889–4904. doi:10.1007/s13277-015-3551-7
- Mazurek, S., Zwerschke, W., Jansen-durr, P., & Eigenbrodt, E. (2001a). Effects of the human papilloma virus HPV-16 E7 oncoprotein on glycolysis and glutaminolysis: role of pyruvate kinase type M2 and the glycolytic-enzyme complex. *Biochemical Journal*, *356*(Pt 1), 247–256. doi:10.1038/sj.onc.1204792
- Mazurek, S., Zwerschke, W., Jansen-durr, P., & Eigenbrodt, E. (2001b). Metabolic cooperation between different oncogenes during cell transformation: interaction between activated ras and HPV-16 E7. *Oncogene*, *20*(47), 6891–6898. doi:10.1038/sj.onc.1204792
- McKay, T. B., Lyon, D., Sarker-Nag, A., Priyadarsini, S., Asara, J. M., & Karamichos, D. (2015). Quercetin Attenuates Lactate Production and Extracellular Matrix Secretion in Keratoconus.

Scientific Reports, 5(9003), 1–7. doi:10.1038/srep09003

- Mehibel, M., Ortiz-martinez, F., Voelxen, N., Boyers, A., Chadwick, A., Telfer, B. A., Mueller-klieser, W., West, C. M., Critchlow, S. E., Williams, K. J., & Stratford, I. J. (2018). Statin-induced metabolic reprogramming in head and neck cancer: a biomarker for targeting monocarboxylate transporters. *Science*, 361(6404), 1–12. doi:10.1126/science.1259111
- Miranda-Gonçalves, V., Bezerra, F., Costa-Almeida, R., Freitas-Cunha, M., Soares, R., Martinho, O., Reis, R. M., Pinheiro, C., & Baltazar, F. (2017). Monocarboxylate transporter 1 is a key player in glioma-endothelial cell crosstalk. *Molecular Carcinogenesis*, 56(12), 2630–2642. doi:10.1002/mc.22707
- Miranda-Gonçalves, V., Granja, S., Martinho, O., Honavar, M., Pojo, M., Costa, B. M., Pires, M. M., Pinheiro, C., Cordeiro, M., Bebiano, G., Costa, P., Reis, R. M., & Baltazar, F. (2016). Hypoxia-mediated upregulation of MCT1 expression supports the glycolytic phenotype of glioblastomas. *Oncotarget*, 7(29), 46335–46353. doi:10.18632/oncotarget.10114
- Mogollón, P., Díaz-Tejedor, A., Algarín, E. M., Paíno, T., Garayoa, M., & Ocio, E. M. (2019). Biological Background of Resistance to Current Standards of Care in Multiple Myeloma. *Cells*, 8(11), 1432. doi:10.3390/cells8111432
- Moriya, H. (2015). Quantitative nature of overexpression experiments. *Molecular Biology of the Cell*, 26(22), 3932–3939. doi:10.1091/mbc.E15-07-0512
- Morris, M. E., & Felmler, M. A. (2008). Overview of the proton-coupled MCT (SLC16A) family of transporters: Characterization, function and role in the transport of the drug of abuse γ -Hydroxybutyric acid. *The AAPS Journal*, 10(2), 311–321. doi:10.1208/s12248-008-9035-6
- Nancolas, B., Guo, L., Zhou, R., Nath, K., Nelson, D. S., Leeper, D. B., Blair, I. A., Glickson, J. D., & Halestrap, A. P. (2016). The anti-tumour agent lonidamine is a potent inhibitor of the mitochondrial pyruvate carrier and plasma membrane monocarboxylate transporters. *Biochemical Journal*, 473(7), 929–936. doi:10.1042/BJ20151120
- Narumi, K., Furugen, A., Kobayashi, M., Otake, S., Itagaki, S., & Iseki, K. (2010). Regulation of Monocarboxylate Transporter 1 in Skeletal Muscle Cells by Intracellular Signaling Pathways. *Biological and Pharmaceutical Bulletin*, 33(9), 1568–1573. doi:10.1248/bpb.33.1568

- Narumi, Katsuya, Kobayashi, M., Otake, S., Furugen, A., Takahashi, N., Ogura, J., Itagaki, S., Hirano, T., Yamaguchi, H., & Iseki, K. (2012). Regulation of human monocarboxylate transporter 4 in skeletal muscle cells : The role of protein kinase C (PKC). *International Journal of Pharmaceutics*, *428*(1–2), 25–32. doi:10.1016/j.ijpharm.2012.02.021
- Nass, J., & Efferth, T. (2018). Drug targets and resistance mechanisms in multiple myeloma. *Cancer Drug Resistance*, *1*, 87–117. doi:10.20517/cdr.2018.04
- Nath, K., Guo, L., Nancolas, B., Nelson, D. S., Shestov, A. A., Lee, S. C., Roman, J., Zhou, R., Leeper, D. B., Halestrap, A. P., Blair, I. A., & Glickson, J. D. (2016). Mechanism of antineoplastic activity of lonidamine. *Biochimica et Biophysica Acta - Reviews on Cancer*, *1866*(2), 151–162. doi:10.1016/j.bbcan.2016.08.001
- Noor, S. I., Dietz, S., Heidtmann, H., Boone, C. D., Mckenna, R., Deitmer, J. W., & Becker, H. M. (2015). Analysis of the Binding Moiety Mediating the Interaction between Monocarboxylate Transporters and Carbonic Anhydrase II. *Journal Of Biological Chemistry*, *290*(7), 4476–4486. doi:10.1074/jbc.M114.624577
- Noor, S. I., Jamali, S., Ames, S., Langer, S., Deitmer, J. W., & Becker, H. M. (2018). A surface proton antenna in carbonic anhydrase II supports lactate transport in cancer cells. *ELife*, *7*, e35176. doi:10.7554/eLife.35176
- Noorolyai, S., Shajari, N., Baghbani, E., Sadreddini, S., & Baradaran, B. (2019). The relation between PI3K/AKT signalling pathway and cancer. *Gene*, *698*, 120–128. doi:10.1016/j.gene.2019.02.076
- Otake, S., Kobayashi, M., Narumi, K., Sasaki, S., Kikutani, Y., Furugen, A., Watanabe, M., Takahashi, N., Ogura, J., & Yamaguchi, H. (2013). Regulation of the Expression and Activity of Glucose and Lactic Acid Metabolism-Related Genes by Protein Kinase C in Skeletal Muscle Cells. *Biological and Pharmaceutical Bulletin*, *36*(9), 1435–1439. doi:10.1002/1097-0134(20010501)43:2<175::AID-PROT1029>3.0.CO;2-%23
- Ovens, M. J., Davies, A. J., Wilson, M. C., Murray, C. M., & Halestrap, A. P. (2010). AR-C155858 is a potent inhibitor of monocarboxylate transporters MCT1 and MCT2 that binds to an intracellular site involving transmembrane helices 7 – 10. *Biochemical Journal*, *425*(3), 523–530. doi:10.1042/BJ20091515

- Pahlman, C., Qi, Z., Murray, C. M., Ferguson, D., & Bundick, R. V. (2013). Immunosuppressive properties of a series of novel inhibitors of the monocarboxylate transporter MCT-1. *Transplant International*, *26*(1), 22–29. doi:10.1111/j.1432-2277.2012.01579.x
- Pang, Z., Laplante, N. E., & Filkins, R. J. (2012). Dark pixel intensity determination and its applications in normalizing different exposure time and autofluorescence removal. *Journal of Microscopy*, *246*(1), 1–10. doi:10.1111/j.1365-2818.2011.03581.x
- Park, S. J., Smith, C. P., Wilbur, R. R., Cain, C. P., Kallu, S. R., Valasapalli, S., Sahoo, A., Guda, M. R., Tsung, A. J., & Velpula, K. K. (2018). An overview of MCT1 and MCT4 in GBM: small molecule transporters with large implications. *American Journal of Cancer Research*, *8*(10), 1967–1976.
- Pascal, L. E., True, L. D., Campbell, D. S., Deutsch, E. W., Risk, M., Coleman, I. M., Eichner, L. J., Nelson, P. S., & Liu, A. Y. (2008). Correlation of mRNA and protein levels: Cell type-specific gene expression of cluster designation antigens in the prostate. *BMC Genomics*, *9*(246), 1–13. doi:10.1186/1471-2164-9-246
- Paul, C., Bundick, R., Craggs, R., Donald, D., Edwards, S., Holness, E., Montgomery, A., Qi, Z., Ekberg, H., & Murray, C. (2017). The effect of Monocarboxylate Transporter (MCT1) inhibitor, ARC117977 on accelerated rejection of cardiac grafts in pre-sensitised rats and concordant xenotransplantation. *Trends in Transplant*, *10*(4), 1–6. doi:10.15761/TiT.1000241
- Payen, V. L., Mina, E., Hée, V. F. Van, Porporato, P. E., & Sonveaux, P. (2019). Monocarboxylate transporters in cancer. *Molecular Metabolism*, *33*, 48–66. doi:10.1016/j.molmet.2019.07.006
- Pérez-Escuredo, J., Dadhich, R. K., Dhup, S., Cacace, A., Van Hée, V. F., De Saedeleer, C. J., Sboarina, M., Rodriguez, F., Fontenille, M. J., Brisson, L., Porporato, P. E., & Sonveaux, P. (2016). Lactate promotes glutamine uptake and metabolism in oxidative cancer cells. *Cell Cycle*, *15*(1), 72–83. doi:10.1080/15384101.2015.1120930
- Phiel, C. J., & Klein, P. S. (2001). Molecular Targets of Lithium Action. *Annual Review of Pharmacology and Toxicology*, *41*(1), 789–813. doi:10.1146/annurev.pharmtox.41.1.789
- Pinheiro, C., Albergaria, A., Paredes, J., Sousa, B., Dufloth, R., Vieira, D., Schmitt, F., & Baltazar, F. (2010). Monocarboxylate transporter 1 is up-regulated in basal-like breast carcinoma.

- Histopathology*, 56(7), 860–867. doi:10.1111/j.1365-2559.2010.03560.x
- Pinheiro, C., Longatto-filho, A., Azevedo-Silva, J., Casal, M., Schmitt, F. C., & Baltazar, F. (2012). Role of monocarboxylate transporters in human cancers: state of the art. *Journal of Bioenergetics and Biomembranes*, 44(1), 127–139. doi:10.1007/s10863-012-9428-1
- Pinheiro, C., Longatto-Filho, A., Pereira, S. M. M., Etlinger, D., Moreira, M. A. R., Jubé, L. F., Queiroz, G. S., Schmitt, F., & Baltazar, F. (2009). Monocarboxylate transporters 1 and 4 are associated with CD147 in cervical carcinoma. *Disease Markers*, 26(3), 97–103. doi:10.3233/DMA-2009-0596
- Pinheiro, C., Longatto-filho, A., Simões, K., Jacob, C. E., Bresciani, C. J. C., Zilberstein, B., Ceconello, I., Alves, V. A. F., Schmitt, F., & Baltazar, F. (2009). The prognostic value of CD147/EMMPRIN is associated with monocarboxylate transporter 1 co-expression in gastric cancer. *European Journal Of Cancer*, 45(13), 2418–2424. doi:10.1016/j.ejca.2009.06.018
- Pinheiro, C., Penna, V., Morais-Santos, F., Abrahão-Machado, L. F., Ribeiro, G., Curcelli, E. C., Olivieri, M. V., Morini, S., Valença, I., Ribeiro, D., Schmitt, F. C., Reis, R. M., & Baltazar, F. (2014). Characterization of monocarboxylate transporters (MCTs) expression in soft tissue sarcomas: distinct prognostic impact of MCT1 sub-cellular localization. *Journal of Translational Medicine*, 12, 118. doi:10.1186/1479-5876-12-118
- Pinheiro, C., Reis, R. M., Ricardo, S., Longatto-filho, A., Schmitt, F., & Baltazar, F. (2010). Expression of Monocarboxylate Transporters 1, 2, and 4 in Human Tumours and Their Association with CD147 and CD44. *Journal of Biomedicine and Biotechnology*, 2010(3191), 427694. doi:10.1155/2010/427694
- Polanski, R., Hodgkinson, C. L., Fusi, A., Nonaka, D., Priest, L., Kelly, P., Trapani, F., Bishop, P. W., White, A., Critchlow, S. E., Smith, P. D., Blackhall, F., Dive, C., & Morrow, C. J. (2014). Activity of the Monocarboxylate Transporter 1 Inhibitor AZD3965 in Small Cell Lung Cancer. *Clinical Cancer Research*, 20(4), 926–938. doi:10.1158/1078-0432.CCR-13-2270
- Porporato, P. E., Saedeleer, C. J. De, Thissen, J., Feron, O., & Sonveaux, P. (2012). Lactate stimulates angiogenesis and accelerates the healing of superficial and ischemic wounds in mice. *Angiogenesis*, 15(4), 581–592. doi:10.1007/s10456-012-9282-0

- Powell, J. M., Plummer, N. W., Scappini, E. L., Tucker, C. J., & Jensen, P. (2019). DEFiNE: A method for enhancement and quantification of fluorescently labeled axons. *Frontiers in Neuroanatomy*, *12*(117), 1–11. doi:10.3389/fnana.2018.00117
- Puig-Kroger, A., Muniz-Pello, O., Selgas, R., Criado, G., Bajo, M.-A., Sánchez-Tomero, J. A., Alvarez, V., Peso, G. del, Sánchez-Mateos, P., Holmes, C., Faict, D., López-Cabrera, M., Madrenas, J., & Corbí, A. L. (2003). Peritoneal dialysis solutions inhibit the differentiation and maturation of human monocyte-derived dendritic cells: effect of lactate and glucose-degradation products. *Journal of Leukocyte Biology*, *73*(4), 482–492. doi:10.1189/jlb.0902451
- Pullen, T. J., Khan, A. M., Barton, G., Butcher, S. A., Rutter, G. A., Pullen, T. J., Khan, A. M., Barton, G., Butcher, S. A., Pullen, T. J., Khan, A. M., Barton, G., Butcher, S. A., Sun, G., & Rutter, G. A. (2010). Identification of genes selectively disallowed in the pancreatic islet. *Islets*, *2*(2), 89–95. doi:10.4161/isl.2.2.11025
- Pullen, T. J., Xavier, S., Kelsey, G., & Rutter, G. A. (2011). miR-29a and miR-29b Contribute to Pancreatic beta-Cell-Specific Silencing of Monocarboxylate Transporter 1 (Mct1). *Molecular And Cellular Biology*, *31*(15), 3182–3194. doi:10.1128/MCB.01433-10
- Quanz, M., Bender, E., Kopitz, C., Grunewald, S., Schlicker, A., Schwede, W., Eheim, A., Toschi, L., Neuhaus, R., Richter, C., Toedling, J., Merz, C., Lesche, R., Kamburov, A., Siebeneicher, H., Bauser, M., & Hagebarth, A. (2018). Preclinical Efficacy of the Novel Monocarboxylate Transporter 1 Inhibitor BAY-8002 and Associated Markers of Resistance. *Molecular Cancer Therapeutics*, *17*(11), 2285–2297. doi:10.1158/1535-7163.MCT-17-1253
- Reyes-Farias, M., & Carrasco-Pozo, C. (2019). The anti-cancer effect of quercetin: Molecular implications in cancer metabolism. *International Journal of Molecular Sciences*, *20*(13), 1–19. doi:10.3390/ijms20123177
- Riethdorf, S., Reimers, N., Assmann, V., Kornfeld, J., Terracciano, L., Sauter, G., & Pantel, K. (2006). High incidence of EMMPRIN expression in human tumors. *International Journal of Cancer*, *119*(8), 1800–1810. doi:10.1002/ijc.22062
- Romero-Cordoba, S. L., Rodriguez-cuevas, S., Bautista-pina, V., Maffu, A., Ippolito, E. D., Cosentino, G., Baroni, S., Iorio, M. V., & Hidalgo-miranda, A. (2018). Loss of function of miR-342-3p results in MCT1 over-expression and contributes to oncogenic metabolic reprogramming in triple negative breast cancer. *Scientific Reports*, *8*(12252), 1–16.

doi:10.1038/s41598-018-29708-9

- Romero-Garcia, S., Moreno-altamirano, M. M. B., Prado-garcia, H., & Sánchez-garcía, F. J. (2016). Lactate Contribution to the Tumor Microenvironment : Mechanisms, effects on immune Cells and Therapeutic Relevance. *Frontiers in Immunology*, *7*(52), 1–11. doi:10.3389/fimmu.2016.00052
- Rosales, K. R., Singh, G., Wu, K., Chen, J., Janes, M. R., Lilly, M. B., Peralta, E. R., Siskind, L. J., Bennett, M. J., David, A., & Edinger, A. L. (2011). Sphingolipid-based drugs selectively kill cancer cells by down-regulating nutrient transporter proteins. *Biochemical Journal*, *439*(2), 299–311. doi:10.1042/BJ20110853
- Rosse, C., Linch, M., Kermorgant, S., Cameron, A. J. M., Boeckeler, K., & Parker, P. J. (2010). PKC and the control of localized signal dynamics. *Nature Reviews Molecular Cell Biology*, *11*(2), 103–112. doi:10.1038/nrm2847
- Saedeleer, C. J. De, Porporato, P. E., Copetti, T., Pérez-Escuredo, J., Payen, V. L., Brisson, L., Feron, O., & Sonveaux, P. (2014). Glucose deprivation increases monocarboxylate transporter 1 (MCT1) expression and MCT1-dependent tumor cell migration. *Oncogene*, *33*, 4060–4068. doi:10.1038/onc.2013.454
- Sattler, U. G. A., Meyer, S. S., Quennet, V., Hoerner, C., Knoerzer, H., Fabian, C., Yaromina, A., Zips, D., Walenta, S., Baumann, M., & Mueller-klieser, W. (2010). Glycolytic metabolism and tumour response to fractionated irradiation. *Radiotherapy and Oncology*, *94*(1), 102–109. doi:10.1016/j.radonc.2009.11.007
- Schindelin, J., Arganda-carreras, I., Frise, E., Kaynig, V., Longair, M., Pietzsch, T., Preibisch, S., Rueden, C., Saalfeld, S., Schmid, B., Tinevez, J., White, D. J., Hartenstein, V., Eliceiri, K., Tomancak, P., & Cardona, A. (2012). Fiji : an open-source platform for biological-image analysis. *Nature Methods*, *9*(7), 676–682. doi:10.1038/nmeth.2019
- Schneider-Poetsch, T., Ju, J., Eyler, D. E., Dang, Y., Bhat, S., Merrick, W. C., Green, R., Shen, B., & Liu, J. O. (2010). Inhibition of Eukaryotic Translation Elongation by Cycloheximide and Lactimidomycin. *Nature Chemical Biology*, *6*(3), 209–217. doi:10.1038/nchembio.304
- Schulze, A., & Harris, A. L. (2012). How cancer metabolism is tuned for proliferation and vulnerable to disruption. *Nature*, *491*(7424), 364–373. doi:10.1038/nature11706

- Schwickert, G., Walenta, S., Suiulfor, K., Rofstad, E. K., & Mueller-kliesser, W. (1995). Correlation of High Lactate Levels in Human Cervical Cancer with Incidence of Metastasis. *Cancer Research*, *55*(21), 4757–4759.
- Sebastian, S., Zhu, Y. X., Braggio, E., Shi, C. X., Panchabhai, S. C., Van Wier, S. A., Ahmann, G. J., Chesi, M., Bergsagel, P. L., Stewart, A. K., & Fonseca, R. (2017). Multiple myeloma cells capacity to decompose H₂O₂ determines lenalidomide sensitivity. In *Blood* (Vol. 129, Issue 8). doi:10.1182/blood-2016-09-738872
- Sekar, R. B., & Periasamy, A. (2003). Fluorescence resonance energy transfer (FRET) microscopy imaging of live cell protein localizations. *The Journal of Cell Biology*, *160*(5), 629–633. doi:10.1083/jcb.200210140
- Semenza, G. J. (2008). Tumor metabolism: cancer cells give and take lactate. *The Journal of Clinical Investigation*, *118*(12), 3835–3837. doi:10.1172/JCI36843
- Serviço Nacional de Saúde. (2018). *Dia Mundial do Cancro*. <https://www.sns.gov.pt/noticias/2019/02/01/Dia-Mundial-Do-Cancro/>.
- Shankavaram, U. T., Reinhold, W. C., Nishizuka, S., Major, S., Morita, D., Chary, K. K., Reimers, M. A., Scherf, U., Kahn, A., Dolginow, D., Cossman, J., Kaldjian, E. P., Scudiero, D. A., Petricoin, E., Liotta, L., Lee, J. K., & Weinstein, J. N. (2007). Transcript and protein expression profiles of the NCI-60 cancer cell panel: An integromic microarray study. *Molecular Cancer Therapeutics*, *6*(3), 820–832. doi:10.1158/1535-7163.MCT-06-0650
- Sharma, P., Nilges, B. S., Wu, J., & Leidel, S. A. (2019). The translation inhibitor cycloheximide affects ribosome profiling data in a species-specific manner. *BioRxiv*. doi:10.1101/746255
- Shim, C.-K., Cheon, E.-P., Kang, K. W., Seo, K.-S., & Han, H.-K. (2007). Inhibition effect of flavonoids on monocarboxylate transporter 1 (MCT1) in Caco-2 cells. *Journal of Pharmacy and Pharmacology*, *59*(1), 1515–1519. doi:10.1211/jpp.59.11.0008
- Singer, K., Gottfried, E., Kreutz, M., & Mackensen, A. (2011). Suppression of T-cell responses by tumor metabolites. *Cancer Immunol Immunother*, *60*(3), 425–431. doi:10.1007/s00262-010-0967-1
- Slomiany, M. G., Grass, G. D., Robertson, A. D., Yang, X. Y., Maria, B. L., Beeson, C., & Toole, B. P. (2009). Hyaluronan, CD44, and Emprin Regulate Lactate Efflux and Membrane

- Localization of Monocarboxylate Transporters in Human Breast Carcinoma Cells. *Cancer Research*, 69(4), 1293–1302. doi:10.1158/0008-5472.CAN-08-2491
- Smith, J. P., Uhernik, A. L., Li, L., Liu, Z., & Drewes, L. R. (2012). Regulation of Mct1 by cAMP-dependent internalization in rat brain endothelial cells. *Brain Research*, 1480, 1–11. doi:10.1016/j.brainres.2012.08.026
- Sonveaux, P., Végran, F., Schroeder, T., Wergin, M. C., Verrax, J., Rabbani, Z. N., De Saedeleer, C. J., Kennedy, K. M., Diepart, C., Jordan, B. F., Kelley, M. J., Gallez, B., Wahl, M. L., Feron, O., & Dewhirst, M. W. (2008). Targeting lactate-fueled respiration selectively kills hypoxic tumor cells in mice. *Journal of Clinical Investigation*, 118(12), 3930–3942. doi:10.1172/JCI36843
- Sotgia, F., Martinez-outschoorn, U. E., & Lisanti, M. P. (2013). Cancer Metabolism: New Validated Targets for Drug Discovery. *Oncotarget*, 4(8), 1309–1316. doi:10.18632/oncotarget.1182
- Staruschenko, A., Pochynyuk, O., & Stockand, J. D. (2005). Regulation of epithelial Na⁺ channel activity by conserved serine/threonine switches within sorting signals. *Journal of Biological Chemistry*, 280(47), 39161–39167. doi:10.1074/jbc.M509608200
- Stern, R. (2009). Hyaluronidases in Cancer Biology. *Seminars in Cancer Biology*, 18(4), 275–280. doi:10.1016/j.semcancer.2008.03.017
- Takimoto, M., Takeyama, M., & Hamada, T. (2013). Possible involvement of AMPK in acute exercise-induced expression of monocarboxylate transporters MCT1 and MCT4 mRNA in fast-twitch skeletal muscle. *Metabolism*, 62(11), 1633–1640. doi:10.1016/j.metabol.2013.06.010
- Talaia, G., Gournas, C., Saliba, E., Barata-Antunes, C., Casal, M., André, B., Diallinas, G., & Paiva, S. (2017). The α -Arrestin Bul1p Mediates Lactate Transporter Endocytosis in Response to Alkalinization and Distinct Physiological Signals. *Journal of Molecular Biology*, 429(23), 3678–3695. doi:10.1016/j.jmb.2017.09.014
- Uhernik, A. L., Li, L., Lavoy, N., Velasquez, M. J., & Smith, J. P. (2014). Regulation of Monocarboxylic Acid Transporter-1 by cAMP Dependent Vesicular Trafficking in Brain Microvascular Endothelial Cells. *Plos One*, 9(1), 1–11. doi:10.1371/journal.pone.0085957
- Ullah, M. S., Davies, A. J., & Halestrap, A. P. (2006). The Plasma Membrane Lactate Transporter

- MCT4, but Not MCT1, Is Up-regulated by Hypoxia through a HIF-1 alpha-dependent Mechanism. *The Journal Of Biological Chemistry*, 281(14), 9030–9037. doi:10.1074/jbc.M511397200
- Van de Lest, C. H. A., Versteeg, E. M. M., Veerkamp, J. H., & Van Kuppevelt, T. H. (1995). Elimination of autofluorescence in immunofluorescence microscopy with digital image processing. *Journal of Histochemistry and Cytochemistry*, 43(7), 727–730. doi:10.1177/43.7.7608528
- Vander Heiden, M. G., Cantley, L. C., & Thompson, C. B. (2009). Understanding the Warburg Effect: The Metabolic Requirements of Cell Proliferation. *Science*, 324(5930), 1029–1033. doi:10.1126/science.1160809
- Végran, F., Boidot, R., Michiels, C., Sonveaux, P., & Feron, O. (2011). Lactate Influx through the Endothelial Cell Monocarboxylate Transporter MCT1 Supports an NF-κB/IL-8 Pathway that Drives Tumor Angiogenesis. *Cancer Research*, 71(7), 2550–2561. doi:10.1158/0008-5472.CAN-10-2828
- Vogelstein, B., & Kinzler, K. W. (2004). Cancer genes and the pathways they control. *Nature Medicine*, 10(8), 789–799. doi:10.1038/nm1087
- Walenta, S., & Mueller-klieser, W. F. (2004). Lactate: Mirror and Motor of Tumor Malignancy. *Seminars in Radiation Oncology*, 14(3), 267–274. doi:10.1016/j.semradonc.2004.04.004
- Walenta, S., Salameh, A., Lyng, H., Evensen, J. F., Mitze, M., Rofstad, E. K., & Mueller-klieser, W. (1997). Correlation of High Lactate Levels in Head and Neck Tumors with Incidence of Metastasis. *American Journal of Pathology*, 150(2), 409–415.
- Walenta, S., Wetterling, M., Lehrke, M., Schwickert, G., Sundfør, K., Rofstad, E. K., & Mueller-klieser, W. (2000). High Lactate Levels Predict Likelihood of Metastases, Tumor Recurrence, and Restricted Patient Survival in Human Cervical Cancers. *Cancer Research*, 60(4), 916–921.
- Wang, G. L., Jiang, B., Rue, E. A., & Semenza, G. L. (1995). Hypoxia-inducible factor 1 is a basic-helix-loop-helix-PAS heterodimer regulated by cellular O₂ tension. *Genetics*, 92, 5510–5514. doi:10.1073/pnas.92.12.5510
- Wang, Q., & Morris, M. E. (2007). Flavonoids Modulate Monocarboxylate Transporter-1-Mediated

- Transport of gamma-Hydroxybutyrate in Vitro and in Vivo. *Drug Metabolism and Disposition*, 35(2), 201–208. doi:10.1124/dmd.106.012369
- Warburg, O. (1956). On the Origin of Cancer Cells. *SCIENCE*, 123(3191), 309–314. doi:10.1126/science.123.3191.309
- Warburg, O., Wind, F., & Negelein, E. (1927). THE METABOLISM OF TUMORS IN THE BODY. *The Journal of General Physiology*, 8(6), 519–530. doi:10.1085/jgp.8.6.519
- Weiss, M. (2004). Challenges and artifacts in quantitative photobleaching experiments. *Traffic*, 5(9), 662–671. doi:10.1111/j.1600-0854.2004.00215.x
- White, J., & Stelzer, E. (1999). Photobleaching GFP reveals protein dynamics inside live cells. *Trends in Cell Biology*, 9(2), 61–65. doi:10.1016/S0962-8924(98)01433-0
- Wilde, L., Roche, M., Domingo, M., Tanson, K., Philp, N., & Martinez-outschoorn, U. (2017). Metabolic Coupling and the Reverse Warburg Effect in Cancer, implications for novel biomarker and anticancer agent development. *Seminars in Oncology*, 44(3), 198–203. doi:10.1053/j.seminoncol.2017.10.004
- Wilson, M. C., Meredith, D., Bunnun, C., Sessions, R. B., & Halestrap, A. P. (2009). Studies on the DIDS-binding site of monocarboxylate transporter 1 suggest a homology model of the open conformation and a plausible translocation cycle. *Journal of Biological Chemistry*, 284(30), 20011–20021. doi:10.1074/jbc.M109.014217
- Wilson, M. C., Meredith, D., Fox, J. E. M., Manoharan, C., Davies, A. J., & Halestrap, A. P. (2005). Basigin (CD147) Is the Target for Organomercurial Inhibition of Monocarboxylate Transporter Isoforms 1 and 4. *The Journal Of Biological Chemistry*, 280(29), 27213–27221. doi:10.1074/jbc.M411950200
- Wilson, M. C., Meredith, D., & Halestrap, A. P. (2002). Fluorescence Resonance Energy Transfer Studies on the Interaction between the Lactate Transporter MCT1 and CD147 Provide Information on the Topology and Stoichiometry of the Complex in Situ*. *The Journal of Biological Chemistry*, 277(5), 3666–3672. doi:10.1074/jbc.M109658200
- Yang, Q. (2016). Semantic Filtering. *Proceedings of the IEEE Conference on Computer Vision and Pattern Recognition*, 4517–4526.
- Yao, H., Ashihara, E., & Maekawa, T. (2011). Targeting the wnt/b-catenin signaling pathway in

humam cancers. *Expert Opinion on Therapeutic Targets*, 15(7), 873–887. doi:10.1007/978-1-4419-8023-6

Zhao, Z., Wu, M., Zou, C., Tang, Q., Lu, J., Liu, D., Wu, Y., Yin, J., Xie, X., Shen, J., Kang, T., & Wang, J. (2013). Downregulation of MCT1 inhibits tumor growth, metastasis and enhances chemotherapeutic efficacy in osteosarcoma through regulation of the NF-κB pathway. *Cancer Letters*, 342(1), 150–158. doi:10.1016/j.canlet.2013.08.042

Zhong, H., Marzo, A. M. De, Laughner, E., Lim, M., Hilton, D. A., Zagzag, D., Buechler, P., Isaacs, W. B., Semenza, G. L., & Simons, J. W. (1999). Overexpression of Hypoxia-inducible Factor 1a in Common Human Cancers and Their Metastases. *Cancer Research*, 59(22), 5830–5835.

Zhou, X., Hao, Q., & Lu, H. (2019). Mutant p53 in cancer therapy-the barrier or the path. *Journal of Molecular Cell Biology*, 11(4), 293–305. doi:10.1093/jmcb/mjy072

Zhu, Y. X., Shi, C. X., Bruins, L. A., Wang, X., Riggs, D. L., Porter, B., Ahmann, J. M., de Campos, C. B., Braggio, E., Bergsagel, P. L., & Stewart, A. K. (2019). Identification of lenalidomide resistance pathways in myeloma and targeted resensitization using cereblon replacement, inhibition of STAT3 or targeting of IRF4. *Blood Cancer Journal*, 9(2), 19. doi:10.1038/s41408-019-0173-0

6. Appendix

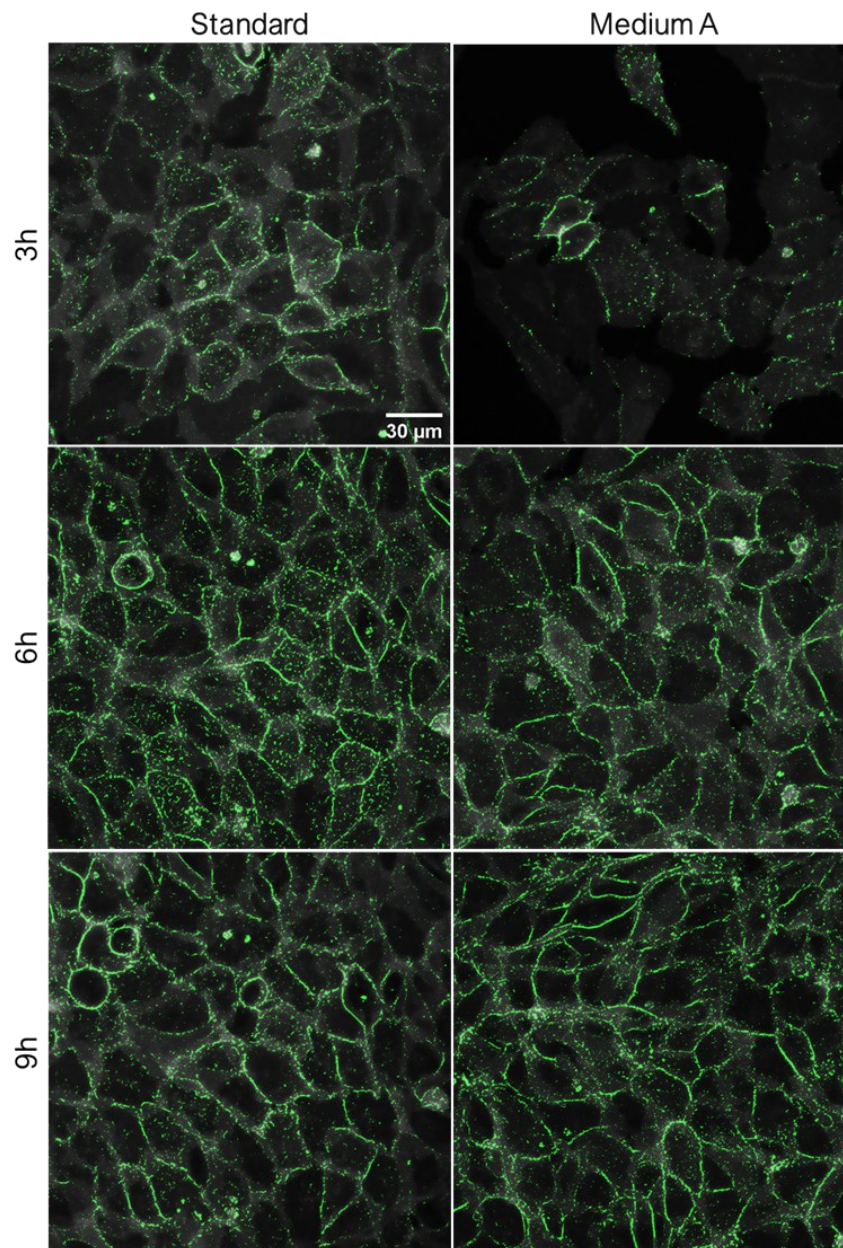


Figure 31 – Image analysis of MCT1 expression after 3 h, 6 h and 9 h of incubation with medium A (no glucose and no glutamine) by confocal microscopy. Images are representative of two independent experiments performed in triplicate. Scale bar corresponds to 30 μm .

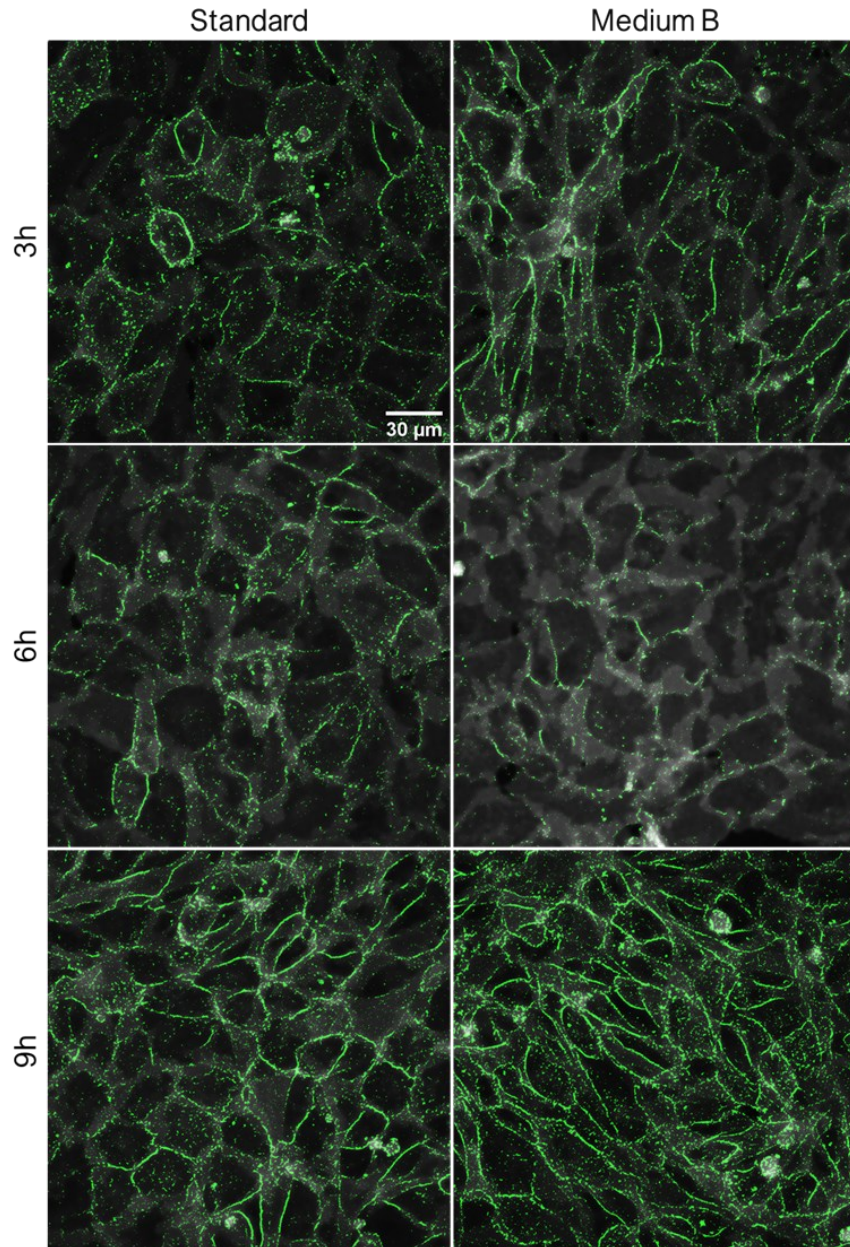


Figure 32 – Image analysis of MCT1 expression after 3 h, 6 h and 9 h of incubation with medium B (with glutamine and without glucose) by confocal microscopy. Images are representative of two independent experiments performed in triplicate. Scale bar corresponds to 30 μm.

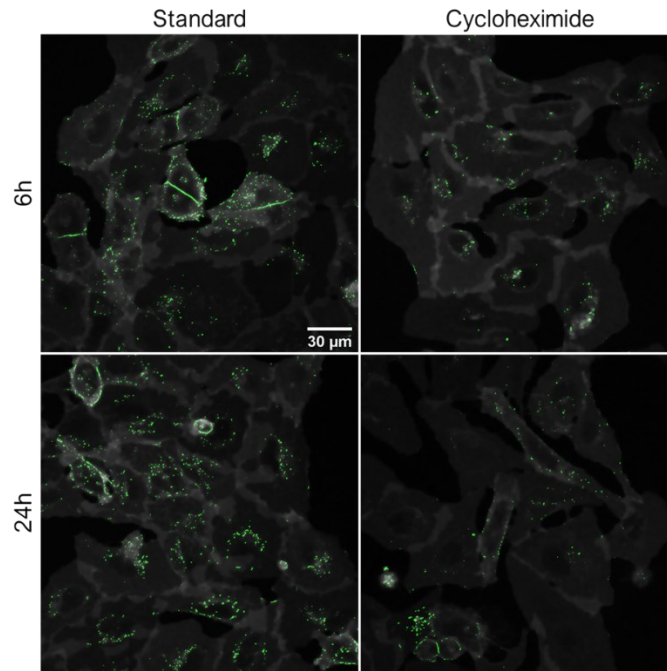


Figure 33 – Image analysis of MCT1 expression after 6 h and 24 h of incubation with cycloheximide by confocal microscopy. Images are representative of two independent experiments performed in triplicate. Scale bar corresponds to 30 μm.

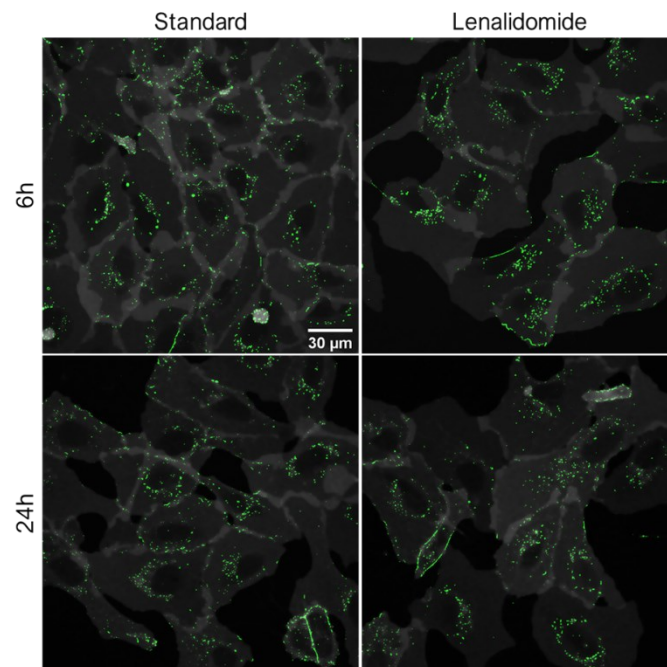


Figure 34 – Image analysis of MCT1 expression after 6 h and 24 h of incubation with lenalidomide by confocal microscopy. Images are representative of three independent experiments performed in triplicate. Scale bar corresponds to 30 μm.

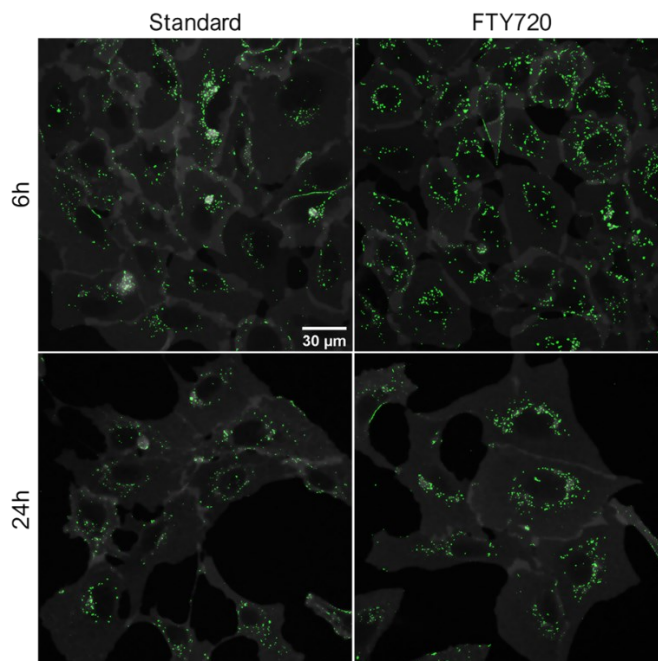


Figure 35 – Image analysis of MCT1 expression after 6 h and 24 h of incubation with FTY720 by confocal microscopy. Images are representative of three independent experiments performed in triplicate. Scale bar corresponds to 30 μm.

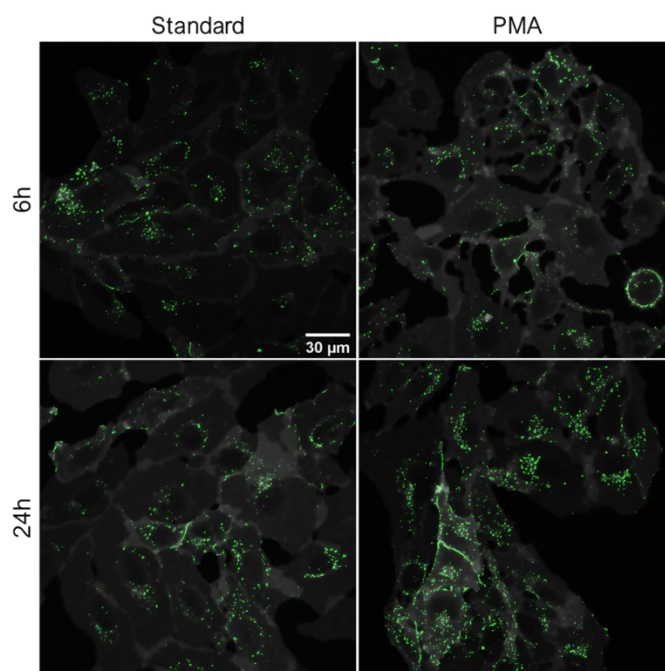


Figure 36 – Image analysis of MCT1 expression after 6 h and 24 h of incubation with PMA by confocal microscopy. Images are representative of two independent experiments performed in triplicate. Scale bar corresponds to 30 μm.

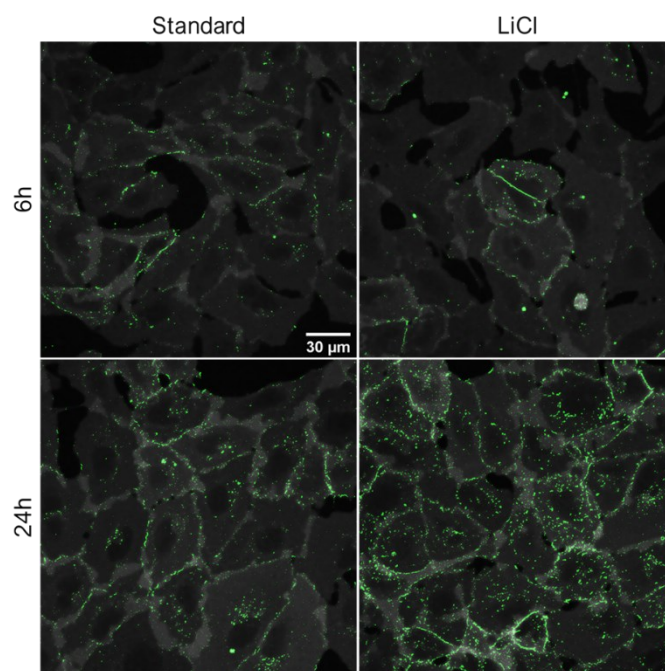


Figure 37 – Image analysis of MCT1 expression after 6 h and 24 h of incubation with LiCl by confocal microscopy. Images are representative of two independent experiments performed in triplicate. Scale bar corresponds to 30 μm .

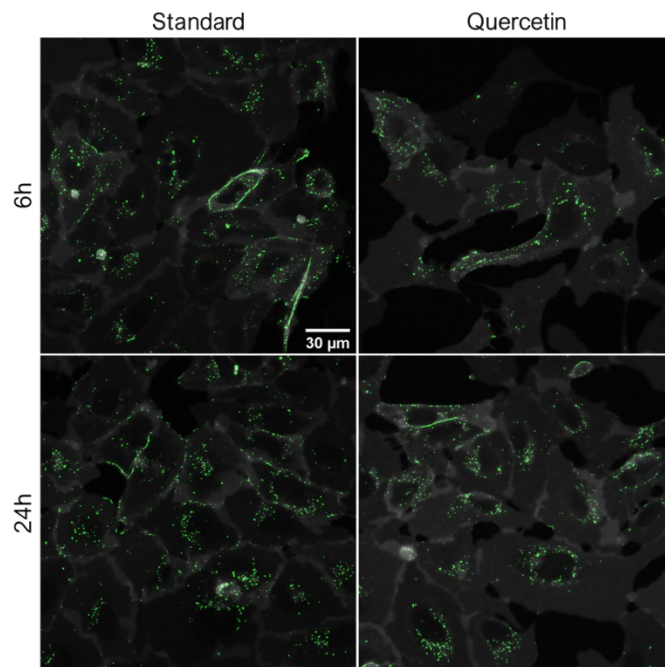


Figure 38 – Image analysis of MCT1 expression after 6 h and 24 h of incubation with quercetin by confocal microscopy. Images are representative of two independent experiments performed in triplicate. Scale bar corresponds to 30 μm .